UNIVERSITÀ DEGLI STUDI DI NAPOLI FEDERICO II

DIPARTIMENTO DI INGEGNERIA CHIMICA

Ph.D. in Chemical Engineering

(XXIII Cycle)

STUDY OF HYBRID MIXTURE EXPLOSIONS

Ph.D. Thesis

Scientific committee:

Prof. Gennaro Russo

Prof. Silvestro Crescitelli

Ing. Roberto Sanchirico

Candidate:

Ing. Anita Garcia Agreda

Table of Contents

Table Captions

Figure Captions

Acknowledgements

I wish to thank prof. Gennaro Russo for providing continued guidance and helpful comments during these three years.

Much gratitude is extended to ing. Linda Di Benedetto, ing. Paola Russo, dott. Ernesto Salzano and ing. Roberto Sanchirico for their help and for providing all the essential technical and theoretical support and advices.

I wish to thank also Mr. Andrea Bizzarro and Mr. Ernesto Marinò for their technical help.

And I gratefully acknowledge the support received for this research from all the people in IRC-CNR that with their kindness made my work more agreeable.

At last, I wish to thank also ing. Olivier Dufaud and Prof. Laurent Perrin for their kind welcome and their availability in their laboratory in France.

Finally a special thank is for my PhD (and not) colleagues and friends with whom I shared either joys and sorrows.

Abstract

The work of this thesis aims at studying the explosive phenomenon of hybrid mixtures to get insights into the driving mechanisms and the explosion features affecting the course of hybrid mixture explosion. This is achieved by means of an extensive experimental study that developed in the following steps:

- Measurement of the ignitability and the explosion severity;
- Study of the flame propagation.

The explosion experiments were performed in a 20 l Siwek bomb; instead, the flame propagation experiments were performed in a new equipment: a tube of 1 m length and 7x7 cm square.
The hybrid mixture under examination was a mixture of methane and nicotinic acid in air.
Results allow the definition of four different regimes of the gas/dust/air mixture explosion in the plane dust concentration vs. fuel concentration. And the flame propagation behaviour of the mixture gives a further contribution to the explanation of the different regimes.

Key words: Hybrid mixture explosion, deflagration index, flame propagation, explosion regimes.

Chapter 1 - Introduction

Every years, in the process industry, many of accidents are imputable to dust explosions which may cause failure to equipment, injuries and damages to people and to the surrounding environment, plant shut-off and, in some cases, the overall destruction of the factory, thus resulting in huge losses and, unfortunately, loss of lives.

Although dust explosion hazard is well known from decades, the recurrence and the destructivity of these phenomena have pushed scientists towards advancement of knowledge for the aims of prediction, prevention and mitigation of industrial equipment. Hence international standards for good engineering practice have been produced worldwide. The American National Fire Protection Association (NFPA) [1] defines any organic powder with surface area to volume ratio greater than that of a 420 micron diameter sphere (i.e. particles capable of passing through a U.S. No. 40 standard sieve) as a potential hazard [2]. Safety management and industrial specialists are nowadays aware of the hazard deriving from even familiar dust substances as sugar, cacao, wheat flour or coffee (Figure 1).

Figure 1 – Sugar can be a dangerous combustible.

Despite the advancement of recent years on the comprehension of the behaviour of dust explosions, further knowledge is required as several aspects of this complex combustion phenomenon are still unclear.

1.1 INDUSTRIAL ACCIDENTS INVOLVING DUST EXPLOSION

As concern dust explosions, many but not exhaustive information can be gathered from several either commercial or public database on industrial accidents occurred worldwide. A main source of data is the Major Accident Reporting System (MARS), a distributed information network for the Member State of the European Union. Other database are produced by IChemE in UK [3]-[4], the ARIA in France [5], ZEMA in Germany [6]; FACT (Failure and Accidents Technical Information System) in the Netherlands [7].

In U.S.A., the agencies involved in enumerating and reporting industrial accidents are the Occupational Safety & Health Administration (OSHA), the main federal agency charged with the enforcement of safety and health legislation, and the Chemical Safety and Hazard Investigation Board (CSB), an independent governmental investigative agency.

In 2006, the CSB published an Investigation Report [8] on the typology of industries that could be involved in dust explosions and fire accidents. CSB investigators carried out a survey on the dust explosions occurred in US from 1980 to 2005, and identified 281 major combustible dust accidents that killed 119 workers, injured 718 others, and destroyed many of the industrial facilities. The main source of statistical data is the OSHA Integrated Management Information System (IMIS) database, a significant source of data concerned with accidents that involve either injuries or fatalities. The result of CBS report are shown in Figure 2.

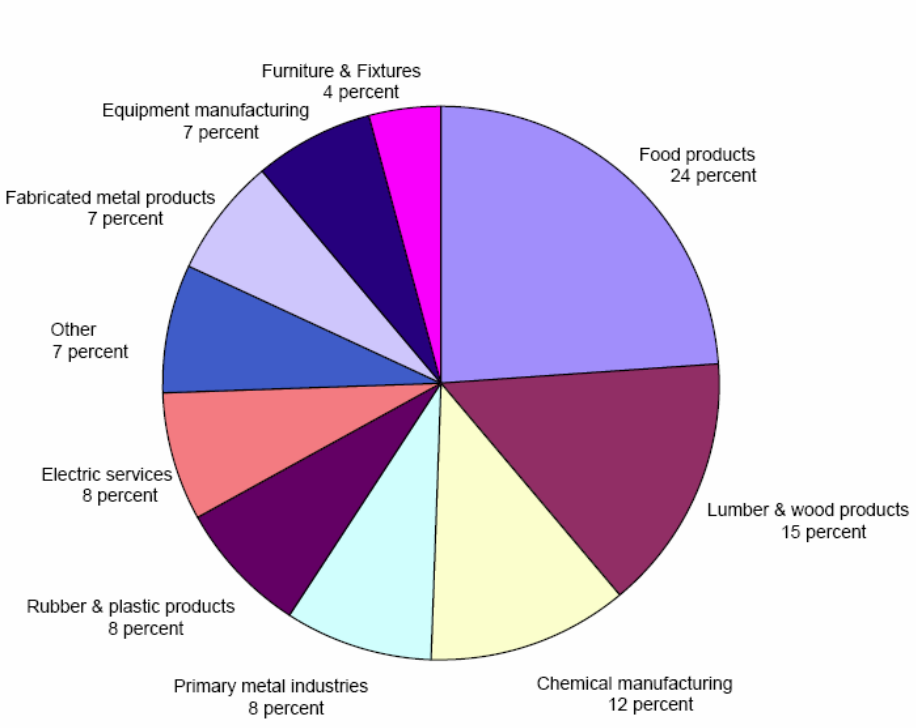

Figure 2 – Distribution of combustible dust accidents by industry.

Dust explosions may occur at any factory that handle combustible dusts, including metal fabrication, plastics, furniture and wood products, pharmaceutical and chemical manufacturing. However, four industry sectors (food products, lumber and wood products, chemicals, and primary metals) account for more than an half of the total accidents. According to CSB, dust collectors are the equipment most often involved in an accident. To this regard, Zalosh et al. [9] reported that dust storage sites account for more than 40 percent of all dust explosions even if grinders, silos, hoppers, and mixers are often involved in accidents.

CBS has analysed the type of materials which have caused combustible dust accidents (Figure 3).

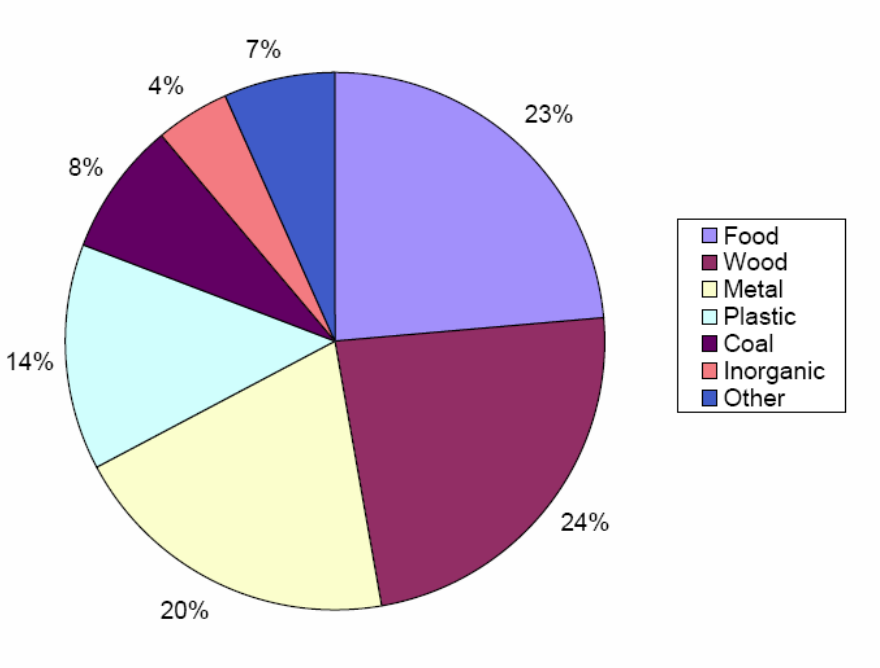

Figure 3 – Distribution of combustible dust accidents by material.

Wood, food-related products, and metals cover over 20 percent of explosions cases, whereas plastics counts for 14 percent.

In these statistics, no attention is paid to the possibility of explosions due to contemporary presence of gas/vapour and dust even if combustible dusts are often dispersed in industrial equipment containing flammable gas or solvents.

Bartknecht [10] defines a dust/air mixture containing flammable gases or vapour in the combustible atmosphere as “hybrid mixture” or even “mixture of two-fold origin”. An example of hybrid mixture explosion can be found in the accident occurred in 1997 at BPS Inc., Arkansas [11]. This event was most likely caused by the decomposition of a bulk sack containing the pesticide Azinphos methyl (AZM), which was placed close to a hot compressor discharge pipe. The heat from the discharge pipe caused the pesticide material to decompose giving rise to the formation of

flammable vapours which resulted in the explosion. Witnesses, including the fire fighters, reported the presence of a product or a powder in addition to smoke in this area. This suggested the formation of a hybrid dust/vapours mixture.

Other examples are reported for pharmaceutical industry [12], and other ones are those reported by Chilworth Technology [13], also mentioned by Amyotte et al. [14] for different field of industries such as fine chemicals, paints and inks, and food stuffs.

1.2 PREVENTING, PROTECTION AND MITIGATION

Prevention and mitigation/protection measures are mandatory for the reduction of the risk.

The prevention measures are concerned with the reduction of the explosion likelihood, whereas the protection measures are adequate to reduce the effects of the explosions.

The prevention measures aim at avoiding the conditions that allow the formation of explosive mixtures and all the possible causes of ignition.

They involve:

- elimination of the dust by cleaning of working environment;
- elimination of oxidant by means of suitable inerting procedures;
- elimination of ignition source by avoiding free flames, hot surfaces, sparks and also installing appropriate electrical system for hazardous areas [15].

The measures to be adopted for the protection are mainly:

- containment of explosion, that is the employment of equipment appropriately dimensioned to withstand the maximum explosion overpressure;
- separation of equipment, that is installation of different apparatus in different places, or physical division of the operations with higher explosion risk;
- explosion suppression by using appropriate extinguishing substances;
- venting: it consists in a surface that can be broken against an unacceptable pressure increase.

Venting is probably the method more extensively used to mitigate dust explosion process. These systems aim at preventing the generation of explosion overpressure taking place in a closed vessel by means of the rupture of a suitable disk.

Important guidelines for the design of the venting area can be found in the NFPA 68 [16]. In this standard, the severity of a dust explosion process is based on the knowledge of explosibility parameters (maximum explosion pressure, P_{MAX}, deflagration index, K_{St}, that will be introduced in the next chapters). In particular the hazard of the dust deflagrations is classified as in Table 1.

Table 1 – Hazard Classes of Dust Deflagrations

Hazard Class	**K_{St} [bar m/s]**	**P_{MAX} [bar]**
St-1	≤ 200	≤ 10
St-2	201 – 300	≤ 10
St-3	> 300	12

Venting area is then calculated as a function of these explosibility parameters:

$$A_v = f\left(V, P_{MAX}, K_{St}\right) \tag{1.1}$$

where A_v is the vent area (m^2), V is the volume of the vessel (m^3), P_{MAX} is the maximum pressure reached during deflagration of an optimum mixture of combustible dust and air in a closed vessel (bar), and K_{St} is the deflagration index of dust cloud (bar m/s). Both P_{MAX} and K_{St} are determined by means of standard test procedures [17].

As concern the design of vent area to mitigate hybrid mixture explosions, according to the current standard, the tendency is that of considering an increasing in the required relief venting area when the effective K_{St} value of most combustible dusts is raised by the admixture of a flammable gas.

NFPA 68 [16] suggests that in the case St-1 and St-2 dusts mixed with gases with combustion characteristics similar to those of propane, the same equation for dust should be used, thus neglecting the effects of gas.

Quite clearly, these options are loosely appropriate and can be adopted for engineering practice only. As matter of fact, indeed, scientific knowledge on hybrid mixture explosion is lacking. These aspects will be discussed in the present work.

Chapter 2 – Background

Gas, dust and hybrid explosions are exothermic chemical reactions (combustion) which produce a fast significant increase of temperature and, in a confined vessel, of pressure.
For the gas explosion to occur, a fuel (gas), an oxidizer and a source of ignition are required (the fire triangle, Figure 4a).
When dust or hybrid explosions are considered, five requirements are needed (Explosion Pentagon, Figure 4b,c):

1. Fuel – combustible dust without or with any flammable gas or vapour;
2. Oxidizer – usually air;
3. Ignition source;
4. Dispersion / mixing of the combustible in the air;
5. Confinement.

When all these requirements are satisfied (i.e. a flammable mixture of dust and air in the right proportion and in a confined space is ignited) the explosion occurs and a propagation of the flame across the cloud takes place.
The velocity and the development of flame propagation depend on several factors such as the nature of dust, the dust particle size, and the nature of combustion by-products.

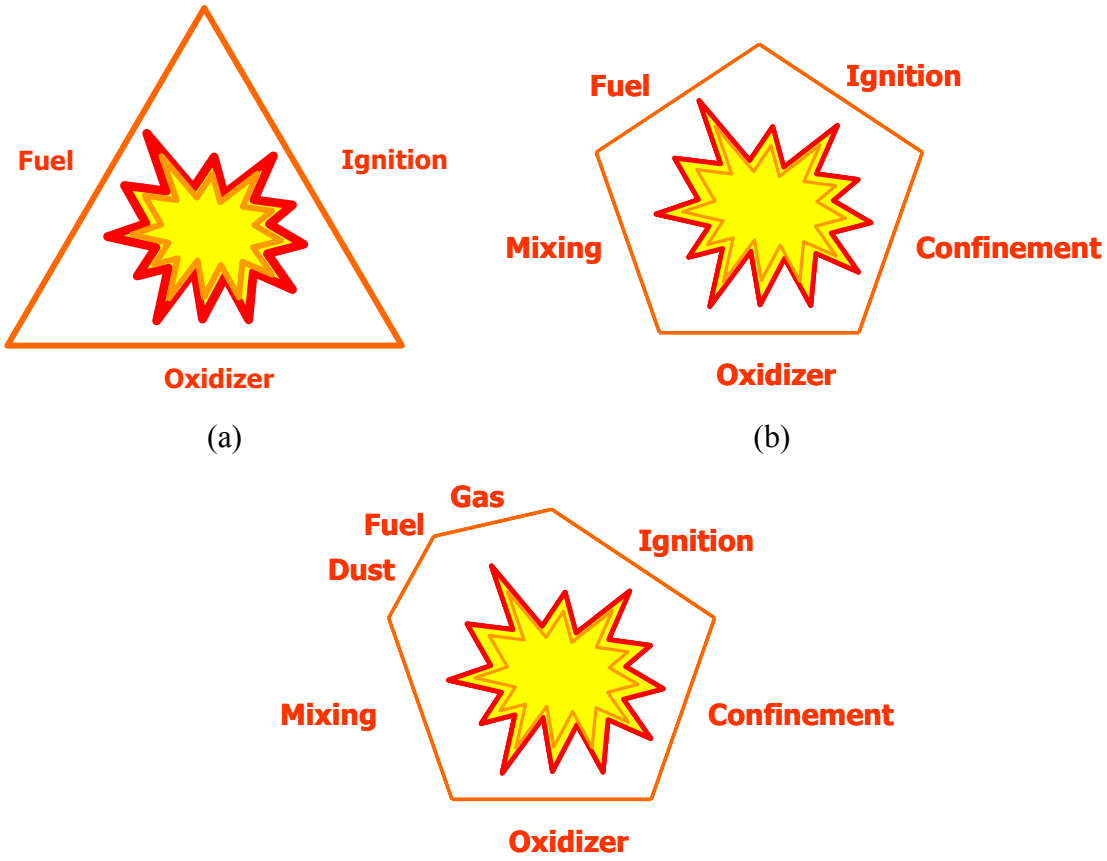

Figure 4 – Fire Triangle (a) , Explosion Pentagon (b), modified Explosion Pentagon (c).

The severity of explosion is affected by several factors: chemical composition of the fuel; moisture content; initial pressure; ignition temperature; distributions of particle sizes and shapes of dust particles; agglomeration of dust particles; initial turbulence; ignition source; and the location of the ignition point [18].

The materials involved in dust explosion can be metals, composed organic, composed organic synthetic, coal and peat. In the case of organic dust producing volatile substances, the explosion occurs in three steps which follow each other in very quick succession [18]:

- pyrolysis/devolatilization;
- gas phase mixing of fuel (released by dusts) and oxidant (usually air);
- gas phase combustion.

A dust explosions can be primarily initiate inside process equipment directly by an ignition source (primary explosion); or due to a primary explosion which originates pressure waves that disperses the dust, thus producing a secondary explosion that is often more destructive than the primary.

Starting from this fundamental knowledge, the following section describes the hybrid mixture explosions.

2.1 HYBRID MIXTURE EXPLOSIONS

More than one century ago, in 1885, Engler [19] observed that mixing coal dusts with methane at concentration even half of its Lower Flammability Limit would allow the explosion of the dust/gas mixture, hence producing unexpected hazardous conditions.

Since then, many studies have been performed to reveal the origin of such behaviour and also to measure the ignition propensity of such dust/gas mixtures frequently named "hybrid" mixtures [10],[20]-[28].

These studies focus their attention on two aspects of the characteristics of the fuel: ignitability and explosivity.

The first characterizes the ability of a fuel to cause a fire or an explosion. The second represents the ability of an airborne fuel mixture to propagate a deflagration after it has been initiated by a sufficient ignition source.

In the next paragraphs, these two aspects are presented separately and are based on the studies carried out in the literature.

2.1.1. Ignitability

The parameters that characterize the ease of ignition are the Minimum Ignition Temperature (MIT), the Minimum Ignition Energy (MIE), the Minimum Explosion Concentration (MEC, for dusts), the Lower and Upper Flammability Limits (LFL and UFL, for gases) and the Limiting Oxygen Concentration (LOC).

The minimum ignition temperature (MIT) is lowest temperature at which a gas/dust cloud will ignite under the specified conditions of test. The minimum ignition energy (MIE) is the lowest spark energy, which is just sufficient to effect ignition of the most ignitable mixture of a given fuel-mixture under specific test conditions. These two parameters are particularly important because they determine a powdered material's sensitivity to various ignition sources such as hot surfaces, electrical or frictional sparks: the lower the MIE and MIT values, the more hazardous the powder.

The minimum explosion concentration (MEC) is the minimum concentration of a combustible dust cloud that is capable of propagating a deflagration through a well dispersed mixture of the dust and air under the specified conditions of test. The Lower (Upper) Flammability Limit (LFL (UFL)) is the lowest (higher) concentration (percentage) of a gas or a vapour in air capable of producing a flash of fire in presence of an ignition source. Finally, The Limiting Oxygen Concentration (LOC) is the minimum concentration of oxygen (displaced by nitrogen) capable of supporting combustion.

The most extensive work on these parameters for hybrid mixtures involved the measurements of the lean flammability limits of coal dust with methane addition [26],[29]. For these mixtures, it was found that dust concentration required for flammability conditions may be predicted by Le Chatelier's Law (Eq. 2.1), originally developed and adopted for homogeneous gas mixtures [30]:

$$LFL_{mix} = \frac{100}{\frac{X_{gas}}{LFL_{gas}} + \frac{X_{dust}}{LFL_{dust}}} \tag{2.1}$$

Le Chatelier's law was derived by considering constant flame temperature for a given class of fuels. In the case of methane and coal dust mixtures such temperatures are comparable and then the correlation is found valid. In Figure 5 other examples, for which the Le Chatelier's law is valid, are shown. However, Cashdollar [27] has found some deviation from Le Chatelier's rule when methane mixes with Pocahontas coal, which is characterised by low content of volatiles. Bartknecht [10] has also shown that if methane is admixed to PVC dust in air, the Lower Flammability Limit of the dust/gas/air mixture decreases with increasing the gas concentration by a second order equation which is known as the curve for flammability limit of hybrid mixtures (Figure 5).

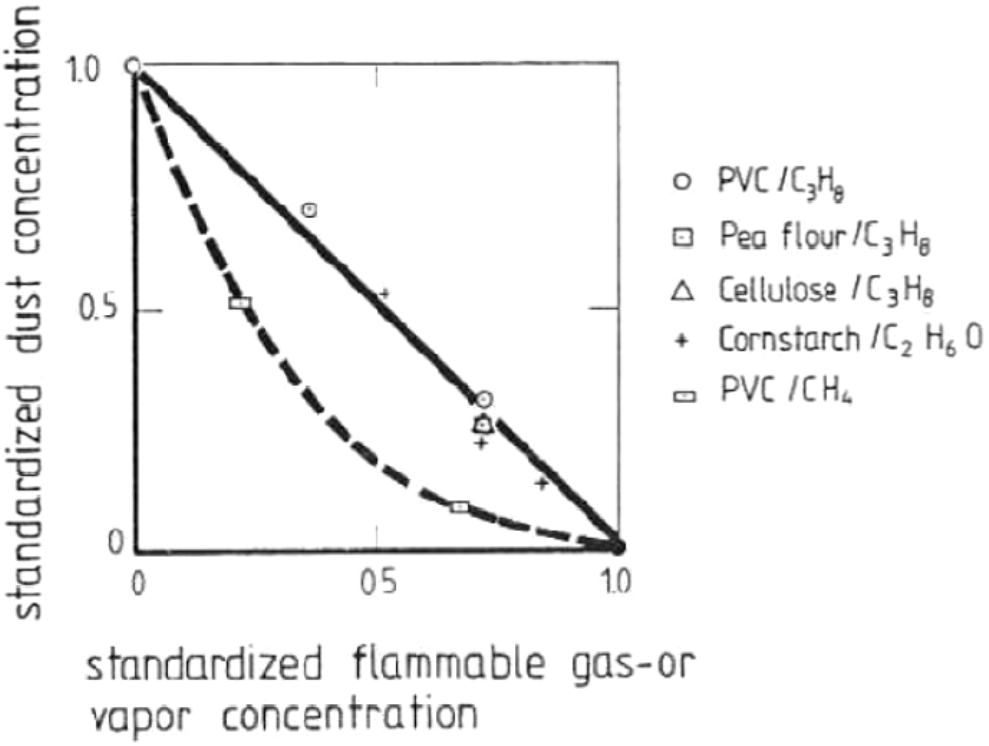

Figure 5 – Standardized presentation of the Lower Flammability Limit of hybrid mixture consisting of combustible dust with flammable gas [31]**.**

The correlation used by Bartknecht is [32]:

$$LFL_{mix} = LFL_{dust} \cdot \left(\frac{C_{gas}}{LFL_{gas}} - 1 \right)^2 \tag{2.2}$$

The data of Gaug, as referred by Hertzberg & Cashdollar [33], for hydrogen addition to cornstarch dust, also have shown significant deviation from Le Chatelier's relationship, thus indicating that a higher amount of dust is required to render the system flammable with respect to that predicted on the basis of Le Chatelier's Law (Figure 6).

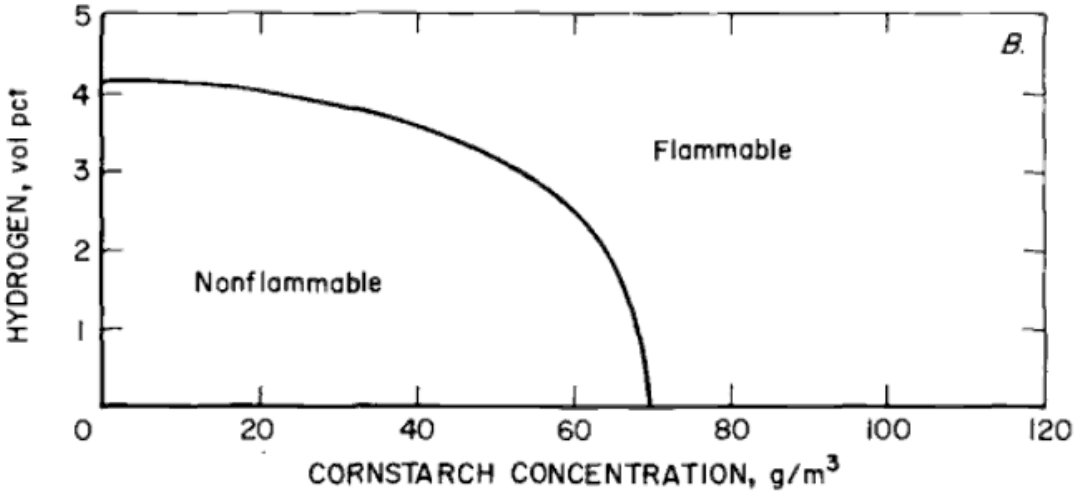

Figure 6 – Lean flammability limit for hybrid mixture of hydrogen and corn starch dust [33].

Chatrathi [28] evaluated the explosibility of hybrid mixture of cornstarch and propane in a 1 m^3 spherical chamber. He measured hybrid lower limits of flammability for pair of fuels, observing that the presence of propane decreases the cornstarch MEC. Similarly, the presence of cornstarch decreases the lower flammable limit of propane. Moreover, he performed tests at higher concentration of both fuels and observed that the violence of hybrid mixture is higher than that of single fuel in turbulent condition.

From all these data it turns out that if the concentration of gas or vapour and dust is respectively lower than Lower Flammability Limit (LFL) and Minimum Explosion Concentration (MEC), an explosion is however likely to occur. Moreover, a flammable gas may push into flammability ranges any dust of such large particle size which would otherwise been non-explosive [34]. Also, it can be deduced that there are different behavior depending on the nature of the specific pair of gas and dust.

2.1.2. Explosion

When a combustible dust is dispersed in a confined or partially confined atmosphere of flammable gas/vapour, and ignited, an hybrid mixture explosion occurs. The severity of this explosion may be quantified by means of the maximum explosion pressure, P_{EX}, and the maximum rate of pressure rise, $(dP/dt)_{EX}$ as for pure gas or dust explosion.

The maximum explosion pressure, P_{EX}, is the pressure in excess of the initial pressure at which the explosive mixture was ignited. The violence of an explosion is dependent on the rate of energy release of chemical reactions. For this reason, the other useful parameter is the maximum rate of pressure rise $(dP/dt)_{EX}$ related to the development of a dust explosion in a closed vessel. The rate of pressure rise is defined as the slope of a tangent laid through the point of inflexion (W_p) in the rising part of the pressure/time curve.

The term $(dP/dt)_{EX}$ depends on the volume of the vessel in which the explosion occurs. In order to take into account the influence of the volume on the course of explosion, the deflagration index, K_{ST}, is defined, by means of Cubic Law, as:

$$\left(\frac{dP}{dt}\right)_{EX} \cdot V^{\frac{1}{3}} = Cost = K_{St} \tag{2.3}$$

The two parameters are typically obtained at any concentration by experimental tests which produce pressure/time plots as in Figure 7.

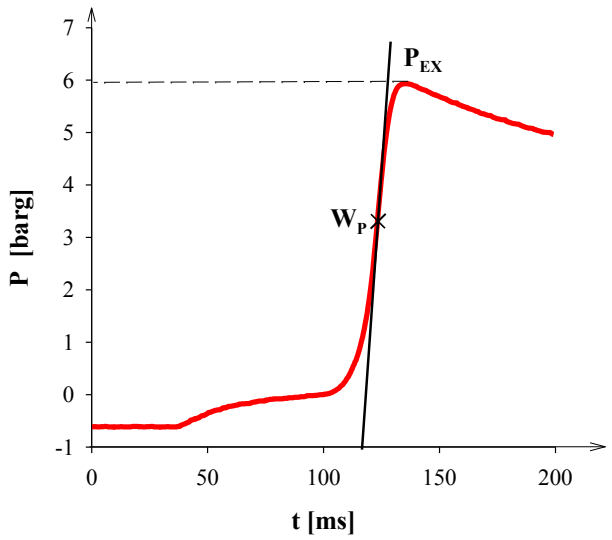

Figure 7 – Pressure/time-diagram of a fuel explosion.

With reference to hybrid explosions, Bartknecht [31] have studied the explosibility of cellulose with adding methane, butane and propane. He concluded that a hybrid mixture constituted by non-explosible dust and non-explosible gas can turn into explosible one. When gas is added, the maximum explosion pressure, P_{EX} was found to have consistent increase, whereas a more dramatic effect was observed on the hybrid deflagration index, K_{st} (higher than 15% of the gas deflagration index K_G, which is defined as in Eq. 2.3).

Pilão et al. [20], [35] investigated the behaviour of the hybrid mixture of methane/cork (Figure 8). They measured explosions parameters as MEC, P_{EX} and $(dP/dt)_{EX}$ for cork dust in methane/air mixture in a near-spherical 22.7 l explosibility test chamber, using 2500 J pyrotechnic chemical igniters. The mixtures investigated are constituted by a lower (40 g/m^3) and a higher (450 g/m^3) cork dust concentration and concentration of methane of 1.98 and 3.5 volume percent, i.e. below the LEL of methane/air mixture [22].

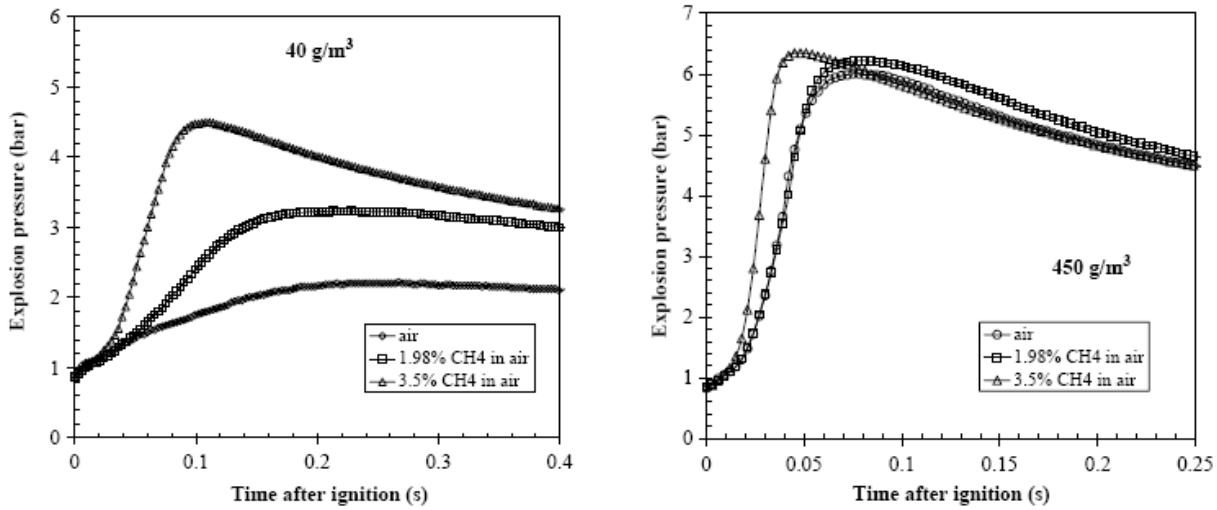

Figure 8 – Pressure history for hybrid mixture of cork (40 g/m^3 and 450 g/m^3) and methane (1.98 – 3.5 %) in air in comparison with that of pure cork [20].

Quite clearly, the presence of methane affects both the explosion severity and the maximum explosion pressure for lower dust concentration, whereas both the parameters are slightly affected in the case of higher dust concentration.

Dufaud et al. [36],[37],[38],[39] have studied the influence of pharmaceutical dusts excipients, vitamins, active principles and their associated solvent (ethanol, di-isopropyl ether, toluene) concentrations on maximum explosion pressure and maximum rate of pressure rise. They investigated three cases: i) magnesium stearate and ethanol; ii) niacin and di-isopropyl ether; iii) antibiotic and toluene, by using the 20 L Sphere Apparatus (see following sections) and 10 kJ due to chemical igniters as ignition energy. It's noteworthy that under thermodynamic prospective

considering poor dust/vapour mixtures the values of P_{EX} correspond well enough to that obtained by means of adiabatic flame temperatures calculation.

In the Figure 9, it's possible to see that the introduction of 0.5% vol. of di-isopropyl ether increases the value of P_{EX} from 7.3 to more than 8 bars at 250 g m^{-3} of niacin in approximately linear way and $(dP/dt)_{EX}$ from 685 to 1100 bar s^{-1} at the same concentration, though not linearly. So, Le Chatelier's law can be applied to hybrid mixture in order to predict the maximum explosion pressure starting from that of pure compounds. On the other hand, the maximum value of the deflagration index is found for dust/gas (or dust/vapors) rather than for the pure fuels, thus concluding that there are more than simple additive effects on explosion severity.

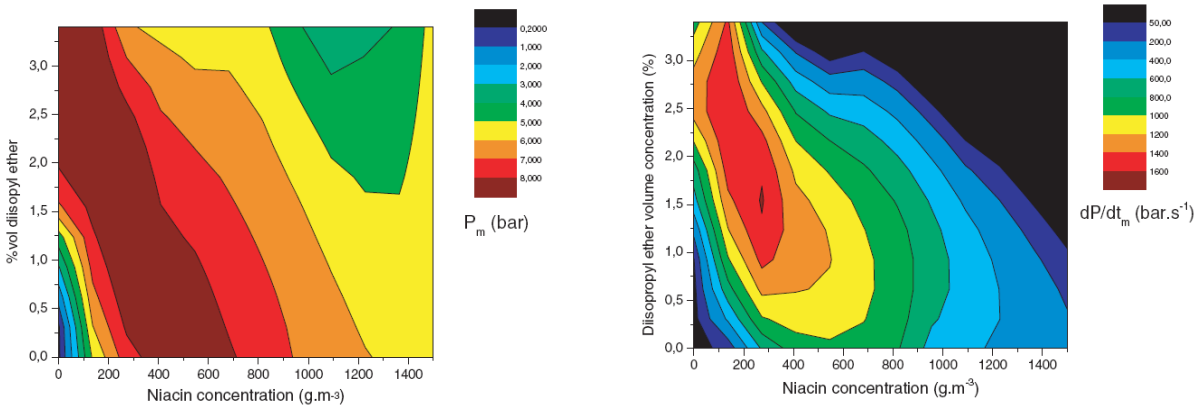

Figure 9 – 2D projection graph of the maximum explosion pressure (left) and of the maximum rate of pressure rise (right) of niacin/di-isopropyl ether hybrid mixtures [39].

All the literature studies were performed in the equipment ad hoc developed for dust explosion tests in which ignition of the dust/air suspension is performed by using two chemical igniters of total 10 kJ [31],[36],[37] or 2.5 kJ [20],[35]. However, the contribution of the gas in the gas/dust/air mixtures with respect to explosion severity and ignitability may be significantly influenced by such ignition energy. To this aim, Landman [40] studied the mixture of coal dust in presence of methane by using a 40-litre explosion vessel and analysing the explosion behaviour of explosive mixtures when exposed to different energy sources, i.e. volumetric ignition (pyrotechnic igniters) and point ignition (electric spark). The author concluded that the explosion of the same mixture initiated by the volumetric source behaves totally differently from that generated by the point source igniter, being the latter much slower and weaker. He noticed also that it is easier and more likely to initiate an explosion with a volumetric source because of more energy introduced with the use of pyrotechnic igniters.

Recently, Denkevits [21],[41] has studied the explosivity of the dust and its influence on the hybrid explosion severity of the graphite/hydrogen/air mixtures with chemical igniters (10 kJ) and with electric sparks in a 20-L sphere apparatus with suitable modifications. The hydrogen concentration is varied from 4% vol., that is the H_2 LEL, to 18% vol.. The graphite dust concentrations were in the range from 25 to 300 g/m^3.

When ignited by 10 kJ chemical igniters, the overpressures reached by the H_2/graphite dust/air mixture explosion are higher than that of hydrogen/air mixtures. More complex is the issue as concerning the maximum rate of pressure rise. When low dust concentrations are considered, two separate phases of the explosion can be distinguished: an initial phase of igniter/hydrogen explosion followed by a slower dust explosion phase (Figure 10). As reported by the author, the small amount of hydrogen acts like an additional ignition source, thus delivering additional combustion energy to the system.

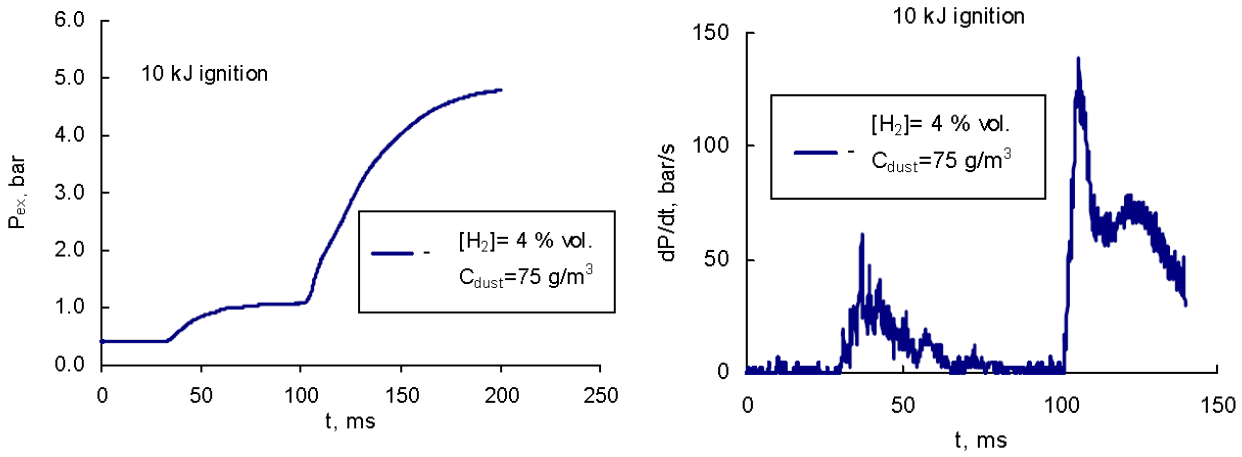

Figure 10 – Pressure-time curve and its derivative for hybrid mixture of hydrogen/graphite dust [H_2] = 4 vol. % C_{dust} = 75 g/m^3 [41].

When higher dust concentrations are considered, only one fast phase in which hydrogen and dust explode like a monofuel is observed (Figure 11).

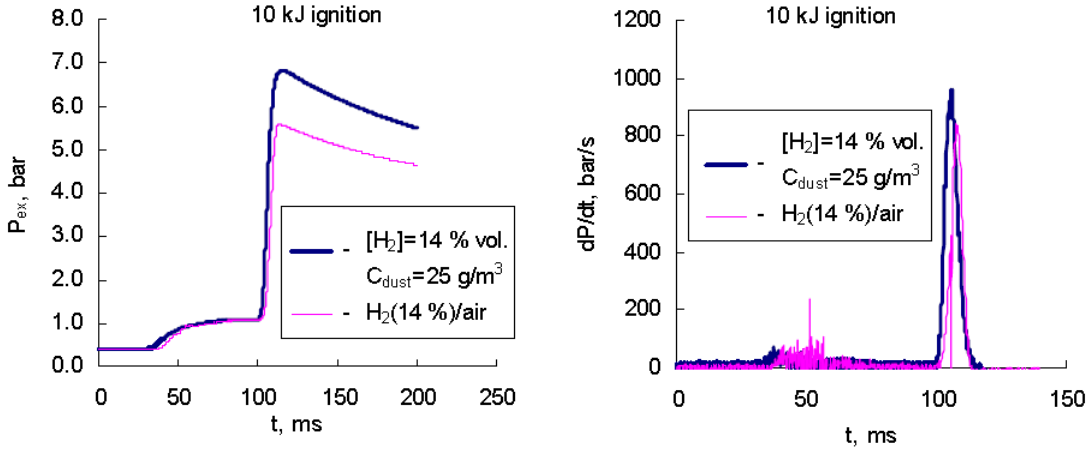

Figure 11 – Pressure-time curve and its derivative for hybrid mixture of hydrogen/graphite dust [H_2] = 14 vol. % C_{dust} = 25 g/m^3 [41].

In this case, chemical igniters are strong ignition sources which overdrive the explosion and the phase relative to igniters is confused with that of hydrogen. For this reason, the author used also electric spark ignition, in order to observe the explosion behaviour when varying hydrogen concentration.

When low concentration of hydrogen is considered, the graphite dust is not involved directly in the explosion and behaves as a heat-sink, i.e. decreasing both the maximum overpressure and the maximum rate of pressure rise (Figure 12).

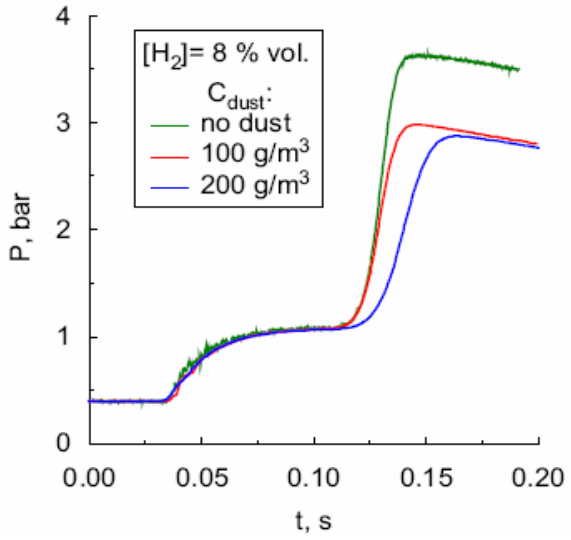

Figure 12 – History of pressure for the hybrid mixture '8 vol. % H_2/100 and 200 g/m^3 4 µm graphite dust'. And for the pure '8 vol. % H_2/air' mixture [41].

When increasing hydrogen concentration, the hybrid explosions is characterised by two distinct phases. Initially, the spark triggers the hydrogen, which reacts similar to the case without dust, and

the dust behaves like a heat-sink. Hence, a second phase is characterised by graphite dust combustion (Figure 13).

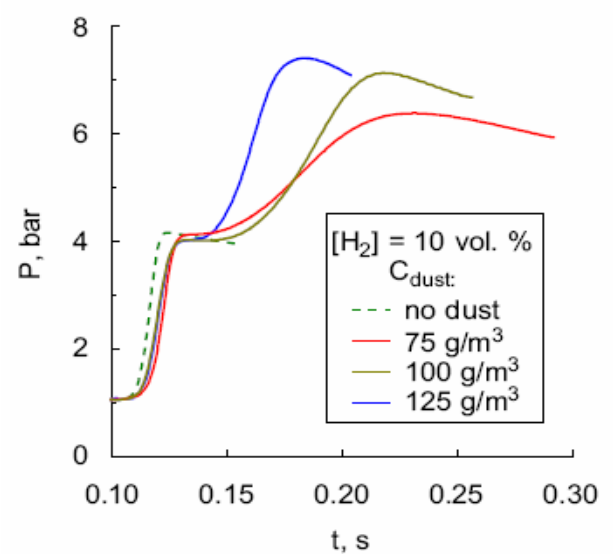

Figure 13 – History of pressure for the hybrid mixture '10 vol. % H_2/75, 100 and 125 g/m^3 4 µm graphite dust'. And for the pure '10 vol. % H_2/air' mixture [41].

When hydrogen concentration is further increased, the hybrid mixtures explode faster than hydrogen alone. Indeed, in this case both dust and hydrogen react at the same time scale and enter in competition for oxygen. Both maximum explosion pressure and maximum rate of pressure rise are higher than pure hydrogen parameters. If the dust concentration reaches some level, (e.g. 75 g/m^3 at 16% vol. of H_2), some hydrogen may remain un-burnt in the combustion products since the system is oxygen limited. This explains the fact that at higher dust concentration the rate of pressure rise is lower than that of the pure H_2/air mixture (Figure 14).

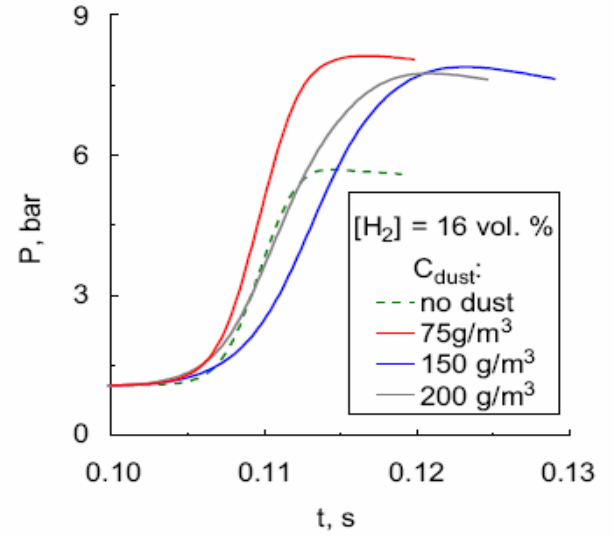

Figure 14 – History of pressure for the hybrid mixture '16 vol. % H_2/75, 150 and 200 g/m^3 4 µm graphite dust'. And for the pure '16 vol. % H_2/air' mixture [41].

Denkevits found that the use of low-energy sparks allowed the identification of different stages of explosion evolution at changing the hydrogen content, which cannot be deduced by the simple combination of the behaviour of the two components.
Denkevits [42] has studied also an hybrid mixture of tungsten/hydrogen-air in the same experimental condition. In this case all mixtures always explode in one step. But this is probably due to the fact that fine tungsten dusts are more sensitive and can be easier ignited by hydrogen explosion than fine graphite dusts.

From these analysed scientific works, it's possible to confirm the complexity of the hybrid explosion phenomenon. In fact, the violence of an hybrid mixture explosion could be not predicted by means of superposition of the effects of the two separate explosions, that of the pure gas/vapour and that of the pure dust. Hence, several questions raise:

- it is not clear how the ignitability and explosibility behaviour of hybrid mixtures can be evaluated from those of pure compounds;
- and it is not yet clarified whether the dust or the gas is driving the explosion phenomena at changing the dust/gas ratio and the fuel/air ratio.

Furthermore, the performance of the explosion seems different depending mainly on gas concentration, dust concentration, particle size and then it's not possible to find an univocal behaviour that can describe the hybrid mixture phenomenon.
Moreover, from these literature studies, it turns out that there is not systematic study able to quantify the role of dust and gas in driving the explosion. Eventually, it becomes essential to understand the mechanisms of hybrid mixture explosions by means of specific experiments with different dusts and gases.

2.1.3. Flame propagation

Explosion phenomenology is based on the fast, spatial propagation of a stable flame. The explosion severity strongly depends on the rate of flame propagation. As a consequence, a complete characterization of the explosion behaviour has also to deal with the study of the flame propagation.
As concern gaseous mixture, the laminar flame propagation is associated with molecular thermal conductivity and diffusion as first suggested by Mallard and Le Chatelier [43], who postulated that the heat transfer controls the flame propagation and the flame consists of two zones separated at the point where the next layer of combustible mixture ignites. This theory was later improved by Zeldovich and Frank-Kamenetzkii, who included the diffusion of molecules in the mechanism of

propagation of the flame. Their theoretical derivation was presented in detail by Semenov [44] and Glassman [30].

If considering a tube with both ends open, assuming a flame front as a geometrical surface of zero thickness and a coordinate system co-moving with the flame front, the unburned fuel mixture moves into the flame front with velocity S_l (the laminar burning velocity) and the combustion products flow out of the flame front with velocity S_b. A relation exists between S_l and S_b for a plane flame front obtained by the condition of conservation of the total mass flux: the total mass of gas entering the flame per unit area of the front must be equal to the mass of combustion products leaving this surface downstream:

$$\rho_u \cdot S_l = \rho_b \cdot S_b \tag{2.4}$$

where ρ_u and ρ_b are the densities of the initial unburned mixture and combustion products [45].

The measure of the laminar burning velocity can be done by means of the burner method or tube method.

The burner system consists of a tube in which the fuel passes and reaches the top part in which the annular space separating the flame from the burner edge provides a continuous ignition source and anchors the flame to burner. In this way is guaranteed the stability of the flame.

The tube system [46] consists of a transparent, semi-open tube in which the ignition system is installed at the open end of the tube. With this last apparatus, two different methods can be used: the "tube" method and the "direct" method.

In the "tube" method, the laminar burning velocity, S_1, is calculated according to the method of Andrews and Bradley [47]

$$S_l = \frac{A'}{A_{fl}} \cdot S_{fl} \tag{2.5}$$

where S_{fl} is the flame velocity, A' is the projected flame area on a plane perpendicular to the direction of flame propagation and A_{fl} is the surface area of the flame front. The flame velocity S_{fl} is calculated as the prime derivative of the distance between the flame front and the ignition point ($\partial x/\partial t$) and in this method is considered uniform over the tube cross section.

In the "direct" method, a local burning velocity is evaluated. More specifically, the laminar burning velocity is directly derived from its definition:

$$S_l = \vec{S} \cdot \vec{n} - \vec{U} \cdot \vec{n} \tag{2.6}$$

where $\vec{S}$ is the flame speed, $\vec{n}$ is the unit vector normal to the flame front at the point under consideration and $\vec{U}$ is the flow velocity (vector). The experimental determination of S_l with this method is very difficult because the evaluation of the quantities have to be sufficiently accurate and $\vec{U}$ has to be determined very close to flame front [46].

The definition of laminar burning velocity of the dusts is essentially similar to that of gases [48] even if, quite clearly, the flame propagates in heterogeneous medium [49]. Hence, two types of flames [50] depending on the nature of the dusts [18] are observed. The first is the Nusselt type flame, where chemical reaction takes place in heterogeneous phase and is controlled by diffusion of oxygen to the surface of individual, solid particles. The second type is the volatile flame, where the rate of gasification, pyrolysis, or devolatilization is the controlling process and the chemical reaction takes place mainly in the homogeneous gas phase. Quite clearly, in this case the volatility of the dust becomes an essential parameter since affects the flame propagation behaviour [51],[52]. Most organic dust explosions are characterised by volatile flame type.

As cited previously, dust explosion needs a dispersion phase before ignition. To this aim, some grade of turbulence is necessary. But turbulence affects the measure of the laminar burning velocity [53]-[55]. These effects should be taken into account when evaluating laminar burning velocity of dusts. Several studies on the flame propagation for the dusts have been carried out [56],[46],[48],[49],[53]-[63] mainly by using tube method, but however the knowledge on the fundamental mechanism of flame propagation in dust-air mixtures is still lacking.

Quite clearly, even less works concern hybrid mixtures [64]-[66]. Bradley et al. [64] studied the laminar burning velocities of methane-air-graphite mixtures in comparison with fine coal dusts by using a burner. They demonstrate that in the dust explosion process the pyrolysis/devolatilization step is very fast and the combustion occurs substantially in the gas phase.

Liu et al. [65] and Chen et al. [66] studied the flame propagation of an hybrid mixture of methane and coal dust in a combustion chamber (tube method). Their results are shown in Figure 15. The results show that the flame propagates first at constant speed for few initial milliseconds; then it has an acceleration, reaches a maximum and then reduces. At its apex, the flame propagation speed reaches value of about 14 m/s, that is much higher than that of single-coal dust flame (2 - 3 m/s [67]) and it's much higher also respect other dust flames [60]-[62].

Liu et al. have explained that the much faster flame propagation speed is due to heat released by the methane which expands combustible products.

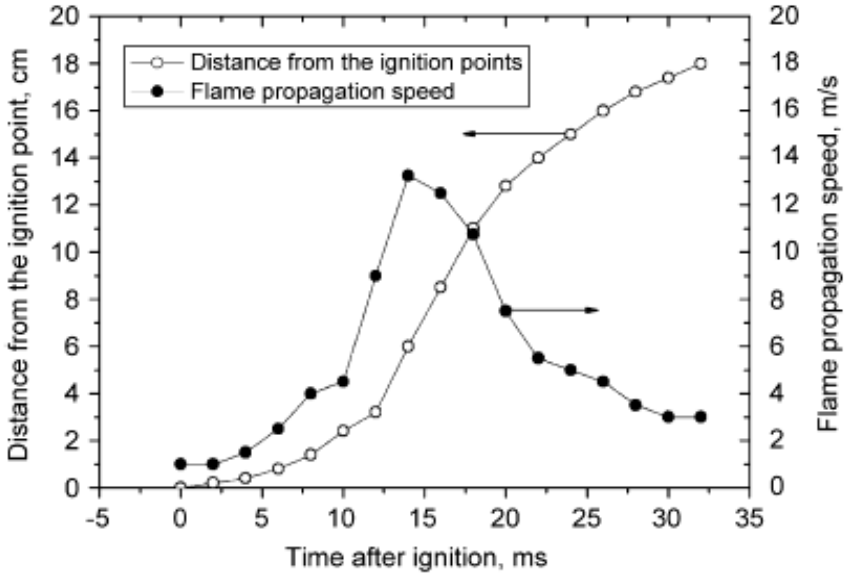

Figure 15 – Relationship between the distance from the ignition point and arrival time of the flame front; coal dust concentration: 127 g/m^3 [65].

Chapter 3 – Aim of the work

The present work aims at studying the explosive phenomenon of hybrid mixtures to get insights into the driving mechanisms and the explosion features affecting the course of hybrid mixture explosion. This is achieved by means of an extensive experimental study that developed in the following steps:

- Measurement of the ignitability and the explosion severity;
- Study of the flame propagation.

3.1 ACTIVITIES

The study involved several activities:

1. The explosion experiments were performed in a 20 l Siwek bomb at Institute of Combustion Research (IRC) of Consiglio Nazionale delle Ricerche (CNR) of Naples and at Dipartimento di Ingegneria Chimica of the Università degli Studi di Napoli Federico II (DIC – UNINA) of Naples.
2. The flame propagation experiments have been performed in a new equipment. It is a tube of 1 m length and 7x7 cm square available at the Laboratoire Réactions et Génie des Procédés (LRGP) at Ecole Nationale Superieure des Industries Chimiques (ENSIC) of Institut national polytechnique de Lorraine (INPL) of Université of Nancy, France.

Chapter 4 – Experimental Apparatus and Methodology

4.1 APPARATUS

4.1.1 Explosion severity tests

The explosion severity experiments are performed by using the standard 20 l sphere apparatus (Figure 16) manufactured by Adolf Kühner AG (CH), with rebound nozzle introduced by Siwek [68].

The tests are performed in accordance with the ASTM Method E 1226 (2000) [17], National Fire Protection Association (NFPA) Standard 68 (1994) [16], German Society of Engineers (VDI) Method 3673 (1995) [69], and International Standards Organization (ISO) Method 6184/1 [70].

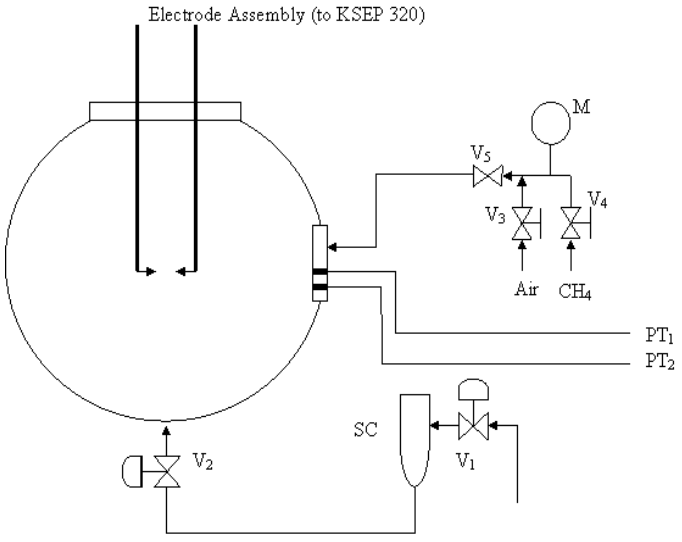

Figure 16 – Siwek 20 l spherical vessels for the determination of dust explosion parameters [71].

The kernel of test facility is a spherical explosion chamber, made of stainless steel and rated to resist at 30 bar static pressure. A water jacket surrounds the spherical bomb for the control of the internal wall temperature.

A flange on the top of combustion chamber allows for the insertion of two electric rods, in order to reach the centre of the sphere for the igniters; the ignition is performed by either chemical igniters or electric spark (Figure 17).

Figure 17 – Chemical igniters (left) and spark electrodes (right).

The chemical ignition is obtained by using two pyrotechnic capsules composed of 40 wt% zirconium, 30 wt% barium nitrate and 30 wt% barium peroxide. The igniters are activated electrically by low-voltage source and provides a dense cloud of hot dispersed particles and very little gas as by-product. The international standards require typically an energy of 10 kJ.

For the electric spark ignition, two electrodes are located at the centre of the sphere. A spark is produced by supplying 15 kV, 30 mA by means of Kühner, KSEP 320, high voltage trasformer. The spark electrodes are two rounded tungsten rod (diameter 2 mm) whose tips are spaced at the standard distance of 6 mm.

At the bottom side of the bomb, the outlet valve V2 (Figure 16) is installed. The outlet valve is connected to a rebound nozzle (Figure 18) placed at the bottom of the bomb for the dispersion of the dust/air mixture. The outlet valve is operated by means of an electro-pneumatic system.

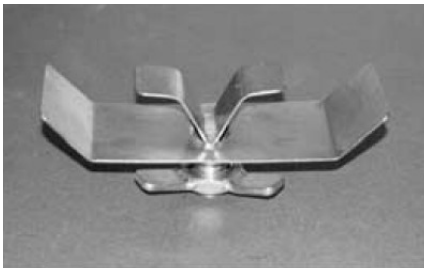

Figure 18 – Rebound nozzle.

The input section of the outlet valve is connected to the sample container SC (V_{SC} = 0.6 liter), by means of which the dust is dispersed in the sphere: the container loaded with dust is pressurized using compressed air at 20 barg.

At the right side of the bomb, two piezoelectric transducer PT1, PT2 (Kistler Type 701A) are mounted. Because the piezoelectric pressure transducers are heat-sensitive, their membranes are

protected by silicon rubber of approx. 2 mm thickness. The use of two completely independent measuring channels gives good confidence against erroneous measurements and allows for self checking.

The sphere is connected at right side with a vacuum line. It is used both to pre-evacuate the sphere and feed the gas mixture. The vacuum outlet is connected to vacuum pump (Vacuubrand RZ9) providing -0.8 barg (for hybrid mixture test) or -0.6 barg (for dust test) evacuation pressure. A pressure transmitter, Dwyer Series 626, M, is used to measure the evacuation pressure. The measurement range of the transmitter is 0 – 3 bar, the accuracy is 0.25% full scale.

The gas mixtures in the chamber are prepared by the partial pressure method; for this reason the vacuum line is linked, by means of two valves, V3 and V4, respectively with air and with the flammable gas cylinder.

All the timing sequences and the acquisition of the pressure signals are performed by means of the electronic module KSEP 332, which is interfaced by a desktop computer for the remote control of the system. The system is also connected to a re-circulating crio-thermostat for the temperature control (Julabo CF31). In all runs water is used as cooling fluid, at 25 °C.

Explosibility tests were then performed on the dusts, gas and respective hybrid mixtures, evaluating the fundamental parameters, maximum explosion pressure and deflagration index.

For the aims of studying hybrid mixture explosions, it was necessary implementing and modifying the sphere apparatus. In Figure 19, a schematic sheet of the system is shown.

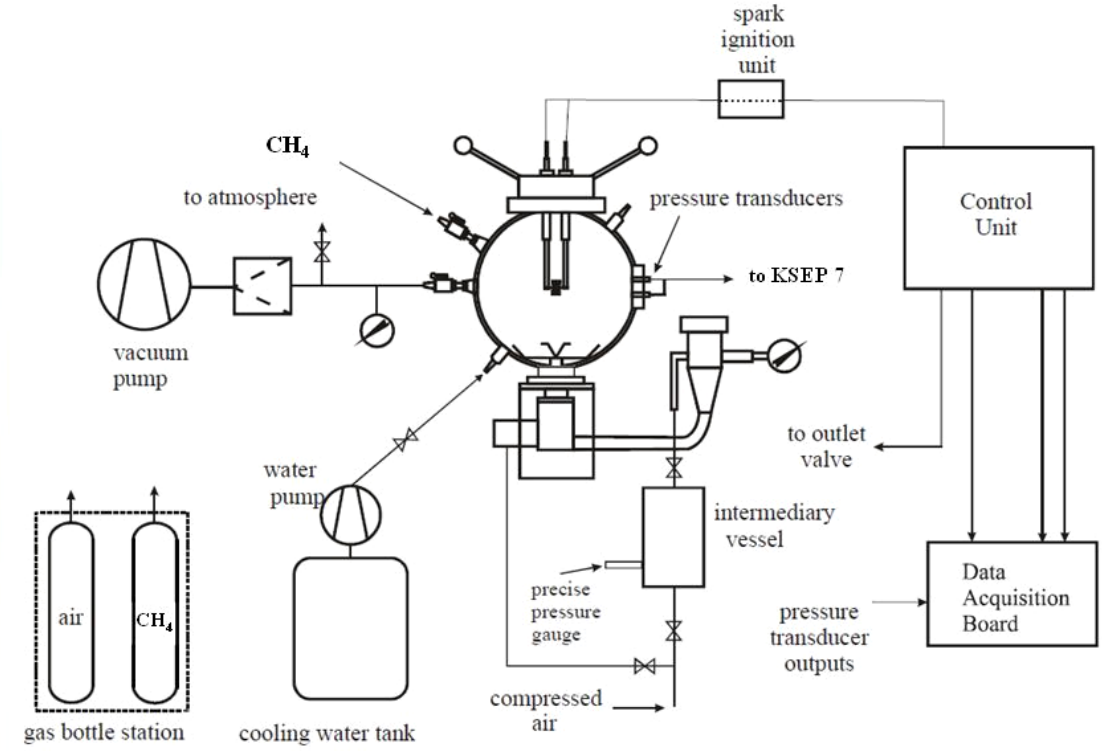

Figure 19 – Scheme of 20 L Sphere Apparatus System [41] adapted for hybrid mixture explosions.

4.1.2 Flame propagation tests

The flame propagation experiments are performed in a square tube 7 cm side, about 1 m length (Figure 20).

Figure 20 – Tube for flame propagation tests.

This tube has a volume of 4.9 L and has two opposite walls made of glass and two opposite wall made of stainless steel.

The combustion chamber is mounted vertically. A removable vent is located at the top of the tube. At the bottom, the tube is attached to a metal base equipped with a dispersion cup. The upper portion of the dispersion cup is nearly hemispherical in shape. The dust placed in the bottom cup prior to the test is dispersed by an air blast from a 0.05 l reservoir powered with a mushroom shaped nozzle at the pressure of about 7 bar, impinging on it in the bottom of the dispersion cup, in order to generate a homogeneous cloud.

Dispersing air is controlled by a 1⁄2-in. (12.7-mm) full port, electrically operated solenoid valve.

The ignition of the dust cloud is obtained by means of a continuous spark between two 2 mm diameter tungsten rods with a spark gap of 6 mm, located near the closed bottom end of the tube.

The power for the igniting spark generation is obtained from a charged capacitor. [72],[73],[74]

The tube is connected also with a vacuum line. The vacuum outlet is connected to vacuum pump (Alcatel PASCAL 2005SD). A pressure transmitter is used to measure the evacuation pressure and used to prepare gas mixture in the chamber by partial pressure method. For this reason the vacuum line is linked by means of a valve to a pre-mixing chamber of about 0.6 l of volume, connected by means of other two valves with an air bottle and a flammable gas bottle.

A PHANTOM v91 camera is used to record ignition of dust cloud with a frame rate of 2000 fps (period: 500.00 μs) and exposure of about 490 μs.

All the timing sequences and the ignition system are controlled remotely by means of electronic system adapted from Hartman tube apparatus [72]. The high speed video camera is directly connected to specific PC by Gigabit Ethernet cable for camera control, image transfer and final acquisition.

A simple scheme of the system is showed in Figure 21. This scheme is similar to that for the standard Hartmann tube test [72], the differences are in the introduction of some line for the vacuum and for the supplying of gas.

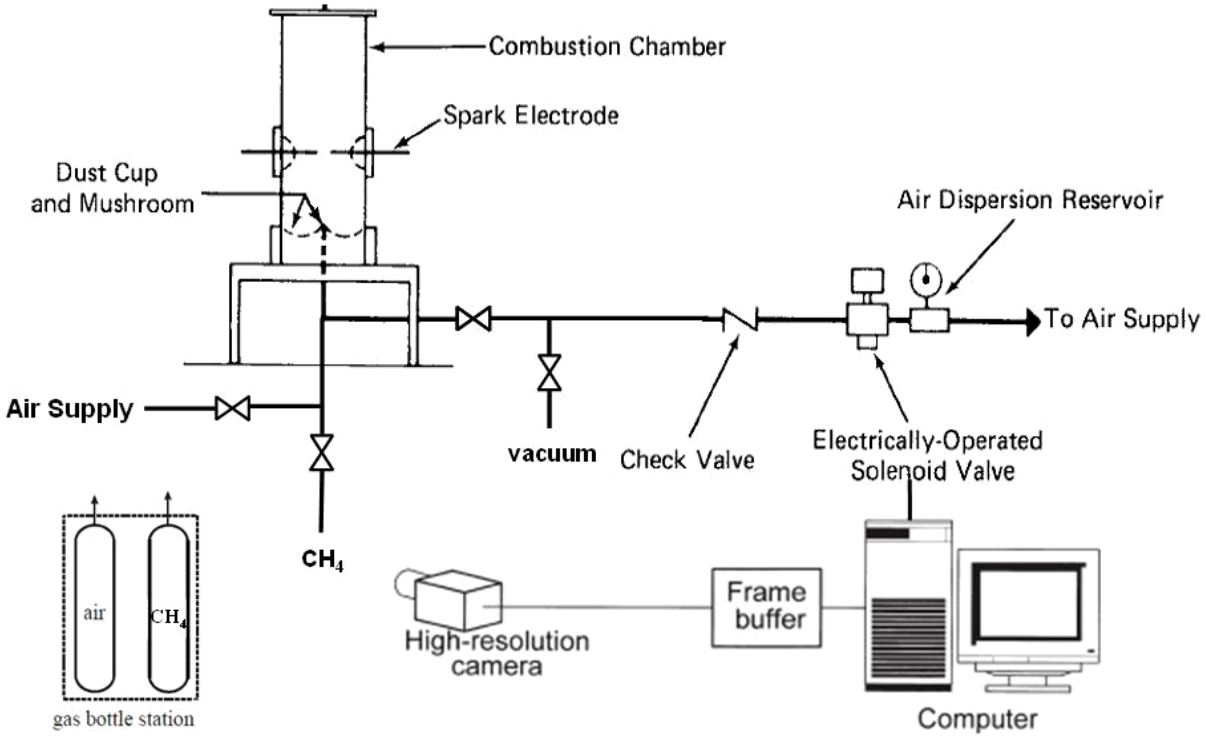

Figure 21 – Modified scheme of Flame Propagation Experiment System [72].

4.2 METHODOLOGIES

4.2.1 Explosion severity tests

A scheme of the experiments that is possible to carry out using the 20 l Sphere is shown in Figure 22.

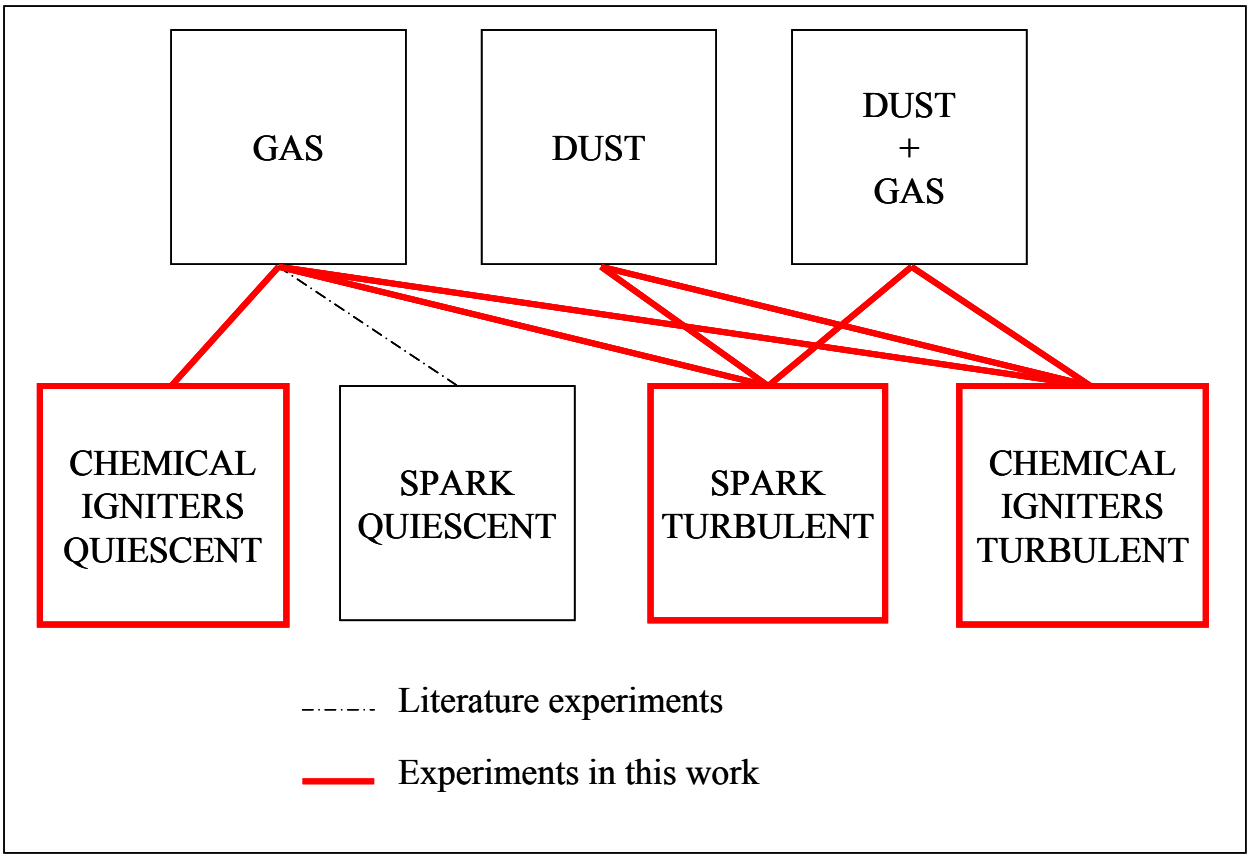

Figure 22 – Type of experiments in the 20 l Sphere.

Experiments may be performed both in quiescent and in turbulent conditions as concern the gas explosions; instead for the own nature of the dust, the experiments on dust explosions may be carried out only in turbulent conditions, that consist in the feeding of the dust by means of an air blast which induces turbulence in the system, as described in the previous paragraph. As a consequence, also for hybrid mixture explosions, the experiments may be performed exclusively in turbulent conditions. Moreover, in both conditions the ignition can be obtained by means of or electric spark or chemical igniters.

In this work, first, explosion experiments were performed for either pure gas, pure dust or hybrid mixture, using a weak electric spark ignition source instead of standard chemical igniters used for dust explosions. The strong ignition energy of chemical igniters may indeed in some cases hide some interplay phenomena between dust and gaseous fuel, overdriving the explosion behaviour.

The effect of the initial turbulence were also studied, by varying the ignition delay time, which significantly affects the explosion development in closed vessels [75]-[79].

Moreover some experiments with chemical igniters were performed for the sake of a comparison between the two type of ignition source.

Experiments with chemical igniters for pure gas, for pure dust and for hybrid mixtures were performed varying the amount of energy between 500 J and 10 kJ. Moreover, as concern the gas, experiments were carried out both in quiescent condition and in turbulent condition to compare the difference of the initial fluid dynamic conditions.

The tests were carried out following the "hybrid mixture" procedure provided by the Software KSEP 7 (Kühner) and setting test conditions as reported in the Table 2

Table 2 – Test conditions procedure.

Test Conditions Procedure	= Hybrid: P_{max}, K_{max}
Ignition source	= Permanent Spark; = Chemical Igniters
Ignition energy IE	≈ (15kV, 30 mA supplied by tension generator) = 500, 1000, 10000 J (Chemical Igniters)
Distance between electrodes	= 6 mm
Ignition delay time t_v	= 0 - 750 ms = Quiescent, 60 – 120 ms
Dispersion pressure P_z	= 20 barg (21 bar absolute, pre-evacuation)
Initial Pressure, P_i	= 0 barg
Volume	= 0.02 m^3

Before each tests, dust is weighted and loaded in the dust container.

For pure gas explosions and for hybrid mixture explosions, the partial pressure method is used for the preparation of mixture with the following steps:

1. the sphere is evacuated up to P_A = -0.8 barg;
2. flammable gas is fed until the required pressure (P_B) to obtain a given gas concentration in air;
3. air is fed up to P_C = - 0.6 barg.

The values of set pressure at different gas concentrations are reported in Table 3. Dry air is fed in the dust container (with or without dust) up to 20 barg pressure. Then outlet valve (V2) is opened reaching the initial pressure (P_0=0.0 barg) in the sphere.

Pressures were measured by means of the manometer M (Dwyer Series 626).

Table 3 – Set pressures for preparation of gas/air mixture in the bomb.

Fuel Gas $_{SET}$ (%v/v)	*P_A (bar g)*	*P_B (bar g)*	*P_C (bar g)*	*P_0 (bar g)*
1	-0.80	-0.79	-0.60	0.0
1.6	-0.80	-0.78	-0.60	0.0
2.3	-0.80	-0.78	-0.60	0.0
3	-0.80	-0.77	-0.60	0.0
3.6	-0.80	-0.76	-0.60	0.0
6	-0.80	-0.74	-0.60	0.0
7.3	-0.80	-0.73	-0.60	0.0
10	-0.80	-0.70	-0.60	0.0

When outlet valve is opened, the dust comes into the sphere chamber through the rebound nozzle producing a dispersion cloud. After a fixed ignition delay time, ignition starts and a possible explosion occurs.

A typical history of evolution of pressure caused by an explosion is showed in Figure 23, where P_d is expansion pressure of storage container, that is difference between "pre-vacuum" and normal pressure (the standard value is 0.6 bar, but 0.55 … 0.7 bar are acceptable value); t_d is time-delay of the outlet valve (that has to be in the range of 30 to 50 ms) ; t_v is ignition delay time; t_2 is induction time, that is time difference between the activation of the ignition and the intersection of the inflexion tangent with the 0 bar line; t_1 is duration of the combustion.

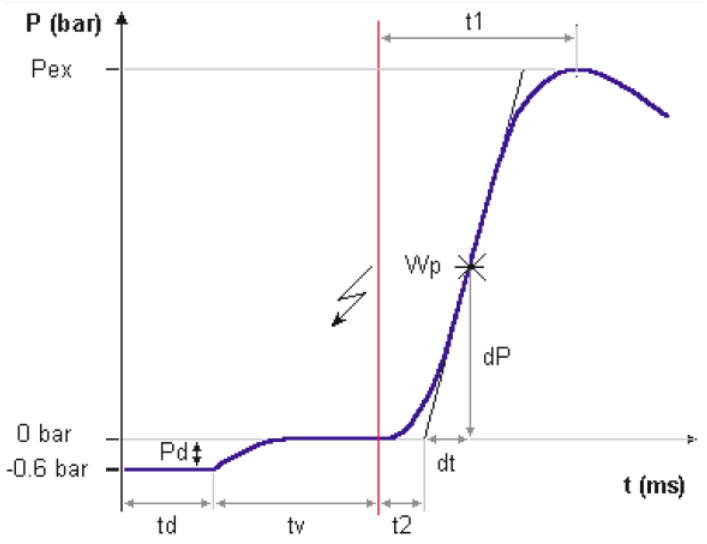

Figure 23 – Pressure/time-diagram of a fuel explosion [71].

Minor hardware modifications on KSEP 320 allowed to adopt different values of the spark delay time, t_v. This parameter is crucial because it determines the turbulence level when the spark is triggered. Ignition delay time, t_v, is defined as the time at which spark ignition is activated in respect to the time at which the pressure starts to rise in the sphere (onset of the dust dispersion).

4.2.2 Flame propagation tests

The tests are carried out setting test conditions as reported in Table 4.

Table 4 – Test conditions.

Test Conditions	
Ignition source	= Capacitive Electric Spark;
Ignition energy IE	= 30 mJ
Distance between electrodes	= 6 mm
Ignition delay time t_v	≈ 150 ms
Dispersion pressure P_z	= 5 barg
Initial Pressure, P_i	≈ - 0.2 barg

The experiments were performed with 30 mJ as ignition energy; and about 150 ms as ignition delay time.

The choice on t_v is justified taking into account the opposite effect of dispersion and turbulence of the dust. Varying this parameter, it is possible both to ensure an acceptable dispersion degree of the dust and to avoid a high grade of turbulence level. The choice of the E_i has been done considering that the value was neither so high to overdrive the system nor so low not to ignite the dust.

The dust is dried in a vacuum oven at 50 °C. After weighting of dusts, the sample dust is loaded in the hemispherical dispersion cup; then after closing the tube, vacuum is made in the tube until P_A = -0.6 bar.

During that time a mixture of 50% v/v air and 50% v/v gas is prepared in a separated pre-mixing bottle of 0.6 l. The mixture obtained is fed until the required pressure (P_B) in the tube. The suitable concentration is achieved by means of partial pressure method.

The values of set pressure at different gas concentrations are reported in Table 5.

Since the tube has an open end, (however closed by means of removable vent before ignition), the initial pressure inside the chamber at the moment of ignition has to be P_0 = -0.24 barg; to provide this value, the pressure in the tube before the entry of the air at 5 barg must be P_C = -0.33 barg.

Table 5 – Set pressures for preparation of gas/air mixture in the tube.

Fuel Gas $_{SET}$ ***(%v/v)***	P_A ***(bar g)***	P_B ***(bar g)***	P_C ***(bar g)***	P_0 ***(bar g)***
0.5	-0.60	-0.338	-0.33	-0.24
1	-0.60	-0.345	-0.33	-0.24
2	-0.60	-0.360	-0.33	-0.24
3	-0.60	-0.376	-0.33	-0.24
4	-0.60	-0.392	-0.33	-0.24
5	-0.60	-0.406	-0.33	-0.24
6	-0.60	-0.422	-0.33	-0.24

The experiments are controlled by using the electronics of the Hartmann tube as concerning the pulse of air necessary for the dispersion of the dust and the ignition system.

When outlet valve is opened, the dust comes into the tube through the mushroom nozzle producing a dispersion cloud. After ignition delay time, ignition starts and it's possible to see a flame propagation, that is recorded by the high speed video camera.

The method used in this work to determine the flame velocity is similar to that used by Proust [56] ('tube' method) [47].

This method is based on a direct visualization of the flame, following the displacement frame by frame of the recorded video.

When ignition starts, the flame grows and propagates; suddenly touches the wall and develops as planar flame. The flame velocity is calculated from the moment when the flame touches the wall until the moment in which the pressure inside the tube is such to open the valve at the top end of the tube; and it is evaluated point by point as first derivative of the displacement of the tip of the flame and then taking the media of these value.

4.3 MATERIALS

The gas/dust mixture used in this work is composed by methane and nicotinic acid. The behaviour of the single substances is well known as literature survey undoubtedly points out.

In the Table 6, some parameters and data are reported for the dust. As concern the explosibility parameters data are available from BGIA database [80] and NFPA 68 [16] and are related to an explosion occurred in 20 l Sphere chamber by means of 10kJ chemical igniters. Chemical – Physical data are, instead, taken from the MSDS given by Sigma-Aldrich.

Table 6 – Literature Properties of Nicotinic Acid.

Particle size [% by weight]	**<71 µm**	90
	<63 µm	-
	<32 µm	50
	<20 µm	10
	median value [µm]	~26
LEL [g/m^3]		30
P_{MAX} [bar]		8.3
K_{St} [bar m/s]		236
Explosibility Class		St 2
Ignition Temperature G-G [°C]		>365
Density [g/m^3]		1.473
Melting point [°C]		236.6
Boiling point [°C]		Sublimes
MIE [mJ]		1.7
Flash Point [°C]		193

For the dust it is possible to report a brief description as concern chemical nature and its utilizations; moreover, the results of tests to characterize its physical – chemical properties are presented.

The ***nicotinic acid*** is an organic compound known as Niacin (Vitamin B3), with the molecular formula $C_6H_5NO_2$ (Figure 24); it is supplied by Sigma Aldrich. It is used mainly in pharmaceutical industries and also is a reference dust for testing dust explosion.

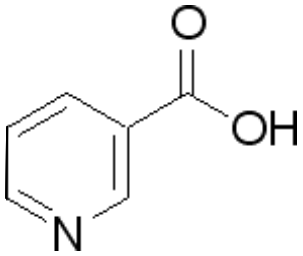

Figure 24 – Structural Formula of nicotinic acid.

Nicotinic acid has been characterized by laser diffraction granulometry using di-ethyl ether as the disperdant solvent (Malvern Instruments Mastersizer 2000); scanning electron microscopy (Philips mod. XL30); simultaneous TG/DSC analysis (TA Instruments SDTQ600).
Details of the granulometric distribution of the nicotinic acid are given in Table 7.

Table 7 – Granulometric distribution of nicotinic acid.

Percentile diameter (µm)	
D (0,1)	5.56
D (0,5)	32.00
D (0,9)	93.06
Surface weighted mean diameter (µm)	
D (3, 2)	14.37
Volume weighted mean diameter (µm)	
D (4, 3)	41.43

The sample structure has been analysed by means of scanning electron microscopy. SEM images of nicotinic acid, reported in Figure 25 at two different magnifications, show that the sample is composed of smooth-faced prismatic particles.

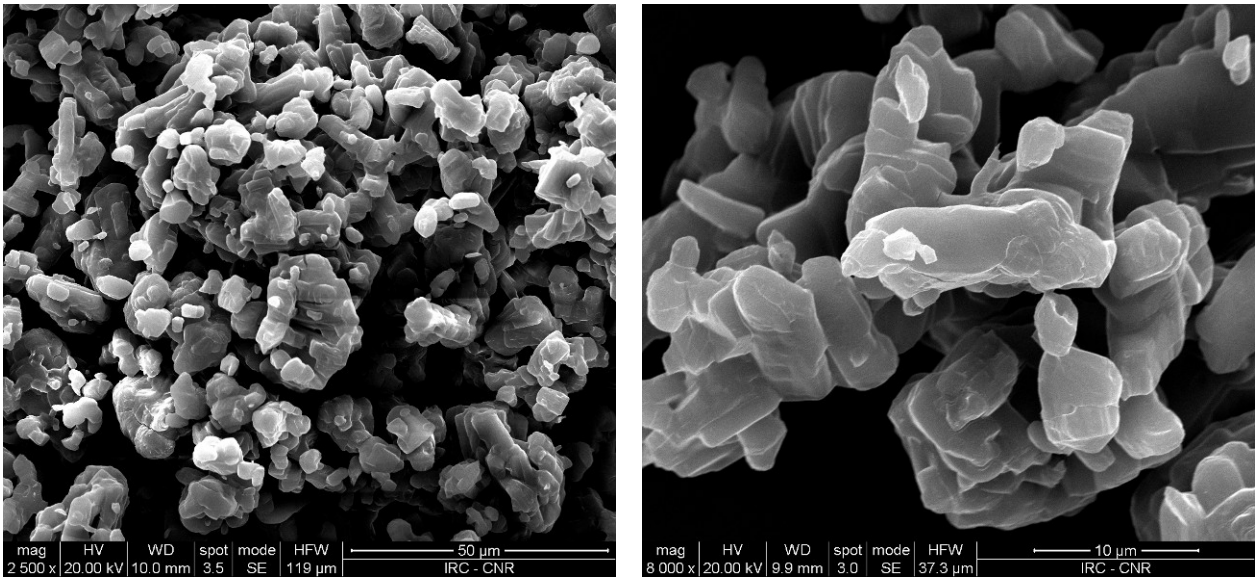

Figure 25 – SEM images of nicotinic acid at 2500x (left) and 8000 x (right) magnification.

The simultaneous TGA-DSC test (N_2 flow rate of 100 ml/min; heating rate of 20°C/min) carried out on the nicotinic acid sample pointed out the absence of moisture in the dust. Furthermore, in the explosion tests cylinder dry air rather than ambient air was used.
The complete combustion of the nicotinic acid is the following:

$$2\ C_6H_5NO_2 + 25/2\ O_2 \rightarrow 12\ CO_2 + 5\ H_2O + N_2 \qquad (1)$$

Methane was used as gaseous fuel. This choice is justified by the lower reactivity of methane in respect to the other fuel gases and to its limited range of flammability. Furthermore, to the aim at validating our experimental results, the wide scientific literature allowed to find a large amount of comparative data. In Table 8, some parameters and data are reported for the methane.

Table 8 – Explosibility parameters of the methane gas.

LFL [% by Vol.]	5
UFL [% by Vol.]	15
P_{MAX} [bar]	7.4
MIE [mJ]	0.29
K_G [bar m/s]	55
Flash Point [°C]	-188
S_u [m/s]	0.1-0.4
Ignition Temperature [°C]	580

4.4 REACTION MECHANISM FOR NICOTINIC ACID EXPLOSION

The hybrid mixture constituted by methane gas, nicotinic acid dust and air is an heterogeneous system. To the aim at elucidating the mechanisms governing the explosion process of these systems, a brief preliminary study on the dust explosion is mandatory.

Nicotinic acid is an organic compound. For this material, it was observed that the dust explosion occurs through different steps [81]:

- internal and external heating;
- pyrolysis/devolatilization;
- gas phase combustion.

All of these steps are mutually dependent and are strongly affected by the particle size. Di Benedetto et al. [81] studied this effect on the dust reactivity developing a model that takes into account all of the steps above mentioned. Varying the dust size, they identified different regimes depending on the values of the characteristic time of each step and several dimensionless numbers (Biot number, Bi; Damköhler number, Da; thermal Thiele number, Th).

This model can be applied to the dust explosion of nicotinic acid. According to Menon et al. [82], the pyrolysis/devolatilization of nicotinic acid can be assumed to occur in one step, the sublimation.

The used model is based on the approach that involves the kinetic mechanism of the sublimation process, inferred from thermo-gravimetric analyses, which allows the solid to decompose over a characteristic temperature range. One or more rate equations can be used to model the rate of change in mass of the small sample as a function of remaining mass and temperature. [81]

Starting from the solid, S, the only sublimation step (k) leads to the formation of volatiles, V:

$S \rightarrow V$

The mass balance equation considered in a dimensionless form is:

$$\frac{d\alpha}{dt} = k \cdot f(\alpha) \qquad (4.\ 1)$$

where α is the fraction reacted of the mass of solid particle (S), f(α) is the expression of the reaction mechanism and k is the reaction rate constant at a specific temperature.

Using the Arrhenius equation, k can be written as:

$$k = A \cdot \exp\left(-\frac{E_a}{R \cdot T}\right) \tag{4. 2}$$

where A is the pre exponential factor, E_a is the energy of activation, R is the universal gas constant and T is the temperature.

Starting from the thermo-gravimetric analysis, A and E_a were calculated assuming a kinetic of zero order ($f(\alpha) = 1$) as found by Menon et al. [82].

On the basis of the work of Di Benedetto et al. [81], it is necessary identifying the process controlling step by the use of dimensionless numbers defined as follows:

$$Bi = \frac{t_c}{t_e} = \frac{d \cdot \left(h_c \cdot \Delta T_i + \varepsilon \cdot \sigma \cdot \Delta T_i^4\right)}{\lambda \cdot \Delta T_i} \tag{4. 3}$$

$$Da = \frac{t_e}{t_{pyro}} = \frac{r_p \cdot \Delta T_i \cdot c_p \cdot d}{h_c \cdot \Delta T_i + \varepsilon \cdot \sigma \cdot \Delta T_i^4} \tag{4. 4}$$

$$Th = \frac{t_c}{t_{pyro}} = \frac{r_p \cdot c_p \cdot d^2}{\lambda} \tag{4. 5}$$

where t_c is the characteristic time of internal heat transfer, t_e is characteristic time of external heat transfer, t_{pyro} is characteristic time of pyrolysis reaction, d is the dust diameter, ΔT_i is the temperature difference between particle and surrounding gases, h_c is the heat transfer coefficient, ε is the emissivity, σ is the Stefan–Boltzmann constant, λ are the thermal conductivity of solid, r_p is the pyrolysis reaction rate, c_p is the specific heat.

On the basis of the values assumed by these number the controlled step can be established [81].

The pyrolysis kinetic and thermodynamic parameters for the nicotinic acid are reported in Table 9.

Table 9 – Pyrolysis kinetic and thermodynamic parameters for nicotinic acid.

Parameter	Value	Reference
ρ (kg/m^3)	1162	ChemCAD Software database
c_p (J/kg K)	1243	ChemCAD Software database
λ (W/m K)	1	ChemCAD Software database
A (1/s)	1.47 x 10^6	Experimental data
E_a (J/mol)	8.44 x 10^4	Experimental data

In Table 10 the Bi, Da and Th numbers are given as calculated for the nicotinic acid dust at the range of particle diameter of interest; moreover Pc, Da Pc, Th Pc, dimensionless numbers are reported too. The Pc numbers is defined as:

$$Pc = \frac{t_{pyro}}{t_{comb}} = \frac{\rho \cdot S_l}{r_p \cdot \delta_F} \qquad (4.\ 6)$$

where t_{comb} characteristic time of combustion reaction, δ_F is the flame thickness (typically, 1 mm) and S_l is the laminar burning velocity assumed equal to 2 m/s, which corresponds to a fully developed turbulent regime typical of the standard 1 m^3 and 20 l spheres.
This number is defined by Di Benedetto et al. [81] to compare the step controlling the pyrolysis process to the combustion rate of the volatiles.

Table 10 – Bi, Da and Th, Pc, Da Pc, Th Pc dimensionless numbers and pyrolysis regimes of nicotinic acid dust.

d (µm)	Bi	Da	Th	Pc	Da•Pc	Th•Pc	Pyrolysis Regime
5	0.12	3.63E+00	4.24E-01	0.17	6.19E-01	7.22E-02	I
10	0.13	1.36E+01	1.70E+00	0.17	2.31E+00	2.89E-01	I
15	0.13	2.89E+01	3.82E+00	0.17	4.91E+00	6.50E-01	I
32	0.15	1.14E+02	1.74E+01	0.17	1.94E+01	2.96E+00	I
45	0.17	2.07E+02	3.44E+01	0.17	3.52E+01	5.85E+00	I
75	0.19	4.92E+02	9.55E+01	0.17	8.37E+01	1.62E+01	I
93	0.21	7.00E+02	1.47E+02	0.17	1.19E+02	2.50E+01	I
100	0.22	7.87E+02	1.70E+02	0.17	1.34E+02	2.89E+01	I

From the value in Table 10, the pyrolysis regime, as defined by Di Benedetto et al. [81], can be identified. In this case the values are Bi<<1 and Da>>1. This implies regime I, that is the conversion occurs under the external heat transfer control.
Moreover, Pc<<1, this means that whatever the dust diameter value is, the pyrolysis reaction rate is faster than the gas combustion rate; also varying the S_l value between 0.1 – 2 m/s, Pc>>1.
For regime I with heat transfer control, the number Da·Pc has to be evaluated:

- for particle diameter lower than 10 µm, Da·Pc<<1;
- for particle diameter higher than 10 µm, Da·Pc>>1.

In the first case, this means that the gas combustion rate controls the overall explosion phenomenon; while, in second case, the external heat transfer is the controlling step of the explosion phenomenon. Since the used dust is constituted by a distribution between 5 – 100 μm, the overall process controlling the explosion phenomenon should be the external heat transfer.
This suggests that the explosion could be influenced by the supplied ignition energy from which the external heat depends.

Chapter 5 – Results and Discussions

In this framework, the efforts is that to clarify the synergetic effects of dust and gas in air during explosion. The approach is that of studying the behaviour of these mixtures as concern the explosibility and as concern the way in which the flame propagates.

5.1 EXPLOSIONS

In the first part, experiments related to study the effect of the turbulence are illustrated.
Then, the work has the objective to identify the explosion regimes for the gas/dust-air mixtures by using weak electric spark ignition. More specifically, the work is addressed to the quantification of the severity of explosion of hybrid mixtures in terms of maximum explosion pressure and deflagration index and to the definition of the most severe zones in the dust-gas concentration plane plot. Moreover, the effect of the ignition (different source and amount) and its link with turbulence were highlighted. Finally, the results of this work may be generalized and utilized as guidelines for estimating and predicting the performances of dust/gas mixtures from those of pure compounds.

5.1.1 Effect of the turbulence

These experiments were carried out varying the ignition delay time (60 ÷ 750 ms), at varying the gas content (6 ÷ 8.6% v/v) in mild ignition conditions, fixing the concentration of nicotinic acid at 30 g/m^3.
A compendium of entire set of results are reported in the Annexes in Table B. 1 and Table B. 2.
As measure of the turbulence, the r.m.s. of flow fluctuations, u', can be used.
Then, the ignition delay time was related to the r.m.s. of flow fluctuations using the experimental data of Dahoe et al. [83] who measured the turbulence level (velocity fluctuation, u') as function of time prior to ignition (ignition delay) in a 20 l explosion sphere (Figure 26).

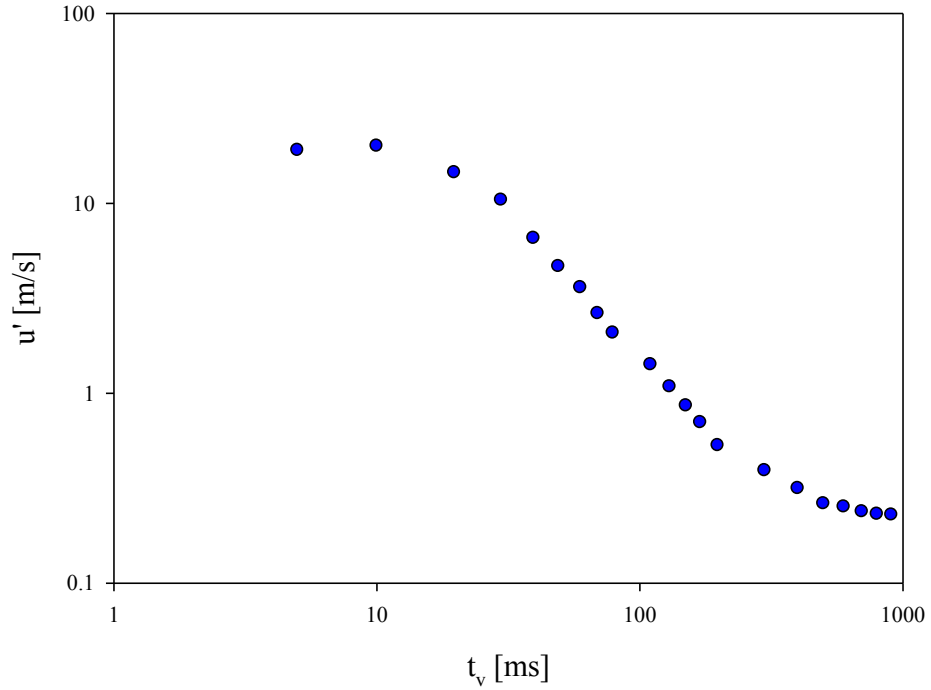

Figure 26 – Root-mean-square values of the velocity fluctuations in function of ignition delay time in the 20-liter sphere with rebound nozzle [83].

It was possible to study the effect of the turbulence level on the deflagration index of methane/nicotinic acid/air mixtures and on the burning velocity at varying the gas content.
The grade of turbulence can be express also in term of turbulent Reynold number, Re_t, by means of r.m.s velocity, u':

$$Re_t = \frac{\rho \cdot u' \cdot R_{sphere}}{\mu} \qquad (5.1)$$

where ρ and μ are respectively the density and the viscosity of the un-burned fuel; and R_{sphere} is the radius of the sphere vessel.
As pointed out in Figure 27; it's possible to observe that the presence of dust even if in concentration below its MEC induces an increase in the deflagration index of the hybrid mixture at every ignition delay time.

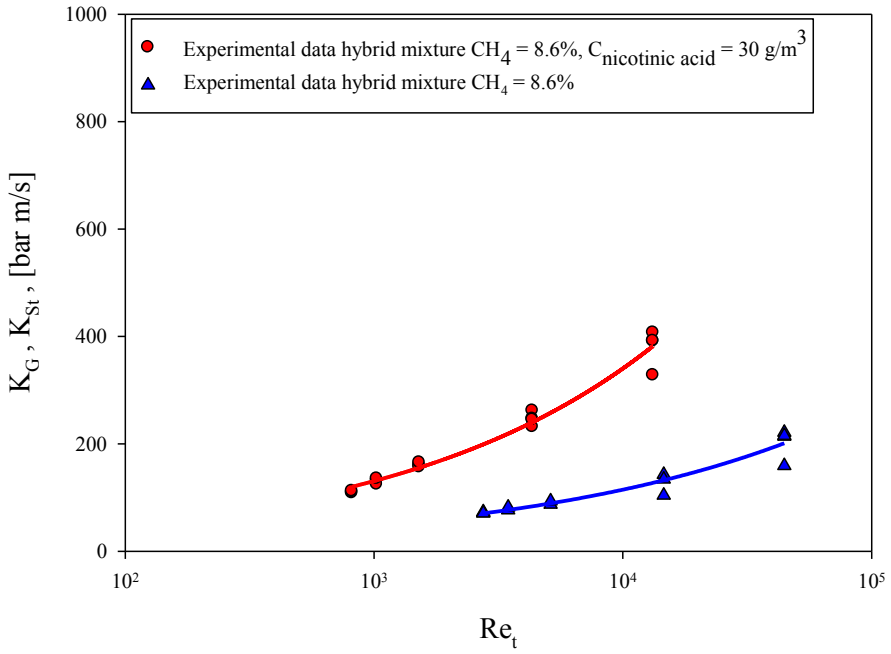

Figure 27 – Deflagration index for pure methane (8.6% v/v) and hybrid mixture of methane (8.6% v/v) and nicotinic acid (30 g/m^3) as function of Re_t.

As concern the burning velocity, it was computed from the measured pressure histories by using the equations by Dahoe et al. [84]-[86] which link the flame radius and the burning velocity to the pressure:

$$r_f = \left(\frac{3 \cdot V}{4\pi}\right)^{1/3} \cdot \left[\left(1 - \frac{P_0}{P}\right)^{1/\gamma} \cdot \left(\frac{P_{MAX} - P}{P_{MAX} - P_0}\right)\right]^{1/3} \tag{5.2}$$

$$S_l = \frac{1}{\left(P_{MAX} - P_0\right)} \cdot \frac{1}{3}\left(\frac{4\pi}{3 \cdot V}\right)^{-1/3} \cdot \left(\frac{P_0}{P}\right)^{1/\gamma} \left[1 - \left(\frac{P_0}{P}\right)^{1/\gamma} \cdot \left(\frac{P_{MAX} - P}{P_{MAX} - P_0}\right)\right]^{-2/3} \cdot \frac{dP}{dt} \tag{5.3}$$

In such equation, the dependence of the deflagration index on the turbulence level was estimated by substituting the laminar burning velocity (S_l) with the turbulent burning velocity (S_t) as function of the velocity fluctuation (u').

The burning velocity S_t was then calculated as function of the ignition delay time. The ignition delay time was related to the r.m.s. of flow fluctuations, as introduced in Figure 26.

The evaluation of the turbulent burning velocity as function of the turbulent fluctuations (u') was performed by using the formula available in the literature.

In Table 11 formulas available from literature for the turbulent burning velocity as function of the turbulence level are reported: formulas 1-3 were obtained for gas [87]-[89], formulas 4-6 for dust [90]-[92], while only formula 7 correlates both gas and dust data [93].
Such formulas depend on the turbulent combustion regimes in which the explosion is occurring.

Table 11 – Formulas of turbulent burning velocity.

N°	St (m/s)	Dust/Gas	Reference
1	$S_l \cdot \left(1+\left(\frac{u'}{S_l}\right)^2\right)^{0.5}$	Gas	Pocheau [87]
2	$S_l \cdot \left(1+2\cdot\frac{u'}{S_l}\right)$	Gas	Phylakotu et al. [88]
3	$S_l \cdot \left(1+\left(\frac{u'}{S_l}\right)^2\right)$	Gas	Clavin and Williams [89]
4	$S_l + 0.45u'$	Dust	Tezok et al. [91]
5	$S_l + Ku'$	Dust	Gieras et al. [90]
6	$S_l \cdot \left(1+1.65\cdot\frac{u'^{0.5}}{S_l}\right)$	Dust	Zhen and Leuckel [92]
7	$6.8\cdot S_l^{0.6} l_t^{0.15} u'^{0.15}$	Dust/Gas	van Wingerden et al. [93]

In all the formulas of S_t the laminar burning velocity is required. For both gas and hybrid mixtures, S_l is assumed equal to the laminar burning velocity of methane, which is in the range (0.15-0.4 m/s) for the methane concentrations investigated (6.0-8.6 % vol.) [83].
Figure 28 reports the experimental values of S_t/S_l, obtained by Eq. 5.3, as function of u'/S_l at different methane concentrations (6.0, 7.3 and 8.6% vol.). For comparison in the same figure the profile of turbulent burning velocity as function of r.m.s. velocity predicted by the formulas 1-3 in Table 11 relevant to gas are shown.
At low value of u'/S_l ratio (≤ 1) the turbulent burning velocity is well predicted by all the formulas; increasing turbulence the S_t given by formula of Clavin and Williams [89] increases much faster. The best agreement is found with the correlation proposed by Pocheau [87] (formula 1,Table 11).

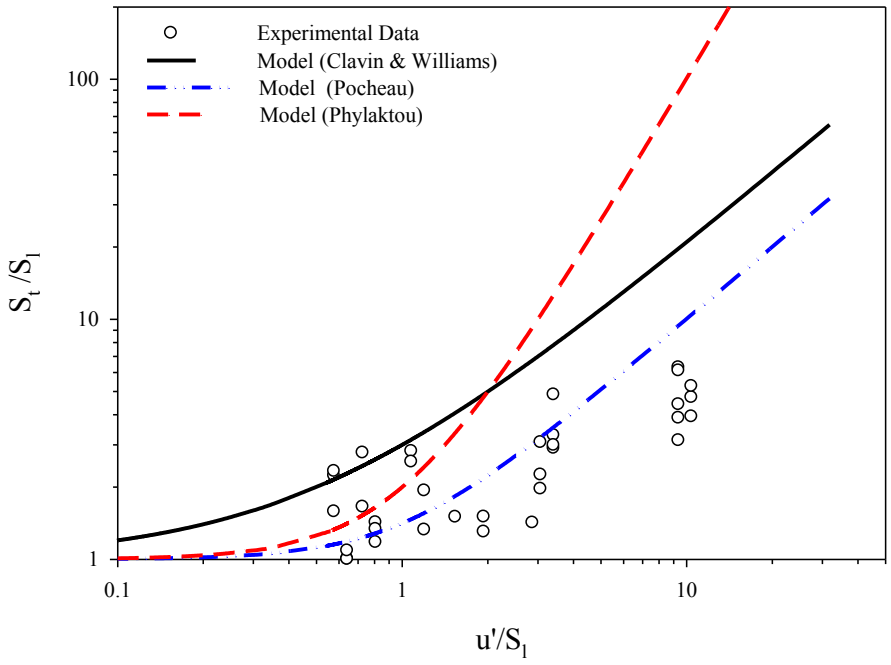

Figure 28 – Turbulent burning velocity (S_t/S_l) as function of u'/S_l for methane/air mixtures.

In Figure 29 to Figure 31 the values of S_t/S_l measured for methane/ nicotinic acid/air mixtures, at different methane concentrations, are shown as function of the turbulence level. The theoretical values obtained by using the formula in Table 11 are also given. In this case, the best agreement is found with the correlation proposed by Tezok et al. [91] (formula 4,Table 11).

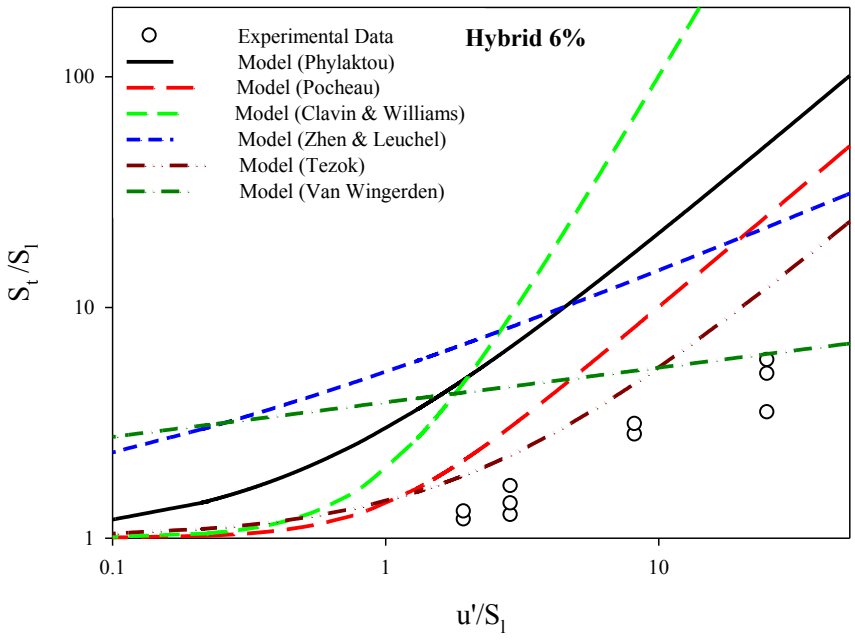

Figure 29 – Turbulent burning velocity (S_t/S_l) as function of u'/S_l for methane/nicotinic acid/air mixtures at different methane content: experimental (symbols) and correlations (lines).

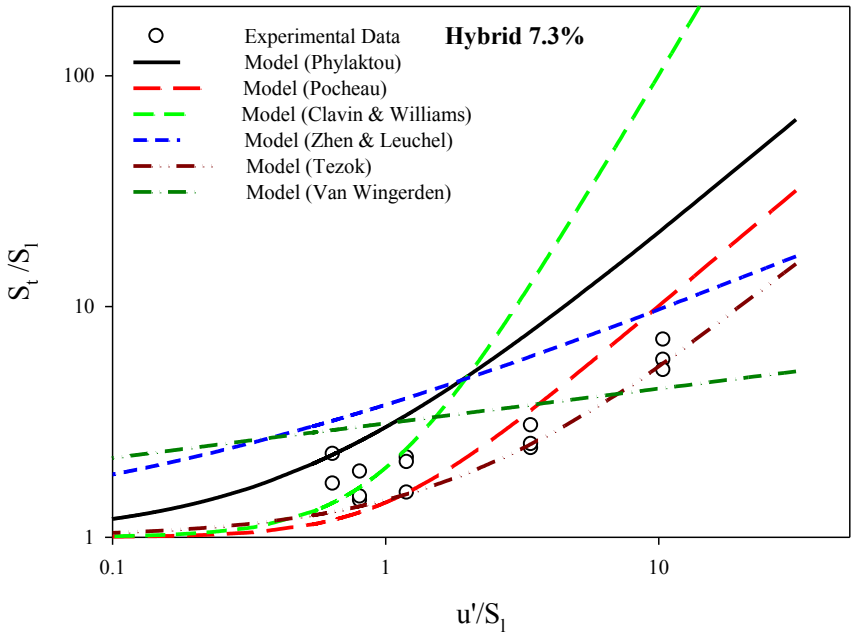

Figure 30 – Turbulent burning velocity (S_t/S_l) as function of u'/S_l for methane/nicotinic acid/air mixtures at different methane content: experimental (symbols) and correlations (lines).

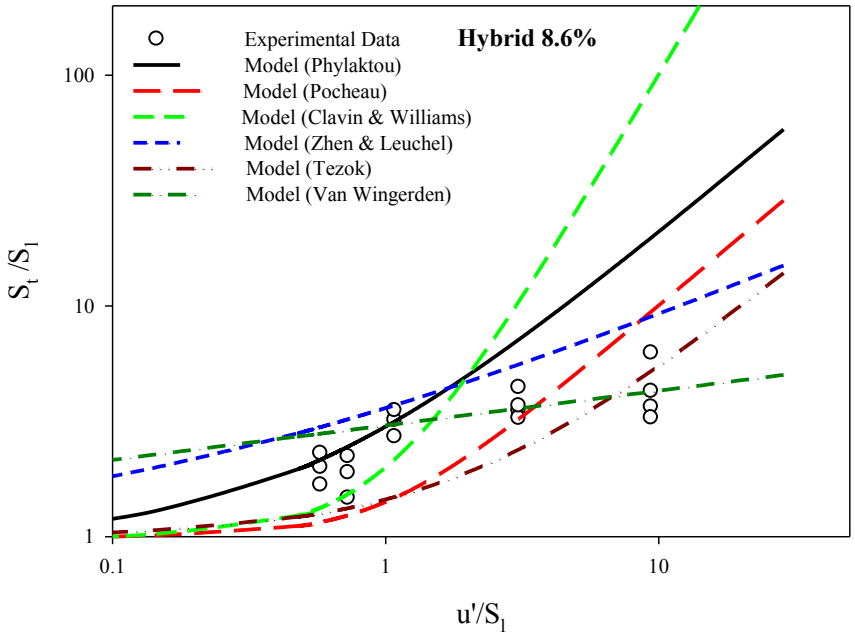

Figure 31 – Turbulent burning velocity (S_t/S_l) as function of u'/S_l for methane/nicotinic acid/air mixtures at different methane content: experimental (symbols) and correlations (lines).

Then, the deflagration index of methane was calculated by means of Eq. 2.3 and Eq. 5.3, using the formula 1 in Table 11 [87], which gives the best agreement with the experimental results Figure 28.

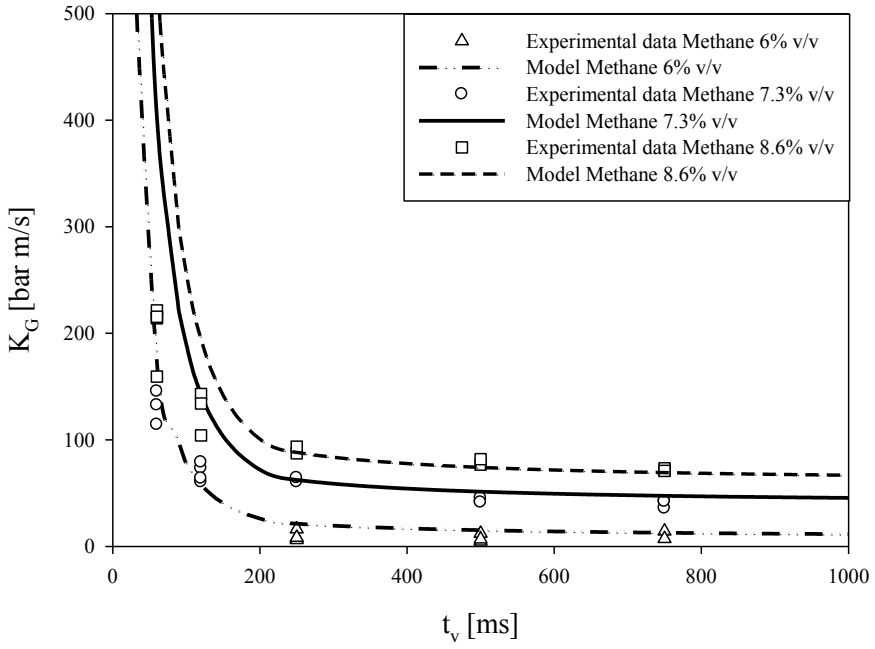

Figure 32 – K_G of methane as function of delay time: experimental (symbols) and model (lines).

In Figure 32 the deflagration index obtained by the model, using the formula 1 in Table 11 [87], for different methane concentrations is plotted as function of the ignition delay time. In the same figure K_G results from experiments are given.

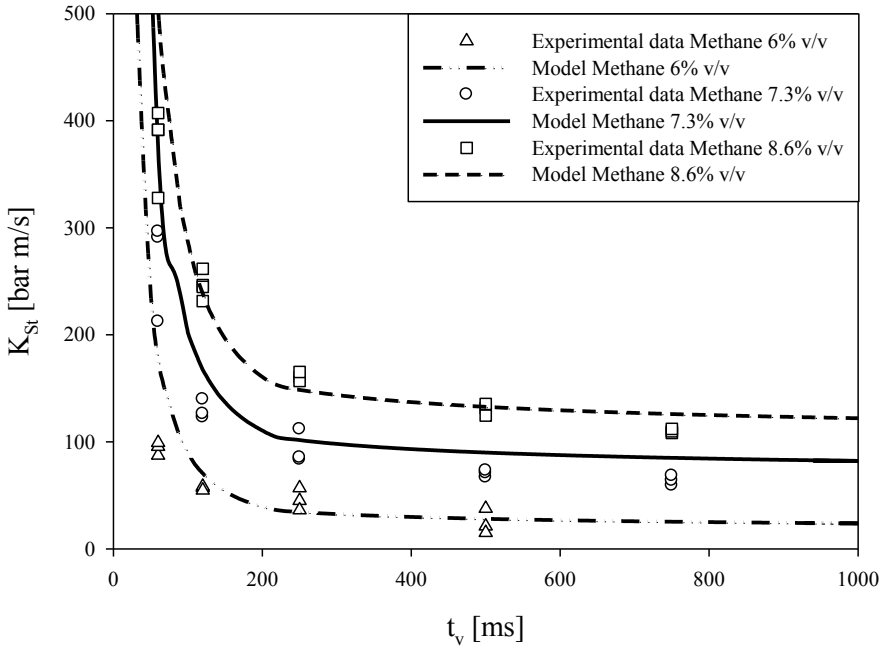

Figure 33 – K_{St} of methane/nicotinic acid mixtures as function of delay time: experimental (symbols) and model (lines).

In Figure 33 the experimental and model K_{St} values of methane/nicotinic acid/ air mixtures are reported as function of t_v. The model values were calculated by using the formula 4 in Table 11 [91] which gives the best agreement with experiments (Figure 29 - Figure 31).

From the results of Figure 32 and Figure 33 it turns out that for both, methane and methane/nicotinic acid explosions, the experimental deflagration index data are almost well predicted by the model especially at values of ignition delay time higher than 60 ms; while, at delay time lower than 60 ms the calculated values over predict the experimental data.

The comparison between deflagration index predicted by the model and the experimental values (t_v>60 ms) is shown in Figure 34 for both methane/air and methane/nicotinic acid/air mixtures. The agreement between calculated and experimental values is quite good (error=35%).

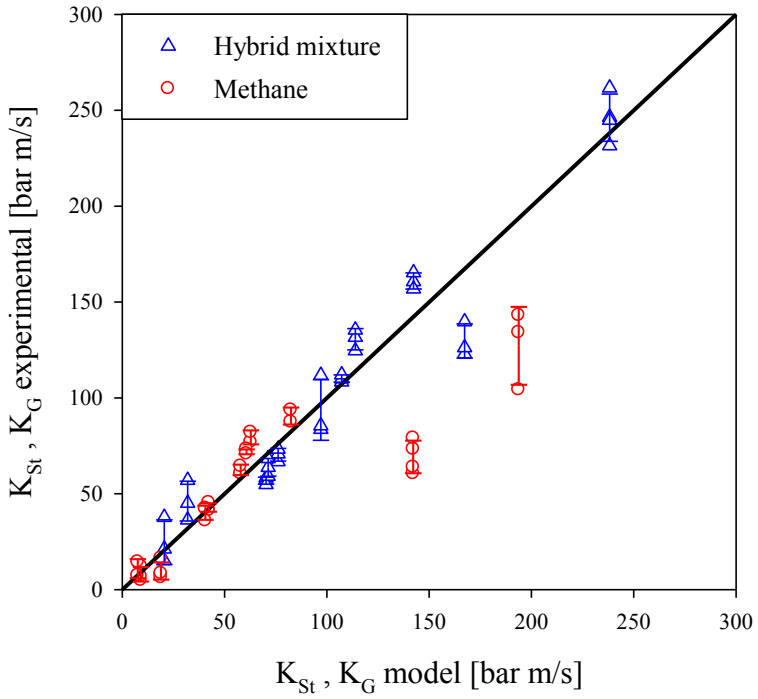

Figure 34 – K_G of methane and K_{St} of methane/nicotinic acid mixtures as calculated by the model as function of the experimental values.

5.1.2 Results: Electric Spark

These tests were all performed at $t_v = 0$. The explosion experiments were performed varying the methane concentration (v/v-%) in the range $1.0 \div 10$ % and for the nicotinic acid in the range $30 \div 250$ g m^{-3}

Experiments were carried out in triplicate: the standard deviation and the accuracy of the data are $P_{EX} \leq \pm 5$ % and $K_{St} \leq \pm 15$ %.

In the following the explosion results obtained in the equipment are reported for each fuel (methane and nicotinic acid) and then the results of the explosion behaviour of their mixture at changing the CH_4/nicotinic acid ratio are discussed. A compendium of entire set of results are reported in the Annexes in to Table B. 3 to Table B. 6.

5.1.2.1 Theoretical evaluation

The measured peak pressures of the mixtures dust/air and methane/air were compared with the theoretical adiabatic pressure. Such parameter was computed by means of the CEA (Chemical Equilibrium with Applications) thermo-equilibrium code [94].

Furthermore, the equilibrium volatile content and the volatile product distribution of nicotinic acid were calculated by using the CEA code.

The CEA code allows the calculation of the equilibrium conditions by minimizing Helmholtz energy at constant temperature and volume; or by minimization of Gibbs free energy, for the chemical equilibrium at constant temperature and pressure.

5.1.2.2 Methane explosion

The explosion behaviour of methane has been widely studied and it is well known in the literature.

Even so, papers dealing with the explosion behaviour measurements of methane/air mixtures in the standard conditions of dust/air explosion in the 20 l bomb are few and are performed at quiescent conditions [95]-[98].

In the present work the ignition of methane/air mixtures was performed at the same conditions as the dust runs (gas mixture injection and $t_v = 0$; spark ignition) in order to allow the comparison between the pure fuel behaviour and the gas/dust-air behaviour.

In Figure 35 the history of explosion pressure recorded in a series of tests carried out on pure methane varying the concentration is shown. For these experiments, the ignition is triggered when the pressure starts to increase in the sphere. The ignition process starts with a certain delay in respect to the energy release. This induction period depends on the type of ignition system adopted. In the case of electric spark, the energy is much lower than that released using the standard chemical igniters. In the case of electric spark, the induction time is longer than in the case of stronger energy like that of chemical igniters. In the next section, this phenomenon will be described.

Starting from the Figure 35, the diagram of Figure 36 is obtained.

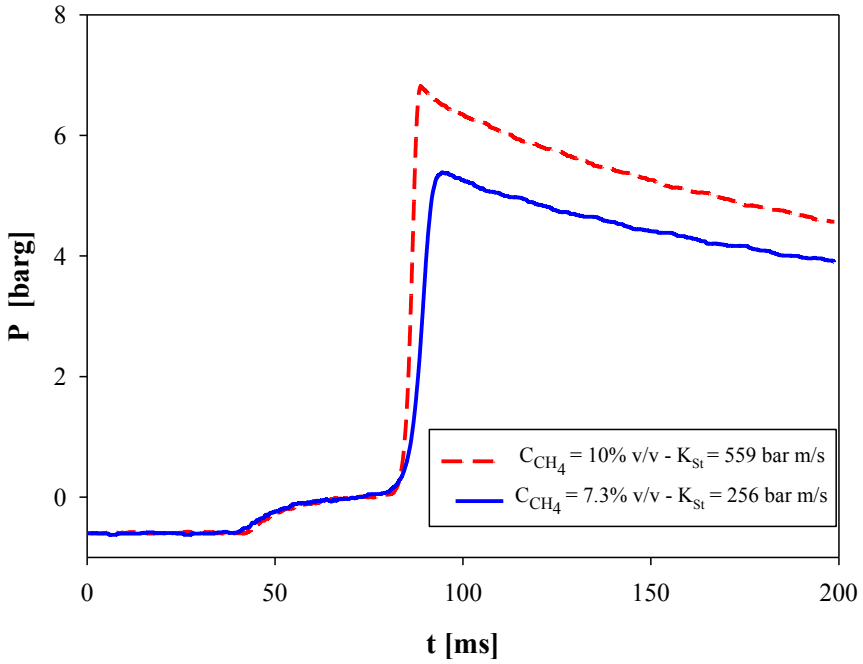

Figure 35 – Explosion pressure vs. time for methane at $t_v = 0$.

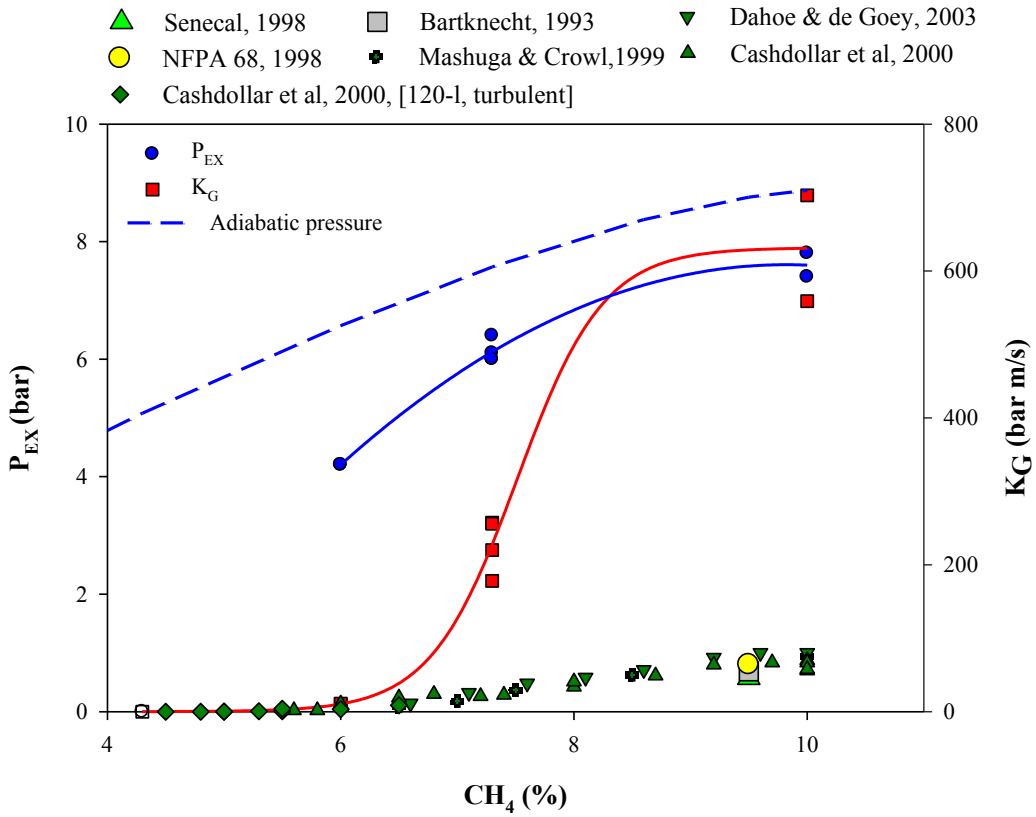

Figure 36 – Maximum explosion pressure and deflagration index as a function of methane concentration. K_G of methane from experiments (spark ignition, $t_v = 0$) and literature data.

Figure 36 shows the maximum pressure and the deflagration index as measured for the methane-air explosion with respect to the fuel concentration. The literature data for the deflagration index as reported by Senecal [98], Bartknecht [99] and NFPA [16] are also given. These values were obtained in apparatus different from the 20 l spherical bomb and are significantly lower than those found in our experiments.

The data of the deflagration index from Dahoe & de Goey [95], Cashdollar et al. [96] and Mashuga & Crowl [97] are also shown, but a significant difference is found due to the highly turbulent conditions, which establish inside the bomb at a delay time $t_v = 0$ used in the present work.

The adiabatic pressure as calculated by means of the CEA code is also shown. The calculated values are higher than the peak pressure measured due to the effect of heat losses.

5.1.2.3 Nicotinic acid explosion

Considering the complete combustion of the nicotinic acid, it is possible to calculate the stoichiometric dust concentration, which results in C = 168 g/m^3.

Some tests were carried out at different concentrations; in Figure 37 some typical pressure curves are shown; in this way it's possible to appreciate the differences varying the concentration of the dust.

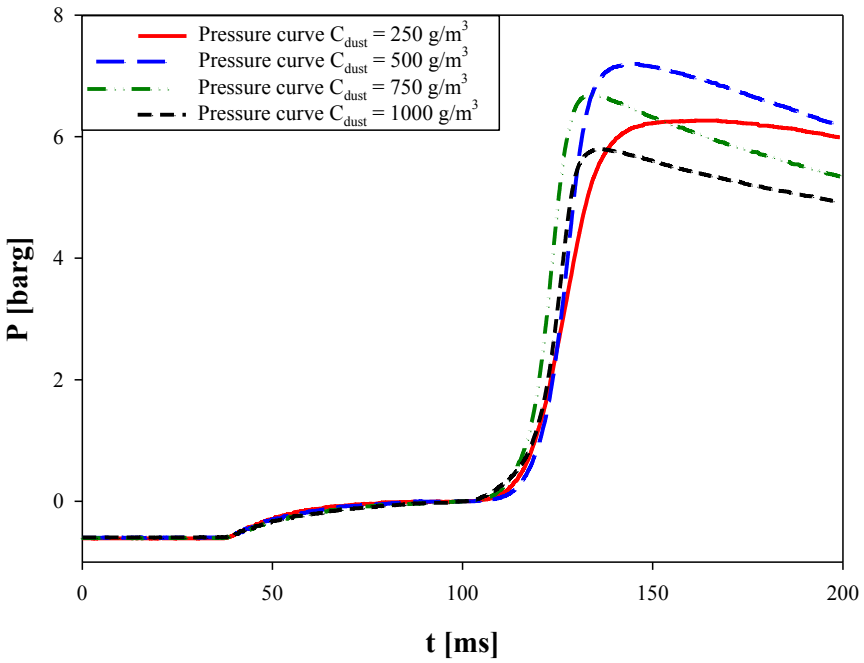

Figure 37 – Explosion pressure vs. time varying concentration of nicotinic acid at $t_v = 0$.

In Figure 38 the maximum pressure ($P_{EX,}$) attained in the sphere and the deflagration index (K_{St}) are shown as a function of the dust concentration. It appears that the maximum value of both P_{EX} and K_{St} is attained at about C = 600 g/m^3, which is much higher than the calculated stoichiometric value, C = 168 g/m^3. These data are similar to those found in the literature [37],[100]-[102] and reported in Table 12.

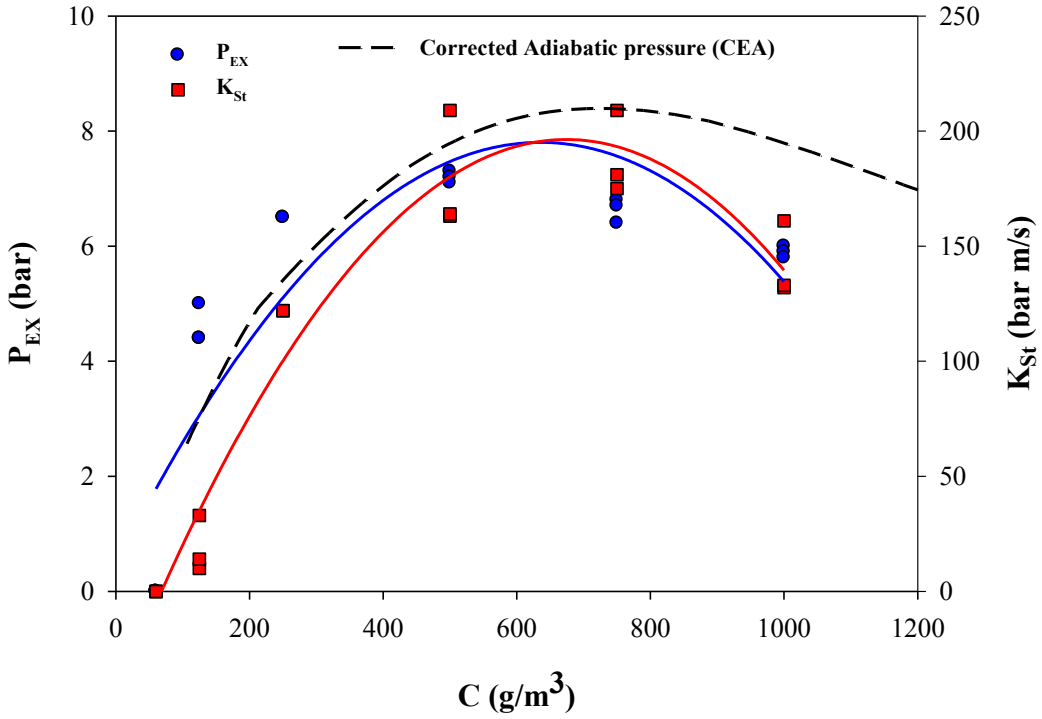

Figure 38 – Maximum explosion pressure and deflagration index as a function of the dust concentration. (Nicotinic acid, spark ignition, $t_v = 0$).

Table 12 – Literature data of nicotinic acid.

P_{max} (bar)	K_{St} (bar m/s)	MEC (g/m^3)	C@ max (g/m^3)	Ignition	Ref.
8.4	214	60	500	2x 5 kJ	[37]
8.0 ± 10%	241 ± 10%	-	520 (P_{max}) 690 (K_{st})	2 x 5 kJ	[100]
8.1 ± 10%	232 ± 10%	-	680 (P_{max}) 880 (K_{st})	2 x 5 kJ	[101]
8.3 ± 10%	236 ± 10%	-	-	2 x 5 kJ	[102]
7.2 ±5%	179 ± 15%	125	600	spark	this work
7.9 ±1%	275 ± 7%	-	500	2 x 5 kJ	this work

In a previous paper Di Benedetto and Russo [103] showed that the explosion of dust can be modelled as the explosion of its volatiles. In order to get insights into this difference, the thermodynamic distribution of the volatiles of nicotinic acid was calculated by using the CEA code. In this regard, it was found that in the range of temperatures from 700 °C to 1800 °C the volatile content ranges from 25 % up to 26 % in weight. This result definitely agrees with the ratio between the stoichiometric dust concentration and the value at which the maximum pressure and deflagration index occurs (168/600 ≈ 0.28). In the following the experimental data are compared with the thermodynamic values estimated at the respective equivalent dust concentration C_{eq} calculated as follows:

$$C_{eq} = \frac{C}{f} \tag{5.4}$$

where C is the experimental concentration, and *f* is the fuel volatiles content of nicotinic acid in the temperature ranges of interest (*f* = 0.26). The factor *f* is here defined as the dust "equivalent" concentration, according to the volatile content.

In the experimental conditions of this work it was found that the Minimum Explosive Concentration (MEC) of the nicotinic acid is equal to 125 g/m^3. This value is higher than those found in the literature (Table 12); this difference is probably related to the weak ignition here used (spark ignition instead of chemical igniters).

In Figure 38 the adiabatic pressure as computed by CEA is also showed. These data are shifted in the concentration range by the factor *f* (Eq. 5.4).

5.1.2.4 Explosion of Nicotinic acid/Methane air mixtures

The explosion behaviour of the methane/nicotinic acid mixture in air has been investigated in the conditions close to the minimum concentration values of both methane (1 % up to 10 %) and nicotinic acid (30 g/m^3 up to 250 g/m^3).

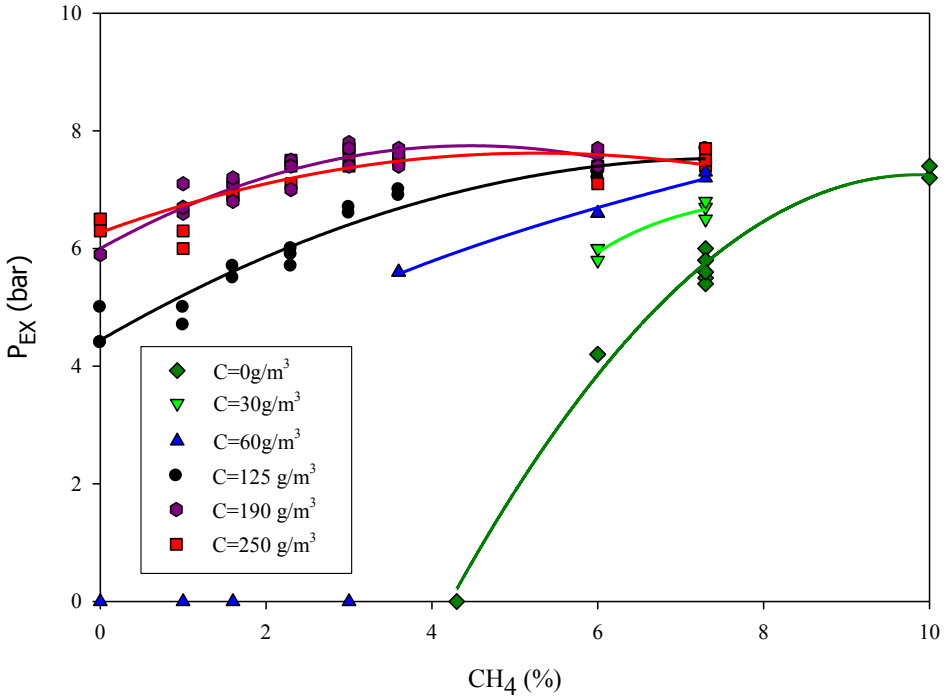

Figure 39 – Maximum pressure as a function of the methane content at different values of the nicotinic acid concentration (spark ignition, $t_v = 0$).

In Figure 39 the maximum pressure is plotted vs. the methane concentration at varying the nicotinic acid concentration in the range C = 0 – 250 g/m^3.

When the dust concentration is lower than MEC = 125 g/m^3 (C = 0, 30 and 60 g/m^3), ignition is observed at CH_4 concentration higher than 3.6 %. On further increasing the methane content the mixture is ignited, even if both the fuels are below their flammability (or explosibility) limits.

At MEC = 125 g/m^3, the maximum pressure is slightly dependent on the methane content. At higher values of dust concentration (190 – 250 g/m^3) the maximum pressure seems to be almost independent on the methane content.

From these results it appears that when methane concentration is lower than lower flammable limit (LFL) the thermodynamic parameters become less sensitive to the methane content when dust concentration goes from non-flammable concentration (C < MEC) to flammable concentration (C > MEC).

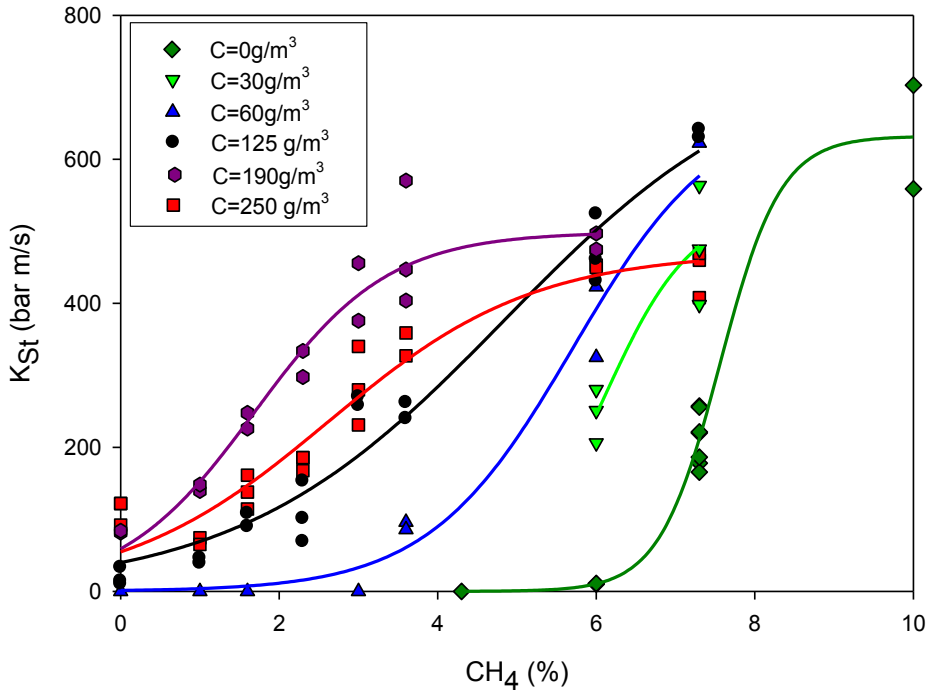

Figure 40 – Deflagration index as a function of the methane content at different values of the nicotinic acid concentration (spark ignition, $t_v = 0$).

In Figure 40 the corresponding data of the deflagration index are given. The results plotted suggest that in the range of concentrations investigated, the presence of methane in a cloud of nicotinic acid makes the dust more violent and reactive than the pure nicotinic acid. Conversely, in the conditions here investigated, it seems that the methane/air mixture explosions (C = 0) are much more severe than that of the methane/nicotinic acid/air mixtures.

At dust concentrations below the MEC (C = 30 and 60 g/m^3), the nicotinic acid alone is unable to ignite, but the presence of methane activates the explosive reaction. At dust concentration equal to the MEC (C = 125 g/m^3), the presence of methane has a significant impact on the violence of explosion: the deflagration index increases (from 20 to 470 bar m/s) about 20 times when increasing the methane content from zero up to the LFL (6 %).

At values of the dust concentration higher than the MEC value (C = 190 and 250 g/m^3), the presence of methane increases the violence of explosion, but its influence is less significant (the deflagration index goes from 80 up to 490 bar m / s and 120 up to 410 bar m / s respectively). As a result, the sensitivity of nicotinic acid/methane/air mixtures to methane content in the non-flammable region of methane (< LFL) decreases when the dust concentration is in the flammable region.

It is worth noting that an inversion occurs: at dust concentration higher than MEC and at low values of the methane content, the highest value of the deflagration index is at the lowest dust

concentration; conversely, at high values of the methane content, the highest value of the deflagration index is at the lowest value of the dust concentration.

From these results it can be concluded that methane and nicotinic acid show comparable thermodynamic pressure and temperature (Figure 39). In the opposite, the kinetic behaviours (Figure 40) are quite different.

Moreover, in these work experiments, it has been found that it is possible to have explosive mixtures also considering concentrations of methane and nicotinic acid below their lower explosion limits. A possible explanation could be that nicotinic acid is an organic volatile dust and the reaction happens effectively in an homogeneous phase. The devolatilized substance of the dust mixes together with methane gas contributing to enhance the combustible fuel whose mixture has a concentration that falls in the range of flammability.

5.1.2.5 Nicotinic acid/methane/air explosion regimes

In order to rationalise all the data, the map of the explosion behaviour of the CH_4/nicotinic acid/air mixtures is developed, where methane content (vol% / LFL) and dust concentration (C / MEC) are respectively the x and y-axes (Figure 41).

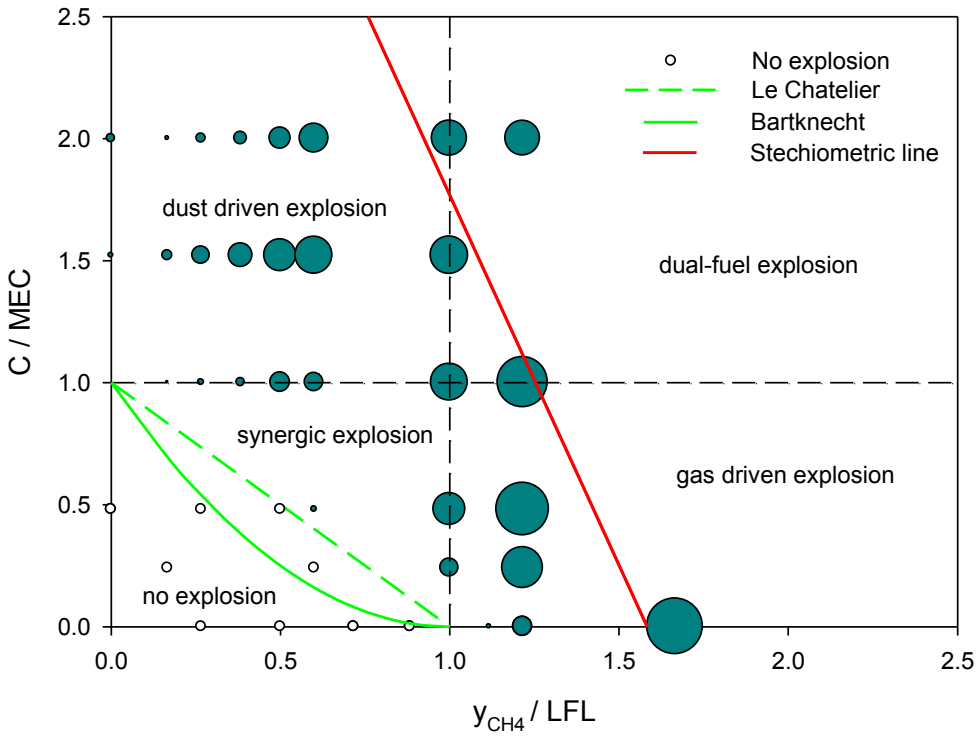

Figure 41 – Explosion regimes in the plane methane content/nicotinic acid concentration.

In the figure, the measured data of the deflagration index are represented by the solid circles whose diameter increases proportionally to the value of K_{st}. White circles refer to experiments where explosion does not occur.

In the same figure, Le Chatelier's line and Bartknecht curve are also shown. These curves delimit the explosive vs. the non-explosive region. Finally, the stoichiometric line (red curve) is also plotted. The equation of this line is the following:

$$\frac{C}{MEC} = 4.8 - 3.03 \cdot \frac{y_{CH_4}}{LFL} \tag{5.5}$$

The white circle symbols lay all below Le Chatelier's line, which limits the non-flammable zone. All the other points represent explosion conditions. Le Chatelier's line well separates the explosive from the non-explosive region since as shown in Figure 41, the adiabatic pressure of methane/air and nicotinic acid/air mixtures (and then temperature) are quite similar.

In the plot of Figure 41, five zones may be identified. The no-explosion zone lays below Le Chatelier's curve.

Above this line the synergic explosion behaviour zone is present. This zone is limited by Le Chatelier's curve and the LFL and MEC lines.

The dust (fuel) driven explosion zone is the region in which the dust (fuel) concentration is higher than the MEC (LFL) and the methane (dust) concentration is lower than the LFL (MEC).

Finally, the dual-fuel explosion zone is above both LFL and MEC concentrations. In this zone both methane and nicotinic acid contribute to the explosion.

From the data of Figure 41 it appears that the maximum values of the deflagration index lay close to the stoichiometric line. When approaching this line the diameter of the solid circles increases. It is also worth noting that in the region where the oxygen is controlling the kinetics of explosion, the diameter of the circle is almost insensitive to both the dust and methane concentrations.

5.1.3 Results: Chemical Igniters

These tests were performed both in quiescent condition (only for the gas) and in turbulent condition with t_v = 60 – 120 ms . The explosion experiments were performed varying the methane concentration (v/v-%) in the range 3.6 ÷ 7.3 % and for the nicotinic acid in the range 30 ÷ 60 g m^{-3}.

Experiments were carried out in duplicate: the standard deviation and the accuracy of the data are $P_{EX} \leq \pm 5$ % and $K_{St} \leq \pm 20$ %.

In the following the explosion results obtained in the equipment are reported for each fuel (methane and nicotinic acid) and then the results of the explosion behaviour of their mixture at changing the CH4/nicotinic acid ratio are discussed. A compendium of entire set of results are reported in the Annexes in the Table B. 7 to Table B. 9.

5.1.3.1 Methane explosion

The ignition of methane/air mixtures is performed at the quiescent conditions using the chemical igniters with an energy of 500, 1000 and 10000 J. Moreover, in order to allow the comparison between the pure fuel behaviour and the gas/dust-air behaviour, experiments were also performed in turbulent conditions varying the ignition delay time, t_v, as the dust runs.

As previously said, the explosion behaviour of methane has been widely studied and it is well known in the literature. In Figure 42, a comparison between experiments performed in quiescent conditions with the 1000 and 10 kJ chemical igniters with some literature data [95]-[97],[104] (quiescent conditions and spark) are shown. Due to mild condition of the methane explosion for these concentration value, the value obtained are well comparable, even if different types of ignition are used.

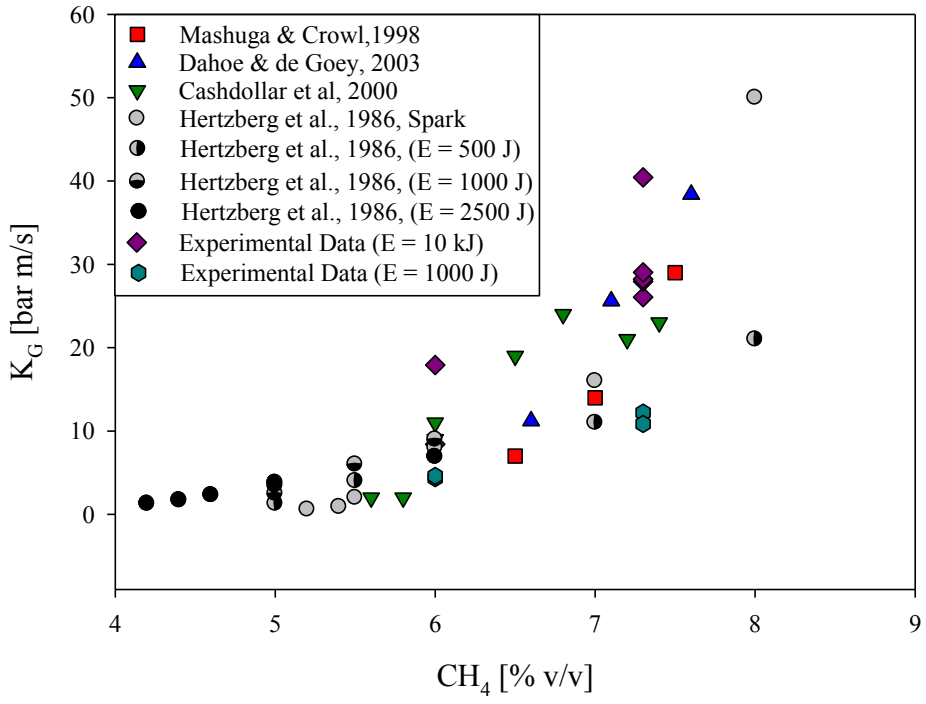

Figure 42 – Deflagration index as a function of methane concentration. K_G of methane from experiments (E = 1000 J - 10 kJ) and literature data in quiescent condition.

Hence, the effect of the turbulence level and of the ignition source were studied varying the methane concentration. The effect of the turbulence was analysed performing experiments varying the ignition delay time. As observable from the Figure 43, passing from quiescent condition, represented at very high value of ignition delay time, t_v, to more turbulent condition, the violence of the explosion, represented by the dimension of the circles, increases. This increase is more remarkable as methane concentration increases. The effect of the ignition energy, on the other hand, was analysed using electric spark (low energy level) and chemical igniters of different size (500, 1000, 10000 J). As the energy level increases deflagration index, K_G, increases slightly. The major difference in the deflagration index, K_G, is observable between the different ignition source, electric spark and chemical igniters.

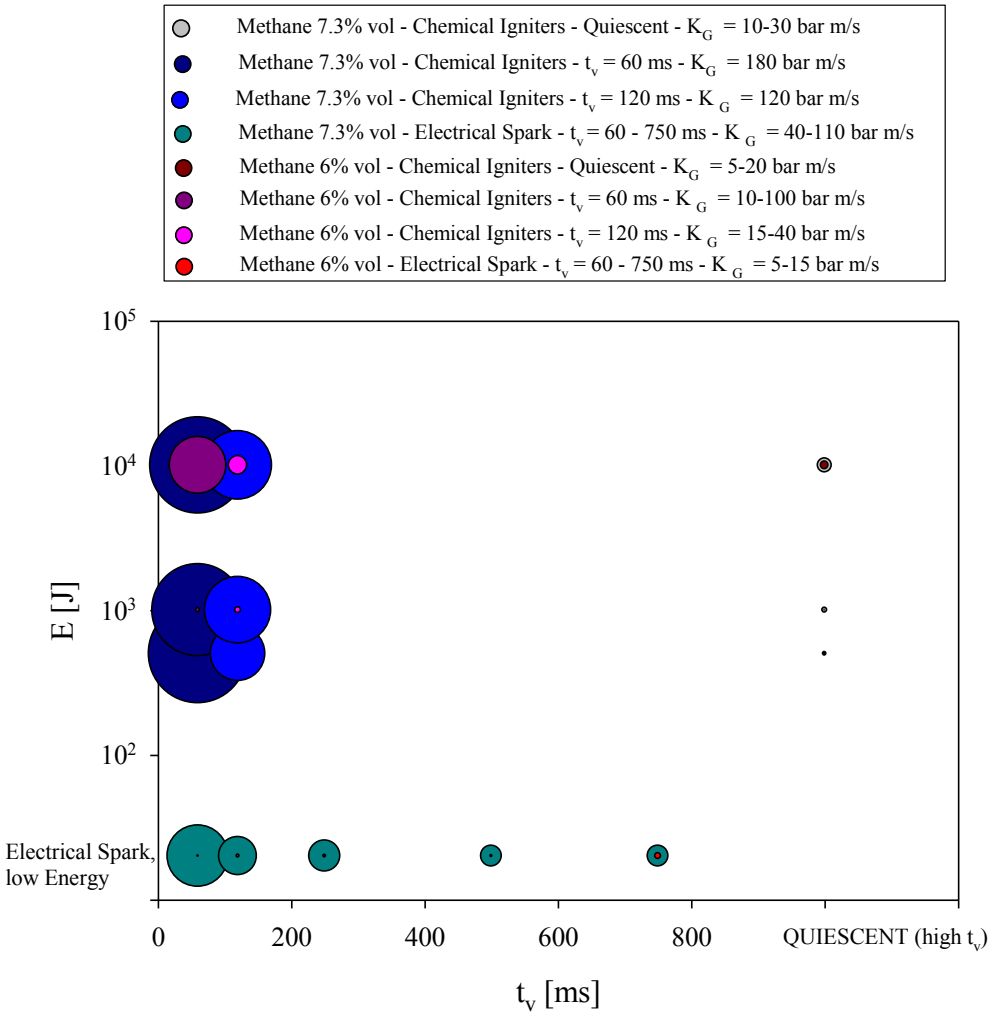

Figure 43 – Effect of the turbulence and of ignition energy on the deflagration index, K_G, of methane explosion. The dimension of the circles is proportional to K_G.

5.1.3.2 Nicotinic acid explosion

Other tests were carried out for pure nicotinic acid. In this case, the chemical igniters with an overall energy of 10 kJ, t_v = 60 ms were used in accordance with ASTM Method E 1226 [17].

Figure 44 and Figure 45 show the comparison between the maximum explosion pressure and the deflagration index with respect of concentration of nicotinic acid obtained from tests, either with 10 kJ chemical igniters or electric spark as ignition source.

As it's possible to see in the Figure 44 and Figure 45, the diagram has the typical behaviour of dust explosion as pointed out by many cases in literature; moreover, the explosion obtained with chemical igniters as ignition source are more reactive than that obtained with electric spark. In fact, in the tests performed with 10 kJ chemical igniters the maximum value of K_{St}, which is reached for a concentration of 500 g/m^3, is about 280 bar m/s against the maximum value reached for tests performed with electric spark of about 160 – 200 bar m/s at the same dust concentration. This is substantially due to the different modality of energy supply to the system: in the case of chemical igniters the overall energy is release to the system instantaneously; instead, in the case of electric spark the overall energy is released over a long interval of time.

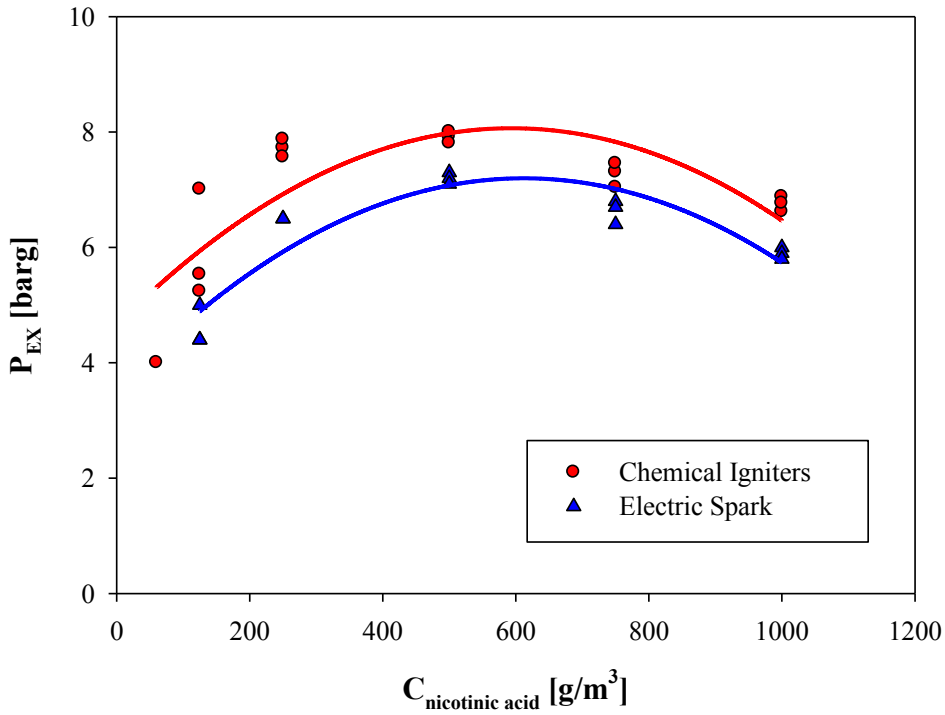

Figure 44 – Comparison of Maximum explosion pressure vs. nicotinic acid concentration between Chemical Igniters and Electric Spark as Ignition Source.

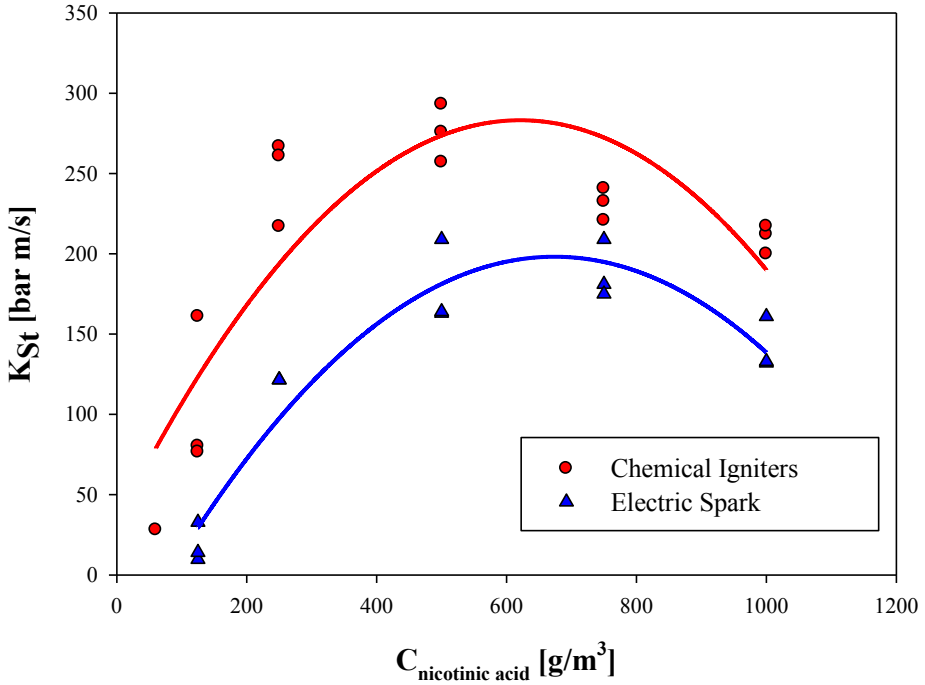

Figure 45 – Comparison of Deflagration Index vs. nicotinic acid concentration between Chemical Igniters and Electric Spark as Ignition Source.

As it is shown in Fig. 45, the use of the different ignition systems (chemical igniters or electric spark) determine different values of the MEC (minimum explosion concentration). In fact, for the lower ignition source of the electric spark, the concentration of nicotinic acid of 60 g/m^3 doesn't ignite, while at this value of concentration, the explosion is possible with chemical igniters of 10 kJ. Moreover, the effect of the turbulence and ignition energy was studied for a dust concentration of 60 g/m^3. In Figure 46 the effect of the turbulence is shown: as the turbulence decreases (higher t_v value), the explosion becomes less violent. As concern the effect of ignition energy, experiments were also carried out with different amount of energy (1000, 10000 J). The explosion didn't occur with the lower ignition energy (1000 J) and also with electric spark ignition.

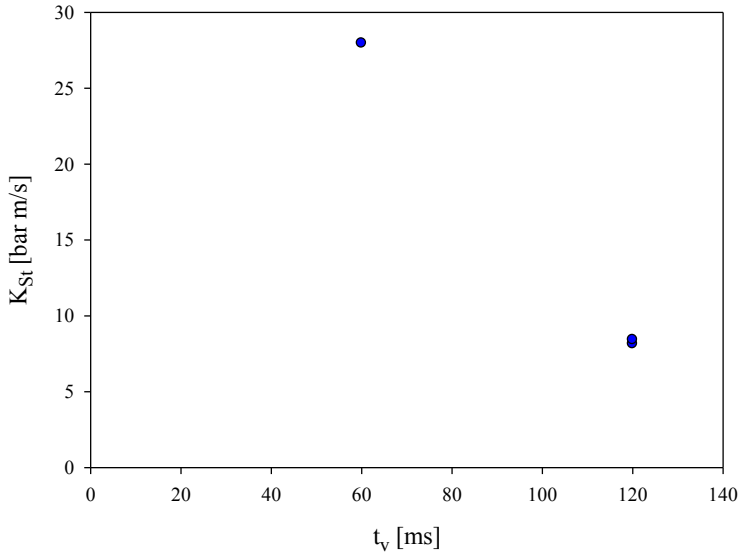

Figure 46 – Effect of turbulence on the dust explosion of 60 g/m^3 of nicotinic acid performed with 10 kJ chemical igniters.

5.1.3.3 Explosion of Nicotinic acid/Methane air mixtures

The explosion behaviour of the methane/nicotinic acid mixture in air was investigated in the conditions close to the minimum concentration values of both methane (6 %) and nicotinic acid (30 - 60 g/m^3). Also in this case, the effect of the turbulence level and of the ignition energy was evaluated. Same considerations as for the methane case can be done: as the turbulence decreases, the K_{St} value decreases; increasing the ignition energy, slight increase of the K_{St} is observable for the case of hybrid mixture constituted by 6% vol. of methane and 60 g/m^3 of nicotinic acid. Instead, for the other case (6% vol. of methane and 30 g/m^3 of nicotinic acid) the increase of the K_{St}, as the energy increase, is more pronounced and the mixture results more sensitive to the ignition energy. This is essentially due to the poorer fuel mixture. Moreover, in Figure 47 and Figure 48, the results of these experiments are shown.

The resultant explosion of hybrid mixture of methane and nicotinic acid is much more violent than the explosion of the pure components, if compared with that of pure components.

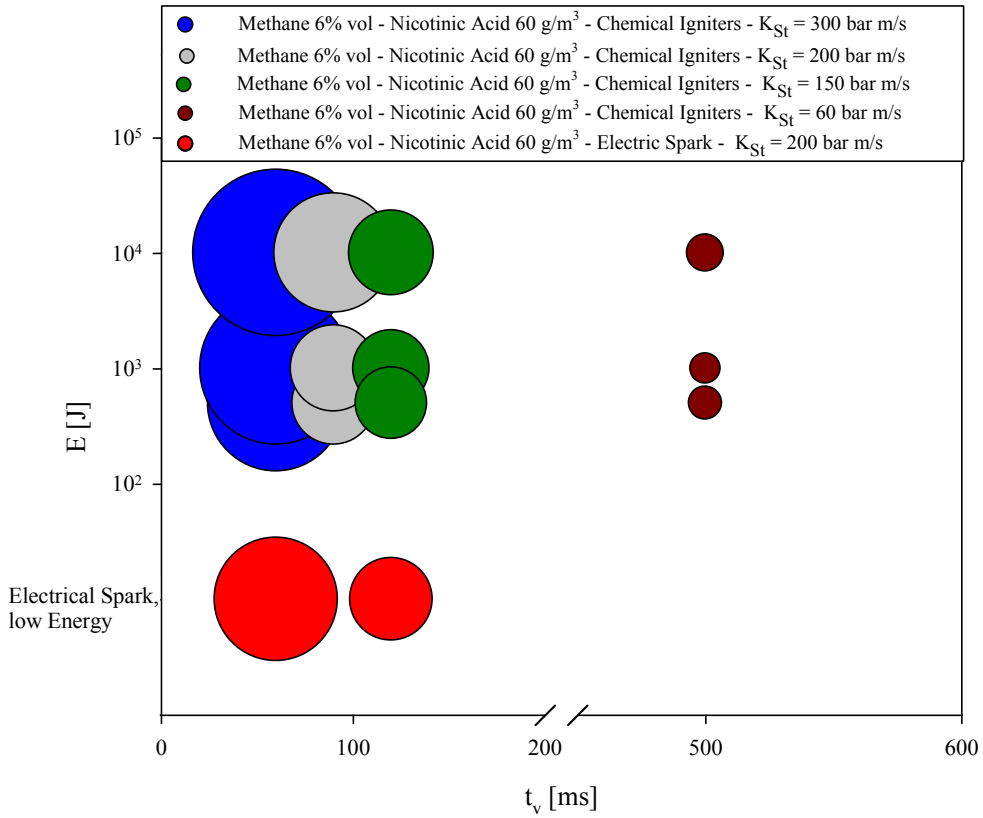

Figure 47 – Effect of the turbulence and of ignition energy on the deflagration index, K_{St}, of a mixture of 6% vol of methane and 60 g/m^3 of nicotinic acid. The dimension of the circles is proportional to K_{St}.

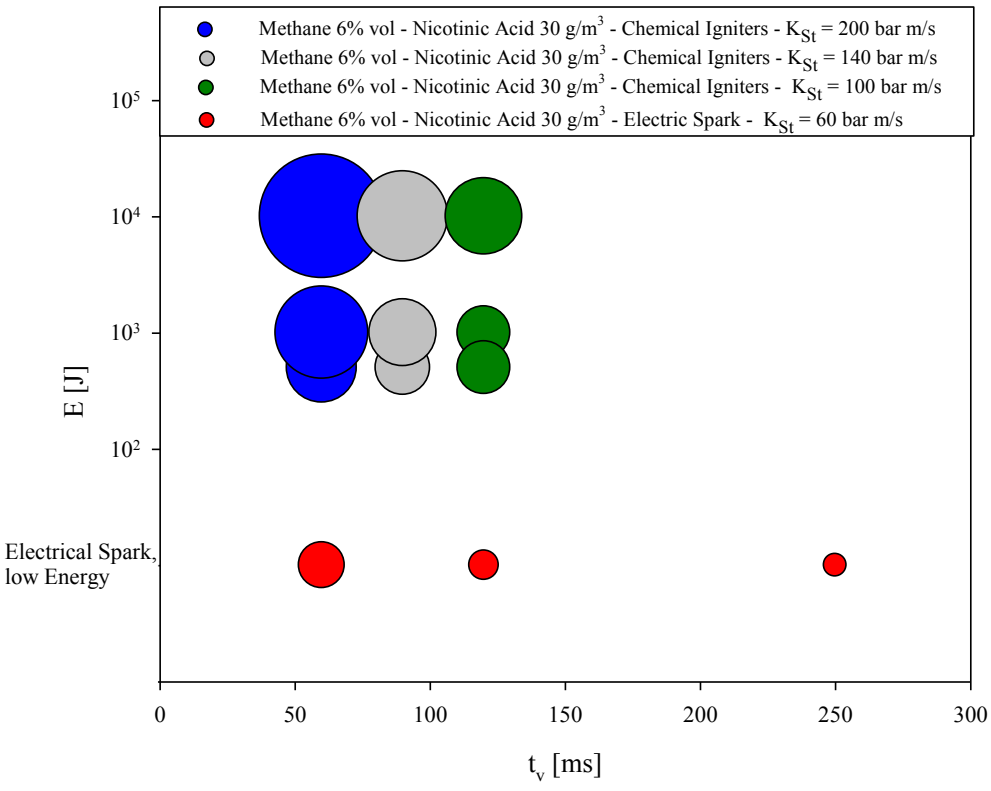

Figure 48 – Effect of the turbulence and of ignition energy on the deflagration index, K_{St}, of a mixture of 6% vol of methane and 30 g/m^3 of nicotinic acid. The dimension of the circles is proportional to K_{St}.

5.1.3.4 Correlation between ignition source and turbulence

As previously said, the effect of ignition energy was studied by using different ignition energies at various turbulence levels. In Figure 49 the pressure time histories of explosions of hybrid mixtures of 6% vol. of methane with 30 g/m^3 of nicotinic acid in air are shown performed with same shorter value of t_v, 60 ms, and with different ignition energies.

This mixture is a poor mixture because the concentration of gas has a value close to the LFL of the gas, while the concentration of the dust is below to the MEC of the dust for these energy values.

The difference in the maximum pressure are probably due to the proximity of the limit conditions of concentration; instead the K_{St} value is influenced by the ignition energy but also by the turbulence in the explosion chamber. A first significant difference in the pressure-time histories is evident when the mixture is exposed to the two different ignition sources: the explosion initiated by the volumetric source (chemical igniters) behaves totally differently from that generated by the point sources ignition (electric spark). Similar results were obtained by Landman [40] with an hybrid mixture of coal dust and methane in air, and the conclusions are also the same; that is, in the case of electric spark ignition, heat is lost near to the point of ignition; then, the reaction takes place at a lower temperature than that of ignition due to chemical igniters, and the reaction rate is much slower; as consequence the overall explosions of the same mixture ignited from the electric spark, are much slower and weaker than those initiated from the chemical igniters.

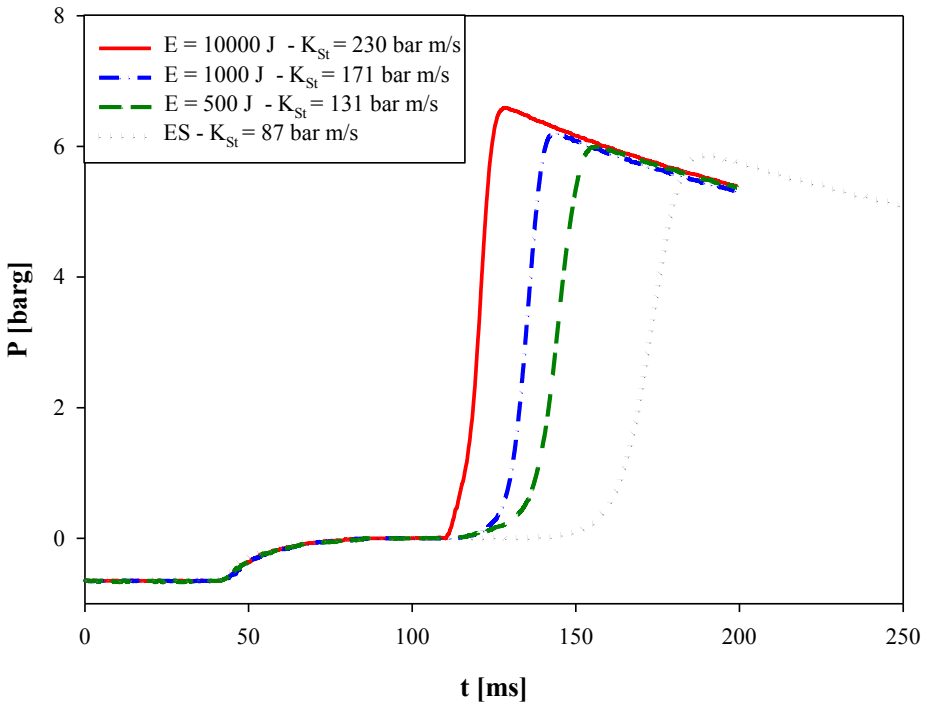

Figure 49 – Pressure time history of mixtures of 6% vol of methane and 30 g/m^3 of nicotinic acid with t_v = 60 ms at different ignition energy (chemical igniters).

Moreover, in the case of Figure 49, minor effects are clear also with different values of energy even if the same type of ignition is used. Similar results in this case are obtained by Zhen & Leuckel [105]: the use of chemical igniters can significantly enhance the rate of pressure rise at the early stage of the explosion in the measure of the amount of energy released; this influence can be as much greater as higher is the amount of ignition energy.

hese observation lead to observe that lower is the ignition energy more time is necessary to trigger the explosion starts: this time is defined as induction time, t_2 (cf. Figure 23); and to conclude that the true turbulence level is determinated by considering the "explosion delay time", t_{ex}, calculated as:

$$t_{ex} = t_v + t_2 \tag{5.6}$$

In Figure 50, the results of the experiments on the pure compound (methane at 6% and 7.3% vol.; dust 60 g/m^3) and two hybrid mixture (methane 6% vol./nicotinic acid 30 g/m^3; methane 6% vol./nicotinic acid 60 g/m^3) are shown. These experiments, performed varying the energy level and type of source of ignition and also the ignition delay time, and reported in term of deflagration index as function of the explosion delay time, t_{ex}, seem to suggest that the ignition energy is related to explosion delay time, t_{ex}.

The violence of the explosion decreases with t_{ex} since, as the t_{ex} increases, the turbulence level decreases.

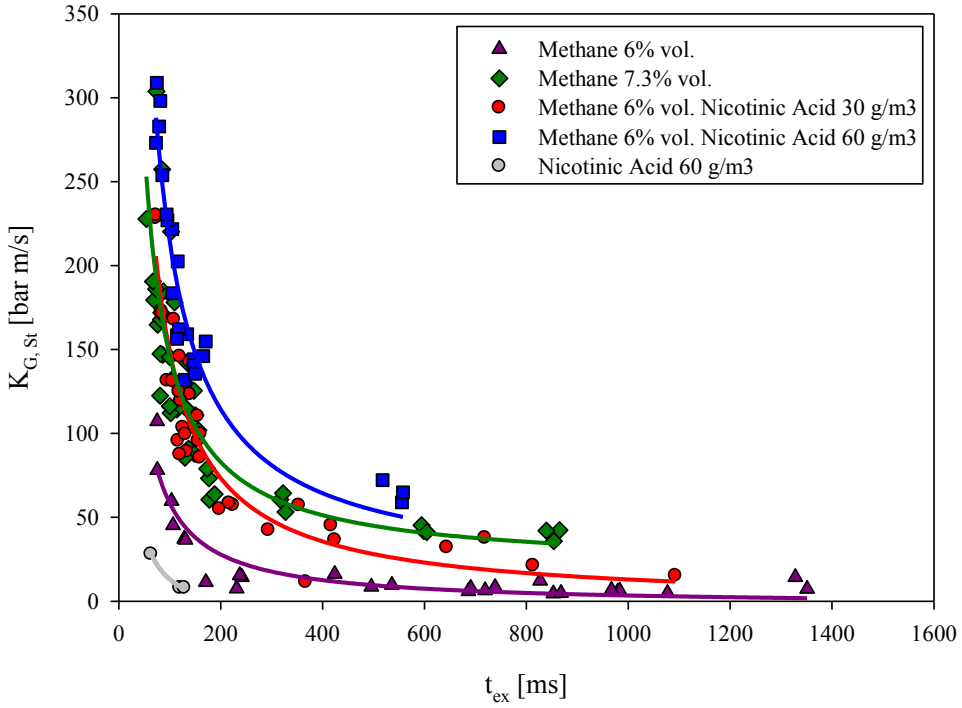

Figure 50 – Deflagration index of experiments on pure compounds (6% - 7.3% vol. of methane – 60 g/m^3 of nicotinic acid) and hybrid mixtures (methane 6% vol./nicotinic acid 30 g/m^3 – methane 6% vol./nicotinic acid 60 g/m^3) as function of explosion delay time.

5.2 FLAME PROPAGATION

The study of the flame propagation was carried out at Nancy. The main goal of this activity was the setting up of a novel apparatus adequate for measuring the flame speed of hybrid mixtures.
The developed equipment was subsequently tested by measuring the flame speed at varying the methane concentration (v/v-%) in the range 0.5 ÷ 7.3 % and the nicotinic acid concentration in the range 60 ÷ 190 g/m^3.

5.2.1 Flame propagation apparatus development

For the hybrid mixture flame propagation study the tube methodology was adopted. The development of the tube was inspired by the Hartmann tube [72].
The main project issues concern the systems for :

1. dust dispersion;
2. feeding and dust/gas mixing;
3. ignition;
4. venting;
5. flame propagation visualization;
6. tests procedure (optimal ignition delay time).

The dust dispersion in the tube is performed by the pneumatic system of the Hartmann tube equipment, for which the air blast is obtained using air from a 0.05 l reservoir pressurized to ~ 7 bar. The issue in this case is that the volume of the tube is different and bigger than that of the Hartmann tube and some modifications as rising the pressure or the volume of the reservoir should be necessary. In fact, this system is able to ensure a uniform and homogeneous dust dispersion but not along the entire length of the tube.

As concern the mixing between the dust, gas fuel and air, no stirred parts are present in the tube. The mixing with dust is guaranteed by means of the air blast. As concern the gas phase, to ensure a good mixing, a pre-mixing cylindrical vessel, in which a mixture of half air and half methane is prepared by means of a dispersing nozzle, external to the tube is used. This is due to avoid some stratification of the gas.

As concern ignition, the Hartmann tube equipment system based on the spark mode was used. The Hartman ignition system was modified in order to implement longer electrical wires to allow changing electrical resistance and then the released energy. The ignition position was located near the closed end of the tube where the dust is dispersed and the gas is fed. When the flame propagates, combustion burned gas are produced and flow in the same direction of the flame front, arising the overall velocity of the flame. Then, a good solution is to put the ignition near the open end of the tube or moving the ignition near the open end or opening the end near the ignition.

The system of venting is design following the Hartmann tube scheme in which the venting pressure is the atmospheric pressure. For this reason to permit the feeding of the gas, the experiments were performed under vacuum condition of about -0.2 barg (i.e., the ignition was triggered when the gas/dust mixture is depressurised). The issue in this case is double: the influence of depressurization, on one hand, and the effects of the vent open, on the other hand, have to be taken into account. The experiments are considered only until the vent open, to avoid the related problems; thus they are performed in a practically closed vessel. A better configuration is that used by Proust [46] an open tube, with the ignition near the open end. In this case, the problem is, instead, related to the feeding of the gas.

The flame propagation visualization was performed by recording the flame images during the propagation by using a camera (14-bit image depth, and 1000 fps at a full resolution of 1632 x 1200 pixels) based on the direct lighting visualization. Several tests were performed in order to get the best contrast to make the flame visible:

- varying the colour of the background of the tube (white, black, orange);
- varying the exposure level of the video camera (between 250 – 990 μs);
- changing the position of the light.

The ultimate adopted solutions are: an orange background and an exposure of 490 μs that permits to have 2000 fps as acquisition frequency with a resolution of 176 x 1200 pixels.

The test procedure used is, also in this case, that used for the Hartmann tube based on the use of a specific Software (Kühner).

The issues arisen by the different configuration of the tube respect to Hartmann tube and by the ignition system have to be taken into account when the ignition energy and ignition delay time are set. A good control of these parameters is not guaranteed with this solution.

5.2.2 Results

Preliminary tests were performed in order to test the developed equipment.

In the following the results obtained in the tube equipment are reported for each fuel (methane and nicotinic acid) and for the hybrid mixture at changing the CH_4/nicotinic acid ratio. A compendium of entire set of results are reported in the Annexes in Table B. 10.

5.2.2.1 Methane flame propagation

Experiments of flame propagation were carried out for pure methane. In Figure 51 images of flame propagation of pure methane at 7.3% v/v are shown with an interval of 5 ms. It's possible to see the displacement of the flame. The methane flame is a blue flame characterized by no hot spot, typical of carbon residual.

The obtained images are not clear because of the colour of the flame; to solve this problem an orange or yellow filter may be used.

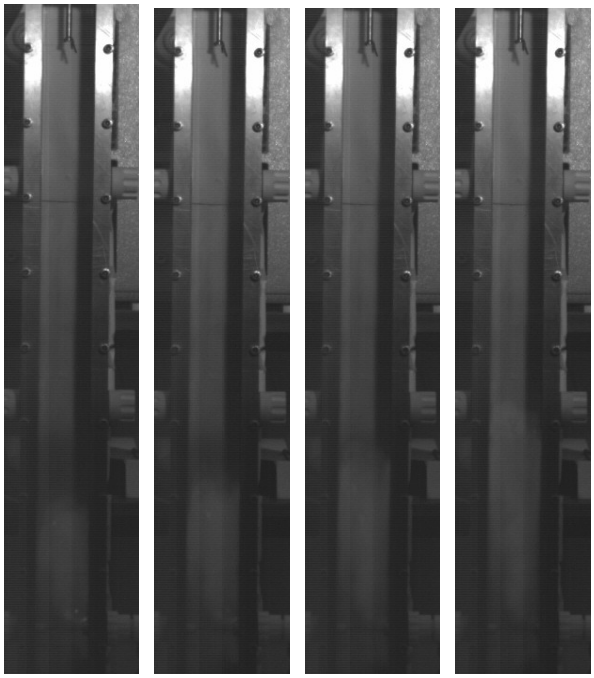

Figure 51 – Images of flame propagation of pure methane (7.3% v/v).

Figure 52 reports the flame velocity of the pure methane by varying its concentration as obtained by post-processing the flame images.

From the measurements it turns out that the LFL here found is about 4% v/v.

The literature data [106]-[108] reported in the same figure are referred to the experiment carried out in spherical or cubic chambers. It's possible to note the large differences in the obtained value of flame velocity. This is due essentially to the high level of turbulence in the tube chamber and in a

less extent to the different shape of the chamber used: in the case of the tube, the walls have a significant rule in disturbing the development of the flame.

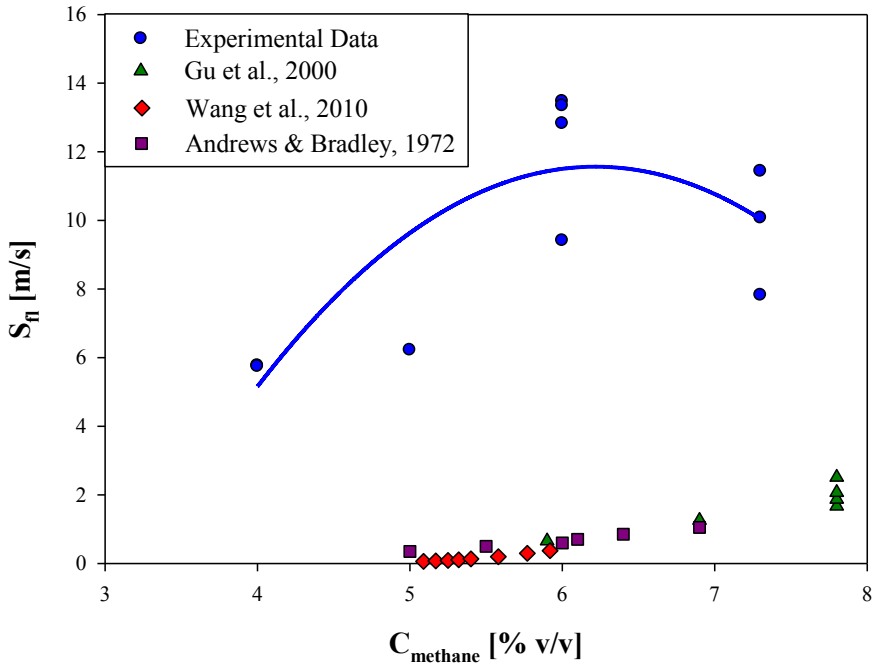

Figure 52 – Flame velocity of pure methane in the tube apparatus designed by LRGP (France): experimental and literature data [106]-[108].

5.2.2.2 Flame propagation of Nicotinic Acid

Tests of flame propagation of nicotinic acid were performed by varying its concentration between 60 and 190 g/m^3 of nicotinic acid. These concentration values were evaluated taking into account only about 1/3 of the tube because the dispersion system was not optimized for this tube and, as consequence, the dispersion didn't regard the entire tube. In Figure 53 images of flame propagation of pure nicotinic acid at concentration of 125 g/m^3 are shown with a time interval equal to 5 ms.
In this case the flame and then the displacement of the flame are more visible than in the case of pure methane, thanks to the radiation of the solid particles of the dust. In some tests we found an over exposure of the flame that in some cases results too much bright.

Figure 53 – Images of flame propagation of pure nicotinic acid (125 g/m^3).

In Figure 54 the results of flow velocities obtained for nicotinic acid are reported.

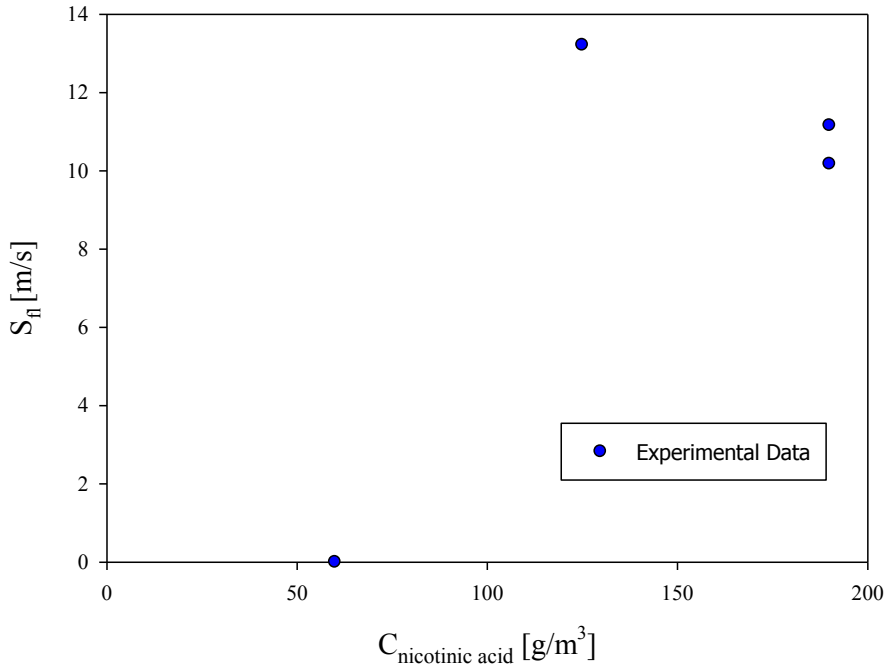

Figure 54 – Flame velocity of pure nicotinic acid in the tube apparatus designed by LRGP (France).

5.2.2.3 Flame propagation of Nicotinic Acid/Methane air mixtures

The flame propagation behaviour of nicotinic acid/methane mixture in air has been investigated by varying the concentration values of methane between 0.5 % up to 6 % and the nicotinic acid content between 60 and 190 g/m^3. In Figure 55 the images of flame propagation of the hybrid mixture of methane at 6% v/v and nicotinic acid at 125 g/m^3 are shown with an interval of 2 ms.

In this case it's possible to observe two flames which may possibly be compared with those of methane and nicotinic acid. Indeed, the more brightness flame could be associated to the dust flame; whereas the clearer one to the gas flame. The methane flame seems to be faster and it seems entraining the dust flame. The colour of the gas flame is not too clear; to solve this problem an orange or yellow filter may be used, as already mentioned; but this solution is not a good choice for the visualization of the dust flame that required opposite type of filters.

Figure 55 – Images of flame propagation of hybrid mixture of methane (6% v/v) and nicotinic acid (125 g/m^3).

In Figure 56 the flame velocity is plotted against the concentration of methane for different values of nicotinic acid content (from 0 to 190 g/m^3). Decreasing the concentration of the nicotinic acid flame velocity increases. An inversion for low values of methane concentration and 60 g/m^3 of concentration of nicotinic acid is observed. This is due to the fact that pure dust at this value of concentration is not flammable; and also a low addition of methane makes the mixture flammable.

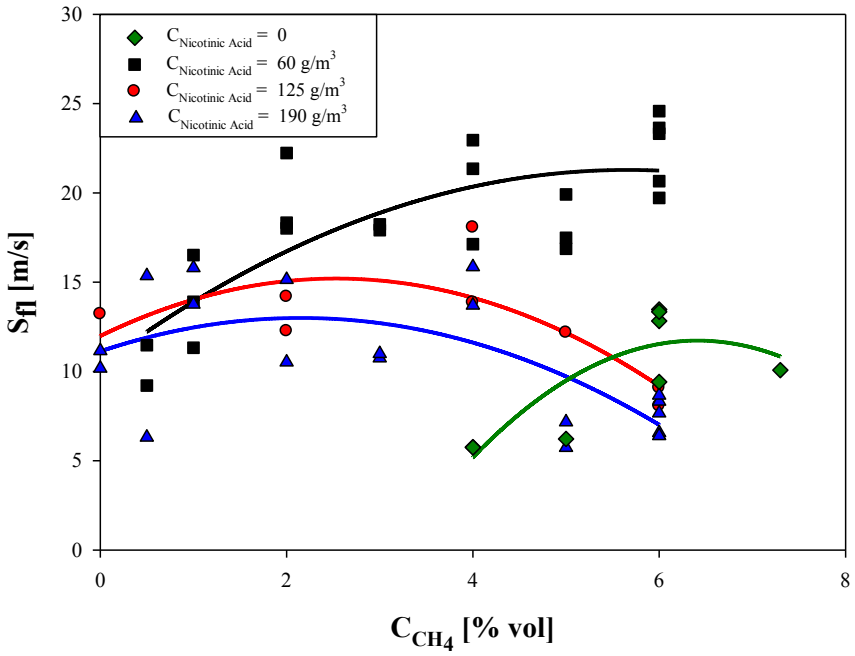

Figure 56 – Flame velocity of nicotinic acid/methane air mixture in the tube apparatus designed by LRGP (France).

Furthermore, it can be observed that the trend of the curve of hybrid mixture with 60 g/m^3 of concentration of nicotinic acid is similar to that of pure methane: there is a shift of the curve towards lower value of methane. All the dust probably devolatilizes increasing the volatile content and so giving a contribute to flame propagation.

5.2.2.4 Nicotinic acid/methane/air explosion regimes

The study of flame propagation is an useful tool to understand the behaviour of the explosion phenomenon. By means of the experiments performed for the study of the flame propagation of the methane/nicotinic acid/air mixtures, in fact, a further contribution to the explanation of the different regimes that are identified for the explosivity behaviour of these mixtures can be given.

For each of the five zones some characteristic experiments can be chosen and a set of frames can be shown in Figure 57 to Figure 61 that are explicative of the behaviour of the mixtures.

No explosion zone

Figure 57 shows the experiment related to the flame propagation of nicotinic acid at 60 g/m^3. In this condition the mixture lies in the no explosion zone in the diagram of regimes. When ignition is activated, the fuel starts reacting but it isn't able to sustain the flame propagation and the flame tends to extinguish.

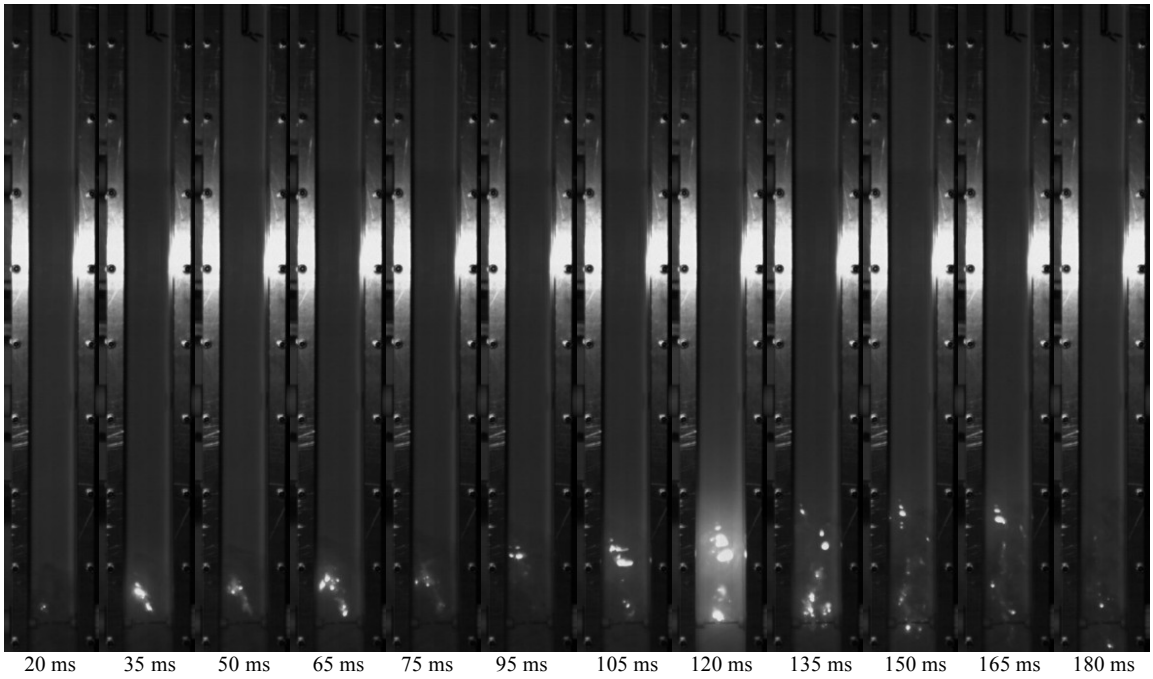

Figure 57 – Set of frames of flame propagation of a mixture of 60 g/m^3 nicotinic acid and related to no explosion zone.

Synergic explosion zone

In Figure 58 the experiment of a mixture of 3% vol. of methane and 60 g/m^3 of nicotinic acid is shown. In this condition of concentrations the mixture lies in the synergic explosion zone in the diagram of regimes. For these concentrations, the separate pure compounds are not able to sustain the propagation of the flame by themselves; instead, the co-presence of the two fuels makes the flame advance along the tube. The flame front is one because the front of the one can't be without the contribution of the other.

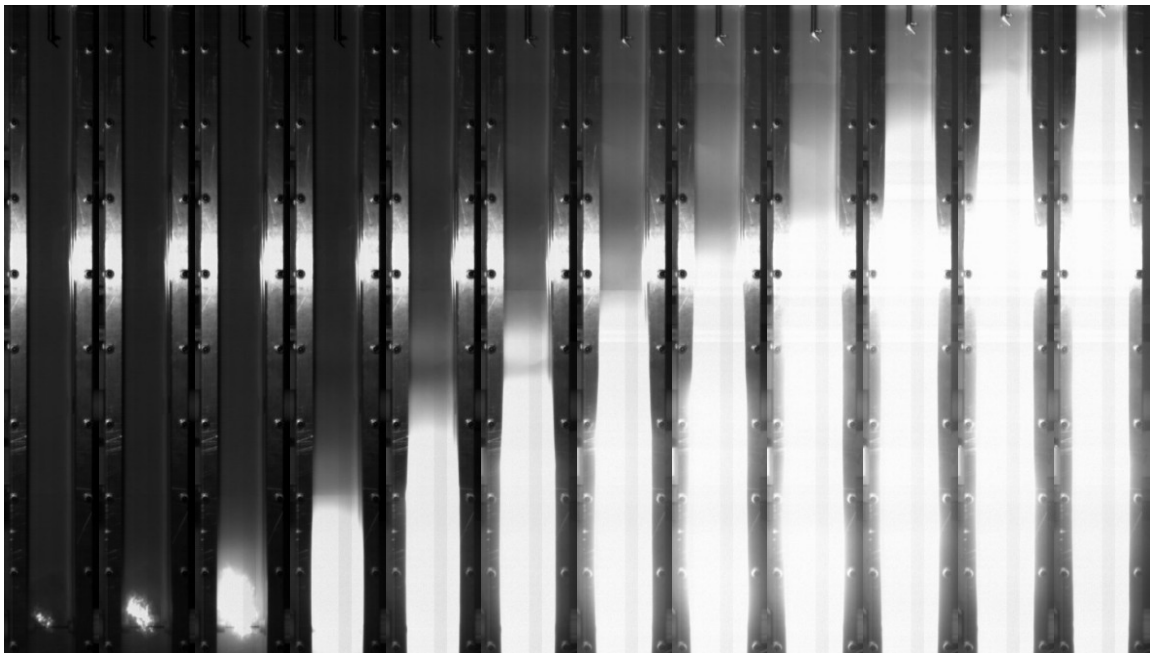

Figure 58 – Set of frames of flame propagation of a mixture of 3% vol methane and 60 g/m^3 nicotinic acid and related to synergic zone.

Dual fuel explosion zone

In Figure 59 the experiment of a mixture of 6% vol. of methane and 190 g/m^3 of nicotinic acid is shown. In this condition of concentrations the mixture lies in the dual fuel explosion zone in the diagram of regimes. For these concentrations, the two flames can be distinguish and develop separately along the tube; the flame of the gas is less bright than that of the dust.

But because of the lack of oxygen that is the limiting reactant in that zone, the two flame are not able to sustain the overall development of the flame and tend to extinguish . The gas flame is faster than that of the dust because it's more reactive.

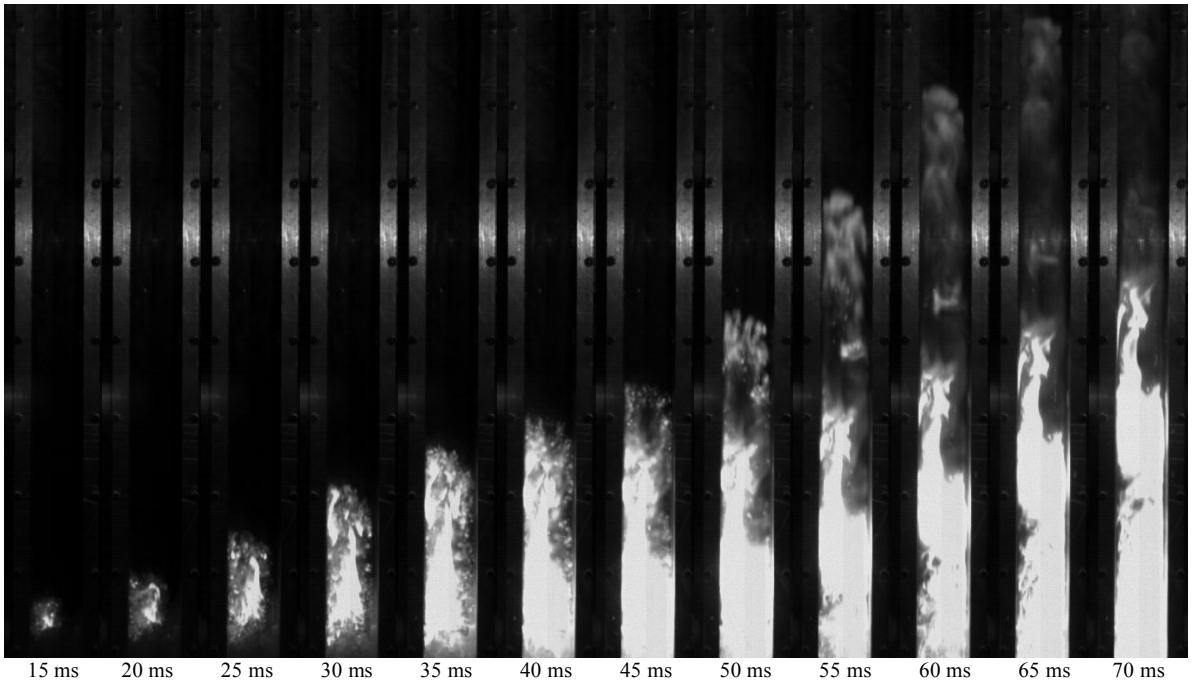

Figure 59 – Set of frames of flame propagation of a mixture of 6% vol. methane and 190 g/m^3 nicotinic acid and related to dual fuel explosion zone.

Gas driven explosion zone

In Figure 60 the experiment of a mixture of 6% vol. of methane and 125 g/m^3 of nicotinic acid is shown. In this condition of concentrations the mixture lies in the gas driven explosion zone in the diagram of regimes. For these concentrations, the gas flame drives the "explosion" phenomenon and this is proved because the gas flame surpasses that of the dust, sustaining and dragging the dust flame.

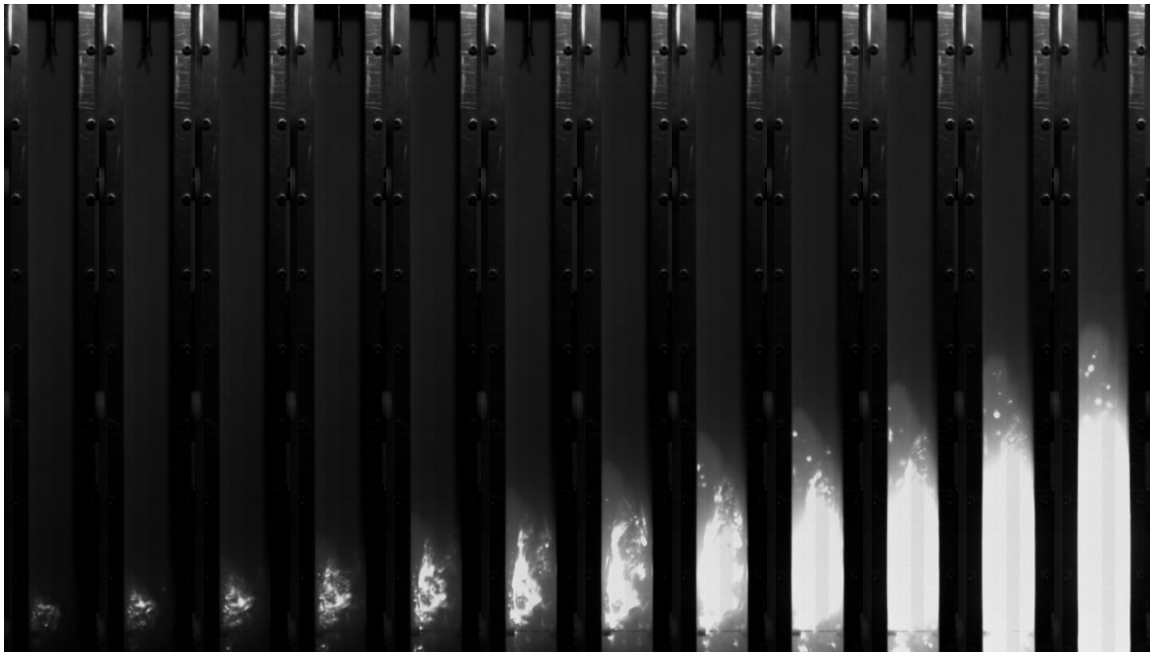

Figure 60 – Set of frames of flame propagation of a mixture of 6% vol. methane and 125 g/m^3 nicotinic acid and related to gas driven explosion zone.

Dust driven explosion zone

In Figure 61 the experiment of a mixture of 3% vol. of methane and 190 g/m^3 of nicotinic acid is shown. In this condition of concentrations the mixture lies in the dust driven explosion zone in the diagram of regimes. For these concentrations, the behaviour is complementary to the previous one; in fact, the flame front of the dust is driven and surpasses that of the gas, sustaining it because it doesn't ignite by itself. In this case, the two flames are not distinguishable because the dust flame is brighter than that of the gas.

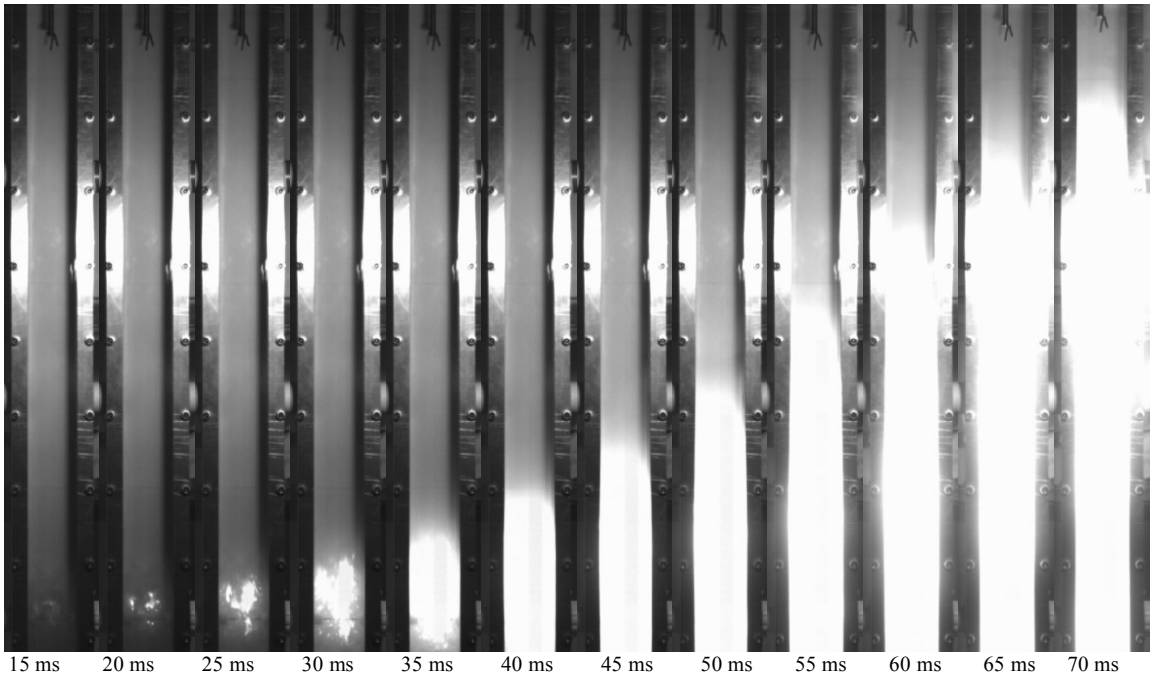

Figure 61 – Set of frames of flame propagation of a mixture of 3% vol. methane and 190 g/m^3 nicotinic acid and related to dust driven explosion zone.

Then, the experiments of flame propagation give further evidence of the existence of the five zones and the behaviour of the mixtures are explained.

5.2.3 Further equipment developments

The experiments of flame propagation suggest that several issues arise in the equipment developed and improvements are needed.

Improvements are related to the following:

- the dust dispersion system has to be improved in order to allow dust dispersion over the entire tube;
- a modification of the ignition position close to the tube open end;
- use of a more adequate video camera, with adequate filters, to get a better resolution;
- or use of two video cameras, implemented to a better visualization one of the methane blue flame (with orange or yellow filter) and other one of the more brightness dust flame;
- implementation of the Schlieren method to light the flame;
- improvement of the pre-mixing apparatus and, then, of the line of feeding of flammable gas;
- development of a specific Software for the control of the process and acquisition of images.

Chapter 6 – Conclusions

In this work explosibility and ignitability of hybrid mixtures was studied. Explosion and flame propagation experiments were performed.

Deflagration index measurements were performed for methane/air and methane/nicotinic acid/air mixtures of different compositions at varying the ignition delay time (60 – 750 ms) and then the turbulence level at ignition.

As result, the effect of turbulence on deflagration index is minor in standard test conditions, while it is significant at high initial turbulence level.

A model is proposed to predict the dependence of the deflagration index on the turbulence level. The model well reproduces the experimental data, provided that the adequate formula for the turbulent burning velocity is used.

Measurements of explosibility of methane/nicotinic acid/air mixtures were carried out in a modified spherical bomb. The experiments were performed varying the methane concentration in the range 1.0 ÷ 7.3 % and the nicotinic acid in the range 30 ÷ 250 g m^{-3}. A spark ignition was used choosing the worst turbulence condition ($t_v = 0$).

From the results obtained the following conclusions may be drawn:

- the volatile content of the dust significantly affects the stoichiometric and the minimum explosive concentration;
- the adiabatic pressure of methane and nicotinic acid are comparable and then their mixture verify Le Chatelier's criterion for flammability: the methane/nicotinic acid mixture may be defined as a similar mixture;
- the explosion behaviour of the methane/nicotinic acid mixture may be classified in four different regimes in the plane dust concentration vs. fuel concentration;
- these results may be extended to all the gas/dust/air mixtures which are similar.

Moreover, the combined effect of the ignition energy and the turbulence were studied varying the methane concentration (v/v-%) in the range 3.6 ÷ 7.3 % and for the nicotinic acid in the range 30 ÷ 60 g m^{-3} using different ignition source, electric spark and chemical igniters of different energy value at different value of ignition delay time, t_v.

A new parameter, the overall explosion delay time, t_{ex}, can be defined. From the obtained results, the violence of the explosion of an hybrid mixture decreases as the overall delay time, t_{ex}, increases independently from ignition energy level. In fact, this parameter takes into account the intrinsic dependence of the ignition energy on the turbulence.

Furthermore, experiments of flame propagation were performed in a new equipment. The experiments were performed varying the methane concentration in the range 0.5 ÷ 7.3 % and the nicotinic acid content in the range 60 ÷ 190 g/m^3. A spark ignition was used.

From the results obtained the following conclusions may be drawn:

- the overall flame of the hybrid mixture is characterized by two flame: one related to gas phase and the other related to dust flame;
- the simultaneous presence of the two fuel has the effect of enhancing the velocity of the resulting flame.

Moreover, the flame propagation behaviour of the methane/nicotinic acid/air mixtures gives a further contribution to the explanation of the different regimes.

The experiments of flame propagation suggest that several issues arise in the equipment developed and improvements are needed.

In conclusion, the results related to ignitability and explosivity of this work can be generalized and utilized as starting point for estimating and predicting the performances of dust/gas mixtures from those of pure compounds.

ANNEXES

A GUIDELINES AND REGULATIONS

The actual prevention and mitigation system against the hazard due to dust explosions are designed following technical standards.

In Europe, the technical standards named "ATEX directive" constitutes the philosophical basis of the entire new generation of European standards on prevention and mitigation of accidental gas/vapour, mist and dust explosions. There are two ATEX directive:

- Directive 94/9/EC of the European Parliament and the Council of 23 March 1994 [109]
- Directive 99/92/EC of the European Parliament and of the Council of 16 December 1999) [110]

The ATEX directive have been originally written with specific reference to gas/vapour explosions, whereas little attention was paid to dust explosion [111], [112]. In fact, in these directives there isn't a sufficient differentiation between combustible gases/vapour, combustible mist, and combustible dusts. This deficiency probably rises from the fact that when combustible dust clouds, mist clouds and gas/vapour are generated, they are similar as concern their burning properties and the way in which they are ignited. While it's more important to consider also the way in which they can be generated. These directives base on the fact that dust clouds can be formed under the same circumstances in which it was envisaged that gas and vapour clouds can be generated. But the formation of the cloud are different for the different combustible.

For example, there are some cases in which the dust cloud can be formed that aren't taken into account by the directives. This is the case when the dusts can be in layers which may be electrically conductive, be thermally insulating and have a potential for self-heating/self-ignition. Sometimes, layers of most organic dusts may produce combustible gases when heated, which, if not ignited immediately, may mix with air and form explosive gas mixtures.

Another hazard case is when a dust contains combustible organic solvents because of the production/treatment/handling process to which it has been subjected. When the dust is dispersed in a cloud, there can be in the surrounding air sufficient solvent vapour to reach the minimum ignition energy of the "hybrid" mixture that is lower than the corresponding value of energy for dry dust in the pure air. Moreover, the vapour fraction in the air that is necessary to trigger an ignition is often well below the lower flammability limit of the pure vapour.

Then, it rises also the need to deal with hybrid clouds mixtures that require special treatments. [111]

The dusts have a behaviour more unpredictable than that of gases or vapour, such that it's more difficult to identify an explosion hazard and so to establish the zone classification.

Up to now there isn't a well clear official distinction for the different combustible and the attempts at extensive "harmonisation" of equipment design concepts for dusts with those existing for gases, cause only confusion and frustration in industry. For this reason, IEC (International Electrotechnical Commission) is encouraged to terminate its efforts to adapt traditional gas/vapour standards to dusts.

To do this, IEC suggests that, for safe design of equipment in the areas containing combustible dusts, two are the important concepts to take into account for ignition protection: first, the dust has to be kept in enclosures to avoid a dispersion in some part of the plant; and it's necessary to keep the enclosures at sufficiently low surface temperatures to prevent ignition of the dust (layer or cloud) under the prevailing conditions.

This is in full accordance with the current philosophy in European standardisation work at committee level, as expressed in EN 50281-1-1 and -2 (CENELEC 1998a, 1999).

This would be the basis of future European standardisation work. And the ATEX directives should be revised as soon as possible to avoid further confusion.

This European philosophy is also in agreement with the prevailing standards and philosophy of standardisation in the USA.

In the U.S.A., also, there aren't significant regulations about dust explosion hazard.

To supply this lack, the Chemical Safety and Hazard Investigation Board (CSB), the agency in charge to investigate industrial chemical accidents, conducts root cause investigations of chemical accidents at fixed industrial facilities. In this way, even if the agency can't issue fines or citations, but it does make recommendations to plants, regulatory agencies such as the United States Department of Labour's Occupational Safety and Health Administration (OSHA) and the Environmental Protection Agency (EPA), industry organizations, and labour groups. The CSB is non-regulatory and independent of other agencies so that its investigations might, where appropriate, review the effectiveness of regulations and regulatory enforcement. [113]

After the accident in Georgia at the Imperial Sugar occurred in the 2008, on demand of CSB, OSHA has created a national regulatory standard for combustible dust hazards called "Combustible Dust National Emphasis Program, NEP" [114]. This work contains policies and procedures for inspecting workplaces that create or handle combustible dusts [8].

Moreover, CSB recommends that OSHA Hazard Communication standard (HCS) and the American National Standards Institute (ANSI) standard Z400.1 to improve the regulatory requirements and suggested format, respectively, for preparing MSDSs to include combustible dust explosion

warning and combustible dust properties and to provide guidance on what information to include on the MSDS.

Besides, in the U.S.A. instead of regulations, consensus standards and codes, there is the National Fire Protection Association (NFPA) that provides guidance for preventing and mitigating hazards. The NFPA provides consensus standards that address combustible dusts. They are voluntary unless they are adopted as law or code by a state or local jurisdiction. [115]

These standards are also followed not only in U.S.A. but also in other parts of the world.

In the Table A. 1 are reported the NFPA standards to be followed for preventing and mitigating the effects of fire and explosions due to the presence of dust in the industry.

Table A. 1 – NFPA Standards.

NFPA 61, Standard for the Prevention of Fires and Dust Explosions in Agricultural and Food Processing Facilities
NFPA 68, Guide for Venting of Deflagrations
NFPA 69, Standard on Explosion Prevention Systems
NFPA 70, National Electrical Code®
NFPA 91, Standard for Exhaust Systems for Air Conveying of Vapours, Gases, Mists, and Non-combustible Particulate Solids
NFPA 120, Standard for Fire Prevention and Control in Metal/Non-metal Mining and Metal Mineral Processing Facilities
NFPA 432, Code for the Storage of Organic Peroxide Formulations
NFPA 480, Standard for the Storage, Handling, and Processing of Magnesium Solids and Powders
NFPA 481, Standard for the Production, Processing, Handling, and Storage of Titanium
NFPA 482, Standard for the Production, Processing, Handling, and Storage of Zirconium
NFPA 484, Standard for Combustible Metals, Metal Powders, and Metal Dusts
NFPA 485, Standard for the Storage, Handling, Processing, and Use of Lithium Metal
NFPA 495, Explosive Materials Code
NFPA 499, Recommended Practice for the Classification of Combustible Dusts and of Hazardous (Classified) Locations for Electrical Installations in Chemical Process Areas
NFPA 505, Fire Safety Standard for Powered Industrial Trucks Including Type Designations, Areas of Use, Conversions, Maintenance, and Operation
NFPA 560, Standard for the Storage, Handling, and Use of Ethylene Oxide for Sterilization and Fumigation
NFPA 654, Standard for the Prevention of Fire and Dust Explosions from the Manufacturing,

Processing, and Handling of Combustible Particulate Solids
NFPA 655, Standard for Prevention of Sulphur Fires and Explosions
NFPA 664, Standard for the Prevention of Fires and Explosions in Wood Processing and Woodworking Facilities
NFPA 1124, Code for the Manufacture, Transportation, Storage, and Retail Sales of Fireworks and Pyrotechnic Articles
NFPA 1125, Code for the Manufacture of Model Rocket and High Power Rocket Motors

Other regulations that can be followed are that drawn up by ASTM International (ASTM).
ASTM International (ASTM), originally known as the American Society for Testing and Materials, is an international standards organization that develops and publishes voluntary consensus technical standards for a wide range of materials, products, systems, and services.
The ASTM standards for dust fire and explosion hazard are presented in Table A. 2.

Table A. 2 – ASTM Standards.

E789-95 Standard Test Method for Dust Explosions in a 1.2 Litre Closed Cylindrical Vessel
E1226-00e1 Standard Test Method for Pressure and Rate of Pressure Rise for Combustible Dusts
E1491-97 Standard Test Method for Minimum Autoignition Temperature of Dust Clouds
E1515-03a Standard Test Method for Minimum Explosible Concentration of Combustible Dusts
E2021-01 Standard Test Method for Hot Surface Ignition Temperature of Dust Layers

At last, there are other publications due to National Materials Advisory Board (NMAB) and International Code Council (ICC) with important classification and code, as reported in Table A. 3.

Table A. 3 – Publications.

NMAB 353-4 (1982), Classification of Dusts Relative to Electrical Equipment in Class II Hazardous Locations.
International Fire Code (ICC)

B TABLE OF RESULTS

In this section the data related to all the experiments are reported.

B.1 EXPLOSION TESTS

Table B. 1 – Explosibility results for pure methane of the experiments performed varying t_v with electric spark ignition.

ID	GAS SAMPLE	C (% v/v)	t_v (ms)	P_{EX} (barg)	dP/dt (bar/s)	K_g (bar m/s)
2_26-10-09	METHANE	6	60	3.9	17	5
3_26-10-09	METHANE	6	60		NO EXPLOSION	
4_26-10-09	METHANE	6	60	3.8	21	6
5_26-10-09	METHANE	6	60		NO EXPLOSION	
6_26-10-09	METHANE	6	60	3.9	24	7
24_26-10-09	METHANE	6	60	4	18	5
7_26-10-09	METHANE	6	120	4.0	22	6
8_26-10-09	METHANE	6	120	4.2	36	10
9_26-10-09	METHANE	6	120	4.2	32	9
10_26-10-09	METHANE	6	250	4.6	60	16
11_26-10-09	METHANE	6	250	4.1	29	8
12_26-10-09	METHANE	6	250	3.9	23	6
13_26-10-09	METHANE	6	250	4.2	31	8
14_26-10-09	METHANE	6	500		NO EXPLOSION	
15_26-10-09	METHANE	6	500	4	18	5
16_26-10-09	METHANE	6	500	4.4	45	12
17_26-10-09	METHANE	6	500	4.2	25	7
18_26-10-09	METHANE	6	500		NO EXPLOSION	
19_26-10-09	METHANE	6	750	4.7	53	14
20_26-10-09	METHANE	6	750		NO EXPLOSION	
21_26-10-09	METHANE	6	750	4	27	7
2_01-10-09	METHANE	7.3	0	5.8	811	220
3_01-10-09	METHANE	7.3	0	5.5	656	178
4_01-10-09	METHANE	7.3	0	5.4	948	257
5_01-10-09	METHANE	7.3	30	5.9	839	228
6_01-10-09	METHANE	7.3	30	5.8	1119	304
7_01-10-09	METHANE	7.3	30	5.5	543	147
8_01-10-09	METHANE	7.3	30	5.6	685	186
9_01-10-09	METHANE	7.3	30	5.5	451	122
27_01-10-09	METHANE	7.3	30	5.7	702	191
10_01-10-09	METHANE	7.3	60	5.7	536	145
11_01-10-09	METHANE	7.3	60	5.5	421	114
12_01-10-09	METHANE	7.3	60	5.7	488	132
13_01-10-09	METHANE	7.3	60	5.6	413	112
28_01-10-09	METHANE	7.3	60	5.5	428	116
14_01-10-09	METHANE	7.3	120	5.4	270	73
15_01-10-09	METHANE	7.3	120	5.3	223	61
16_01-10-09	METHANE	7.3	120	5.5	291	79
17_01-10-09	METHANE	7.3	120	5.5	235	64
18_01-10-09	METHANE	7.3	250	5.4	223	61
19_01-10-09	METHANE	7.3	250	5.5	237	64
20_01-10-09	METHANE	7.3	250	5.4	196	53
21_01-10-09	METHANE	7.3	500	5.3	154	42
22_01-10-09	METHANE	7.3	500	5.3	167	45
23_01-10-09	METHANE	7.3	500	5.1	152	41

24_01-10-09	METHANE	7.3	750	5.4	156	42
25_01-10-09	METHANE	7.3	750	5.2	132	36
26_01-10-09	METHANE	7.3	750	5.5	155	42
2_05-10-09	METHANE	8.6	60	6.7	1282	348
3_05-10-09	METHANE	8.6	60	6	587	159
4_05-10-09	METHANE	8.6	60	6.2	816	221
5_05-10-09	METHANE	8.6	60	6.3	789	214
6_05-10-09	METHANE	8.6	60	6.4	794	216
7_05-10-09	METHANE	8.6	120	6	384	104
8_05-10-09	METHANE	8.6	120	6.3	527	143
9_05-10-09	METHANE	8.6	120	6.3	494	134
10_05-10-09	METHANE	8.6	120	6.1	535	145
11_05-10-09	METHANE	8.6	250	6	322	87
12_05-10-09	METHANE	8.6	250	6.2	345	94
13_05-10-09	METHANE	8.6	250	6.4	441	120
14_05-10-09	METHANE	8.6	250	6.2	328	89
15_05-10-09	METHANE	8.6	500	6.2	283	77
16_05-10-09	METHANE	8.6	500	6.1	287	78
17_05-10-09	METHANE	8.6	500	6.3	302	82
18_05-10-09	METHANE	8.6	750	6.1	263	71
19_05-10-09	METHANE	8.6	750	6.4	270	73
20_05-10-09	METHANE	8.6	750	6.3	261	71
3_28-09-09	METHANE	10	0	7.2	2590	703
4_28-09-09	METHANE	10	30	7.3	1544	419
5_28-09-09	METHANE	10	30	7.2	1715	466
6_28-09-09	METHANE	10	30	6.9	1649	448
7_28-09-09	METHANE	10	60	6.9	1134	308
8_28-09-09	METHANE	10	60	7.1	1146	311
9_28-09-09	METHANE	10	60	7.2	1391	378
10_28-09-09	METHANE	10	60	7.1	1185	322
11_28-09-09	METHANE	10	120	7	726	197
12_28-09-09	METHANE	10	120	7.1	847	230
13_28-09-09	METHANE	10	120	6.9	777	211
14_28-09-09	METHANE	10	250	7.1	688	187
15_28-09-09	METHANE	10	250	7.1	676	183
17_28-09-09	METHANE	10	250	7	579	157
18_28-09-09	METHANE	10	250	6.9	532	144
19_28-09-09	METHANE	10	250	7	609	165
20_28-09-09	METHANE	10	500	6.8	456	124
21_28-09-09	METHANE	10	500	6.8	408	111
22_28-09-09	METHANE	10	500	6.9	439	119
24_28-09-09	METHANE	10	750	6.7	356	97
25_28-09-09	METHANE	10	750	6.6	351	95

Table B. 2 – Explosibility results for hybrid mixtures of methane – nicotinic acid of the experiments performed varying t_v with electric spark ignition.

ID	GAS SAMPLE	C (% v/v)	DUST SAMPLE	C (g/m3)	t_v (ms)	P_{EX} (barg)	dP/dt (bar/s)	Kst (bar m/s)
4_19-10-09	METHANE	6	NICOTINIC ACID	30	60	4.5	42	11
5_19-10-09	METHANE	6	NICOTINIC ACID	30	60	5.9	322	87
6_19-10-09	METHANE	6	NICOTINIC ACID	30	60	5.9	352	96
7_19-10-09	METHANE	6	NICOTINIC ACID	30	60	5.9	366	99
8_19-10-09	METHANE	6	NICOTINIC ACID	30	120	5.7	211	57
9_19-10-09	METHANE	6	NICOTINIC ACID	30	120	5.7	215	58
10_19-10-09	METHANE	6	NICOTINIC ACID	30	120	5.5	156	42
11_19-10-09	METHANE	6	NICOTINIC ACID	30	120	5.5	202	55
12_19-10-09	METHANE	6	NICOTINIC ACID	30	250	5.8	210	57
13_19-10-09	METHANE	6	NICOTINIC ACID	30	250	5.4	118	32
14_19-10-09	METHANE	6	NICOTINIC ACID	30	250	5.5	166	45
15_19-10-09	METHANE	6	NICOTINIC ACID	30	250	5.4	134	36
16_19-10-09	METHANE	6	NICOTINIC ACID	30	500	5.4	139	38
17_19-10-09	METHANE	6	NICOTINIC ACID	30	500	5.1	78	21
18_19-10-09	METHANE	6	NICOTINIC ACID	30	500	4.9	56	15
19_19-10-09	METHANE	6	NICOTINIC ACID	30	500	NO EXPLOSION		
20_19-10-09	METHANE	6	NICOTINIC ACID	30	500	NO EXPLOSION		
21_19-10-09	METHANE	6	NICOTINIC ACID	30	500	NO EXPLOSION		
18_20-10-09	METHANE	6	NICOTINIC ACID	30	500	NO EXPLOSION		
1_26-10-10	METHANE	6	NICOTINIC ACID	60	60	7	836	227
2_26-10-10	METHANE	6	NICOTINIC ACID	60	60	7.1	849	230
3_26-10-10	METHANE	6	NICOTINIC ACID	60	120	7	538	146
4_26-10-10	METHANE	6	NICOTINIC ACID	60	120	6.8	570	155
3_20-10-09	METHANE	7.3	NICOTINIC ACID	30	60	7.1	1072	291
4_20-10-09	METHANE	7.3	NICOTINIC ACID	30	60	7	782	212
5_20-10-09	METHANE	7.3	NICOTINIC ACID	30	60	7.1	1092	296
6_20-10-09	METHANE	7.3	NICOTINIC ACID	30	120	6.6	453	123
7_20-10-09	METHANE	7.3	NICOTINIC ACID	30	120	6.5	465	126
8_20-10-09	METHANE	7.3	NICOTINIC ACID	30	120	6.8	515	140
9_20-10-09	METHANE	7.3	NICOTINIC ACID	30	250	6.3	308	84
10_20-10-09	METHANE	7.3	NICOTINIC ACID	30	250	6.4	315	86
11_20-10-09	METHANE	7.3	NICOTINIC ACID	30	250	6.7	412	112
12_20-10-09	METHANE	7.3	NICOTINIC ACID	30	500	6.4	246	67
13_20-10-09	METHANE	7.3	NICOTINIC ACID	30	500	6.5	261	71
14_20-10-09	METHANE	7.3	NICOTINIC ACID	30	500	6.4	270	73
15_20-10-09	METHANE	7.3	NICOTINIC ACID	30	750	6.2	218	59
16_20-10-09	METHANE	7.3	NICOTINIC ACID	30	750	6.4	235	64
17_20-10-09	METHANE	7.3	NICOTINIC ACID	30	750	6.4	252	68
2_21-10-09	METHANE	8.6	NICOTINIC ACID	30	60	7.6	1442	391
3_21-10-09	METHANE	8.6	NICOTINIC ACID	30	60	7.5	1100	299
4_21-10-09	METHANE	8.6	NICOTINIC ACID	30	60	7.4	844	229
5_21-10-09	METHANE	8.6	NICOTINIC ACID	30	60	7.7	1500	407
11_22-10-09	METHANE	8.6	NICOTINIC ACID	30	60	7.6	931	253
12_22-10-09	METHANE	8.6	NICOTINIC ACID	30	60	7.5	1208	328
13_22-10-09	METHANE	8.6	NICOTINIC ACID	30	60	7.6	1443	392
6_21-10-09	METHANE	8.6	NICOTINIC ACID	30	120	7.5	782	212
7_21-10-09	METHANE	8.6	NICOTINIC ACID	30	120	7.4	634	172
8_21-10-09	METHANE	8.6	NICOTINIC ACID	30	120	7.5	964	262

9_21-10-09	METHANE	8.6	NICOTINIC ACID	30	120	7.4	908	246
14_22-10-09	METHANE	8.6	NICOTINIC ACID	30	120	7.4	853	232
15_22-10-09	METHANE	8.6	NICOTINIC ACID	30	120	7.4	902	245
16_22-10-09	METHANE	8.6	NICOTINIC ACID	30	250	7.2	592	161
17_22-10-09	METHANE	8.6	NICOTINIC ACID	30	250	7.3	578	157
18_22-10-09	METHANE	8.6	NICOTINIC ACID	30	250	7.3	609	165
19_22-10-09	METHANE	8.6	NICOTINIC ACID	30	500	7.2	485	132
20_22-10-09	METHANE	8.6	NICOTINIC ACID	30	500	7.1	459	125
21_22-10-09	METHANE	8.6	NICOTINIC ACID	30	500	7.2	499	135
22_22-10-09	METHANE	8.6	NICOTINIC ACID	30	750	7.1	399	108
23_22-10-09	METHANE	8.6	NICOTINIC ACID	30	750	7	405	110
24_22-10-09	METHANE	8.6	NICOTINIC ACID	30	750	7.1	413	112

Table B. 3 – Explosibility results for methane gas for different ignition delay time, t_v, with electric spark ignition.

ID	GAS SAMPLE	C (% v/v)	t_v (ms)	P_{EX} (barg)	dP/dt (bar/s)	K_g (bar m/s)
10_13-07-09	METHANE	1.6	0	NO EXPLOSION		
11_13-07-09	METHANE	3	0	NO EXPLOSION		
5_14-09-09	METHANE	4.3	0	NO EXPLOSION		
7_14-09-09	METHANE	4.3	60	NO EXPLOSION		
8_14-09-09	METHANE	4.3	60	NO EXPLOSION		
9_14-09-09	METHANE	5.3	60	NO EXPLOSION		
10_14-09-09	METHANE	5.3	60	NO EXPLOSION		
6_09-07-09	METHANE	6	0	4.2	35	10
9_09-07-09	METHANE	6	0	4.2	39	11
10_09-09-09	METHANE	6	30	NO EXPLOSION		
11_09-09-09	METHANE	6	40	4.2	38	10
8_09-09-09	METHANE	6	60	4.3	44	12
3_14-09-09	METHANE	6	60	NO EXPLOSION		
4_14-09-09	METHANE	6	60	4	29	8
9_09-09-09	METHANE	6	120	3.9	22	6
11_14-09-09	METHANE	6.7	60	5.2	282	77
12_14-09-09	METHANE	6.7	60	5.1	215	58
2_01-12-09	METHANE	7.3	0	5.6	816	221
3_01-12-09	METHANE	7.3	0	5.8	610	166
4_01-12-09	METHANE	7.3	0	5.6	687	186
12_09-09-09	METHANE	7.3	40	5.7	652	177
13_09-09-09	METHANE	7.3	40	5.3	339	92
14_09-09-09	METHANE	7.3	40	5.5	544	148
16_09-09-09	METHANE	7.3	60	5.8	591	160
17_09-09-09	METHANE	10	40	7	1318	358
18_09-09-09	METHANE	10	40	7.1	1437	390
20_09-09-09	METHANE	10	60	6.9	1230	334

Table B. 4 – Explosibility results for nicotinic acid dust with electric spark ignition.

ID	SAMPLE	C (g/m^3)	P_{EX} (barg)	dP/dt (bar/s)	K_{St} (bar m/s)
3_15-07-09	NICOTINIC ACID	60	NO EXPLOSION		
4_15-07-09	NICOTINIC ACID	60	NO EXPLOSION		
5_15-07-09	NICOTINIC ACID	60	NO EXPLOSION		
12_13-07-09	NICOTINIC ACID	125	4.4	36	10
13_13-07-09	NICOTINIC ACID	125	4.4	52	14
14_13-07-09	NICOTINIC ACID	125	5	121	33
3_15-12-09	NICOTINIC ACID	190	5.9	301	82
4_15-12-09	NICOTINIC ACID	190	6.7	492	134
5_15-12-09	NICOTINIC ACID	190	5.9	310	84
I-5_27-05-09	NICOTINIC ACID	250	6.5	448	122
III-5_27-05-09	NICOTINIC ACID	250	6.5	448	122
I-10_27-05-09	NICOTINIC ACID	500	7.3	769	209
II-10_27-05-09	NICOTINIC ACID	500	7.2	602	163
III-10-27-05-09	NICOTINIC ACID	500	7.1	604	164
I-15_27-05-09	NICOTINIC ACID	750	6.8	769	209
II-15_27-05-09	NICOTINIC ACID	750	6.4	665	181
III-15_27-05-09	NICOTINIC ACID	750	6.7	644	175
I-20_27-05-09	NICOTINIC ACID	1000	6	487	132
II-20_27-05-09	NICOTINIC ACID	1000	5.9	489	133
III-20_27-05-09	NICOTINIC ACID	1000	5.8	594	161

Table B. 5 – Explosibility results for nicotinic acid dust with chemical igniters.

ID	SAMPLE	C (g/m^3)	P_{EX} (barg)	dP/dt (bar/s)	K_{st} (bar m/s)
I-2.5_17-03-09	NICOTINIC ACID	125	5.5	295	80
II-2.5_18-03-09	NICOTINIC ACID	125	5.2	282	76
III-2.5_18-03-09	NICOTINIC ACID	125	7.0	593	161
I-5_17-03-09	NICOTINIC ACID	250	7.7	982	267
II-5_18-03-09	NICOTINIC ACID	250	7.9	961	261
III-5_18-03-09	NICOTINIC ACID	250	7.6	799	217
I-10_17-03-09	NICOTINIC ACID	500	7.9	1015	276
II-10_18-03-09	NICOTINIC ACID	500	7.8	1080	293
III-10_18-03-09	NICOTINIC ACID	500	8.0	947	257
I-15_17-03-09	NICOTINIC ACID	750	7.3	886	241
II-15_18-03-09	NICOTINIC ACID	750	7.0	813	221
III-15_18-03-09	NICOTINIC ACID	750	7.5	856	232
I-20_17-03-09	NICOTINIC ACID	1000	6.9	781	212
II-20_18-03-09	NICOTINIC ACID	1000	6.6	800	217
III-20_18-03-09	NICOTINIC ACID	1000	6.8	736	200

Table B. 6 – Explosibility results for hybrid mixtures of methane – nicotinic acid with electric spark ignition.

ID	GAS SAMPLE	C (% v/v)	DUST SAMPLE	C (g/m^3)	P_{EX} (barg)	dP/dt (bar/s)	K_{St} (bar m/s)
13_01-12-09	METHANE	7.3	NICOTINIC ACID	250	7.4	1694	460
14_01-12-09	METHANE	7.3	NICOTINIC ACID	250	7.5	1503	408
15_01-12-09	METHANE	7.3	NICOTINIC ACID	250	7.7	1729	469
10_01-12-09	METHANE	7.3	NICOTINIC ACID	125	7.7	2047	556
11_01-12-09	METHANE	7.3	NICOTINIC ACID	125	7.5	2363	641
12_01-12-09	METHANE	7.3	NICOTINIC ACID	125	7.5	2321	630
8_01-12-09	METHANE	7.3	NICOTINIC ACID	60	7.2	2294	623
9_01-12-09	METHANE	7.3	NICOTINIC ACID	60	7.3	2612	709
5_01-12-09	METHANE	7.3	NICOTINIC ACID	30	6.5	1467	398
6_01-12-09	METHANE	7.3	NICOTINIC ACID	30	6.7	1751	475
7_01-12-09	METHANE	7.3	NICOTINIC ACID	30	6.8	2076	564
5_01-07-09	METHANE	6	NICOTINIC ACID	250	7.4	1668	453
10_09-07-09	METHANE	6	NICOTINIC ACID	250	7.1	1656	450
6_15-12-09	METHANE	6	NICOTINIC ACID	190	7.6	1746	474
7_15-12-09	METHANE	6	NICOTINIC ACID	190	7.7	1749	475
8_15-12-09	METHANE	6	NICOTINIC ACID	190	7.4	1831	497
12_09-07-09	METHANE	6	NICOTINIC ACID	125	7.3	1929	524
14_09-07-09	METHANE	6	NICOTINIC ACID	125	7.2	1699	461
15_09-07-09	METHANE	6	NICOTINIC ACID	125	7.3	1586	431
6_15-07-09	METHANE	6	NICOTINIC ACID	60	6.3	1823	495
7_15-07-09	METHANE	6	NICOTINIC ACID	60	6.6	1197	325
8_15-07-09	METHANE	6	NICOTINIC ACID	60	6.6	1560	423
4_20-07-09	METHANE	6	NICOTINIC ACID	30	6	1033	280
3_21-07-09	METHANE	6	NICOTINIC ACID	30	6	759	206
4_21-07-09	METHANE	6	NICOTINIC ACID	30	5.8	924	251
12_21-07-09	METHANE	3.6	NICOTINIC ACID	250	7.5	1324	359
13_21-07-09	METHANE	3.6	NICOTINIC ACID	250	7.5	1206	327
21_15-12-09	METHANE	3.6	NICOTINIC ACID	190	7.7	1647	447
22_15-12-09	METHANE	3.6	NICOTINIC ACID	190	7.6	1488	404
23_15-12-29	METHANE	3.6	NICOTINIC ACID	190	7.4	2102	571
9_21-07-09	METHANE	3.6	NICOTINIC ACID	125	7	964	262
11_21-07-09	METHANE	3.6	NICOTINIC ACID	125	6.9	886	240
16_15-07-09	METHANE	3.6	NICOTINIC ACID	60	5.6	354	96
17_15-07-09	METHANE	3.6	NICOTINIC ACID	60	5.6	316	86
1_20-07-09	METHANE	3.6	NICOTINIC ACID	30	NO EXPLOSION		
2_20-07-09	METHANE	3.6	NICOTINIC ACID	30	NO EXPLOSION		
3_20-07-09	METHANE	3.6	NICOTINIC ACID	30	NO EXPLOSION		
8_16-12-09	METHANE	3	NICOTINIC ACID	250	7.6	851	231
9_16-12-09	METHANE	3	NICOTINIC ACID	250	7.4	1031	280
10_16-12-09	METHANE	3	NICOTINIC ACID	250	7.7	1253	340
15_15-12-09	METHANE	3	NICOTINIC ACID	190	7.4	711	193
16_15-12-09	METHANE	3	NICOTINIC ACID	190	7.8	1385	376
17_15-12-09	METHANE	3	NICOTINIC ACID	190	7.7	1679	456
16_09-07-09	METHANE	3	NICOTINIC ACID	125	6.7	994	270
18_09-07-09	METHANE	3	NICOTINIC ACID	125	6.6	950	258
9_15-07-09	METHANE	3	NICOTINIC ACID	60	NO EXPLOSION		
10_15-07-09	METHANE	3	NICOTINIC ACID	60	NO EXPLOSION		
12_15-07-09	METHANE	3	NICOTINIC ACID	60	NO EXPLOSION		

14_16-12-09	METHANE	2.3	NICOTINIC ACID	250	7.1	618	168
15_16-12-09	METHANE	2.3	NICOTINIC ACID	250	7.5	684	186
16_16-12-09	METHANE	2.3	NICOTINIC ACID	250	7.4	684	186
12_15-12-09	METHANE	2.3	NICOTINIC ACID	190	7.5	1230	334
13_15-12-09	METHANE	2.3	NICOTINIC ACID	190	7	685	186
14_15-12-09	METHANE	2.3	NICOTINIC ACID	190	7.4	1097	298
5_21-07-09	METHANE	2.3	NICOTINIC ACID	125	5.7	255	69
7_21-07-09	METHANE	2.3	NICOTINIC ACID	125	5.9	562	153
8_21-07-09	METHANE	2.3	NICOTINIC ACID	125	6	373	101
11_16-12-09	METHANE	1.6	NICOTINIC ACID	250	6.9	421	114
12_16-12-09	METHANE	1.6	NICOTINIC ACID	250	7.1	508	138
13_16-12-09	METHANE	1.6	NICOTINIC ACID	250	6.9	594	161
18_15-12-09	METHANE	1.6	NICOTINIC ACID	190	7.1	833	226
19_15-12-09	METHANE	1.6	NICOTINIC ACID	190	7.2	913	248
20_15-12-09	METHANE	1.6	NICOTINIC ACID	190	6.8	481	131
4_13-07-09	METHANE	1.6	NICOTINIC ACID	125	5.5	333	90
5_13-07-09	METHANE	1.6	NICOTINIC ACID	125	5.7	399	108
13_15-07-09	METHANE	1.6	NICOTINIC ACID	60	NO EXPLOSION		
14_15-07-09	METHANE	1.6	NICOTINIC ACID	60	NO EXPLOSION		
15_15-07-09	METHANE	1.6	NICOTINIC ACID	60	NO EXPLOSION		
17_16-12-09	METHANE	1	NICOTINIC ACID	250	6.3	274	74
19_16-12-09	METHANE	1	NICOTINIC ACID	250	6	240	65
9_15-12-09	METHANE	1	NICOTINIC ACID	190	7.1	859	233
10_15-12-09	METHANE	1	NICOTINIC ACID	190	6.6	514	140
11_15-12-09	METHANE	1	NICOTINIC ACID	190	6.7	546	148
21_15-07-09	METHANE	1	NICOTINIC ACID	30	NO EXPLOSION		
22_15-07-09	METHANE	1	NICOTINIC ACID	30	NO EXPLOSION		
23_15-07-09	METHANE	1	NICOTINIC ACID	30	NO EXPLOSION		
6_13-07-09	METHANE	1	NICOTINIC ACID	125	4.7	145	39
9_13-07-09	METHANE	1	NICOTINIC ACID	125	5	170	46

Table B. 7 – Explosibility results for methane gas for different ignition delay time, t_v, with chemical igniters.

ID	SAMPLE	C (% v/v)	E (J)	t_v (ms)	P_{EX} (barg)	dP/dt (bar/s)	K_G (bar m/s)
01_06-10-10	METHANE	7.3	500	Quiescent	4.8	35	9
01_07-10-10	METHANE	7.3	500	Quiescent	4.7	37	10
02_07-10-10	METHANE	7.3	1000	Quiescent	5.1	45	12
03_07-10-10	METHANE	7.3	1000	Quiescent	5.1	40	11
03_06-10-10	METHANE	7.3	10000	Quiescent	5.6	96	26
04_06-10-10	METHANE	7.3	10000	Quiescent	5.7	149	40
04_07-10-10	METHANE	7.3	10000	Quiescent	5.4	103	28
05_07-10-10	METHANE	7.3	10000	Quiescent	6.8	104	28
06_07-10-10	METHANE	7.3	10000	Quiescent	5.6	107	29
11_07-10-10	METHANE	7.3	500	60	5.8	541	147
12_07-10-10	METHANE	7.3	500	60	6	680	185
09_07-10-10	METHANE	7.3	1000	60	5.9	618	168
10_07-10-10	METHANE	7.3	1000	60	5.8	633	172
07_07-10-10	METHANE	7.3	10000	60	6	607	165
08_07-10-10	METHANE	7.3	10000	60	6.3	661	179
19_07-10-10	METHANE	7.3	500	120	5.9	383	104
20_07-10-10	METHANE	7.3	500	120	5.9	375	102
17_07-10-10	METHANE	7.3	1000	120	5.8	462	125
18_07-10-10	METHANE	7.3	1000	120	5.9	408	111
21_07-10-10	METHANE	7.3	10000	120	6	315	86
22_07-10-10	METHANE	7.3	10000	120	6	423	115
3_11-10-10	METHANE	6	500	Quiescent	2.2	23	6
4_11-10-10	METHANE	6	500	Quiescent	3.2	10	3
5_11-10-10	METHANE	6	1000	Quiescent	3.8	16	4
6_11-10-10	METHANE	6	1000	Quiescent	4	17	5
7_11-10-10	METHANE	6	10000	Quiescent	4.7	66	18
8_11-10-10	METHANE	6	10000	Quiescent	4	31	8
9_11-10-10	METHANE	6	500	60	NO EXPLOSION		
10_11-10-10	METHANE	6	500	60	NO EXPLOSION		
11_11-10-10	METHANE	6	1000	60	NO EXPLOSION		
14_11-10-10	METHANE	6	1000	60	4.3	42	11
12_11-10-10	METHANE	6	10000	60	5.4	395	107
13_11-10-10	METHANE	6	10000	60	5.2	288	78
1_3-11-10	METHANE	6	10000	90	5.2	220	60
2_3-11-10	METHANE	6	10000	90	5	167	45
3_3-11-10	METHANE	6	1000	90	4.6	57	15
17_11-10-10	METHANE	6	1000	120	4.1	28	8
18_11-10-10	METHANE	6	1000	120	4.3	53	14
15_11-10-10	METHANE	6	10000	120	4.5	137	37
16_11-10-10	METHANE	6	10000	120	4.8	135	37

1_11-10-10	METHANE	3.6	500	Quiescent	NO EXPLOSION		
2_11-10-10	METHANE	3.6	500	60	NO EXPLOSION		
23_07-10-10	METHANE	3.6	10000	Quiescent	3	170	46
24_07-10-10	METHANE	3.6	10000	60	3.2	128	35

Table B. 8 – Explosibility results for nicotinic acid dust for different ignition delay time, t_v, with chemical igniters.

ID	SAMPLE	C (g/m^3)	E (J)	tv (ms)	P_{EX} (barg)	dP/dt (bar/s)	K_{St} (bar m/s)
1_13-10-10	NICOTINIC ACID	60	10000	60	4	103	28
2_13-10-10	NICOTINIC ACID	60	1000	60	NO EXPLOSION		
3_13-10-10	NICOTINIC ACID	60	10000	120	2.4	30	8
4_13-10-10	NICOTINIC ACID	60	10000	120	2.6	31	8

Table B. 9 – Explosibility results for hybrid mixture of methane and nicotinic acid for different ignition delay time, t_v, with chemical igniters.

ID	SAMPLE	C (% v/v)	SAMPLE	C (g/m^3)	E (J)	tv (ms)	P_{EX} (barg)	dP/dt (bar/s)	K_{St} (bar m/s)
16_3-11-10	METHANE	6	NICOTINIC ACID	60	500	60	7.2	1098	298
17_3-11-10	METHANE	6	NICOTINIC ACID	60	500	60	7.1	935	254
7_13-10-10	METHANE	6	NICOTINIC ACID	60	1000	60	6.9	1042	283
8_13-10-10	METHANE	6	NICOTINIC ACID	60	1000	60	6.8	678	184
5_13-10-10	METHANE	6	NICOTINIC ACID	60	10000	60	7.2	1138	309
6_13-10-10	METHANE	6	NICOTINIC ACID	60	10000	60	7.2	1006	273
14_3-11-10	METHANE	6	NICOTINIC ACID	60	500	90	6.9	746	202
15_3-11-10	METHANE	6	NICOTINIC ACID	60	500	90	6.8	576	156
12_3-11-10	METHANE	6	NICOTINIC ACID	60	1000	90	6.6	584	159
13_-3-11-10	METHANE	6	NICOTINIC ACID	60	1000	90	6.8	597	162
10_3-11-10	METHANE	6	NICOTINIC ACID	60	10000	90	7.2	817	222
11_3-11-10	METHANE	6	NICOTINIC ACID	60	10000	90	7.1	676	183
18_3-11-10	METHANE	6	NICOTINIC ACID	60	500	120	6.7	518	141
19_3-11-10	METHANE	6	NICOTINIC ACID	60	500	120	6.8	499	135
11_13-10-10	METHANE	6	NICOTINIC ACID	60	1000	120	6.6	531	144
12_13-10-10	METHANE	6	NICOTINIC ACID	60	1000	120	6.7	516	140
9_13-10-10	METHANE	6	NICOTINIC ACID	60	10000	120	6.9	486	132
10_13-10-10	METHANE	6	NICOTINIC ACID	60	10000	120	6.6	586	159
22_3-11-10	METHANE	6	NICOTINIC ACID	60	500	500	6.3	239	65
21_3-11-10	METHANE	6	NICOTINIC ACID	60	1000	500	6.1	217	59
20_3-11-10	METHANE	6	NICOTINIC ACID	60	10000	500	6.6	266	72
14_26-10-10	METHANE	6	NICOTINIC ACID	30	500	60	6.2	632	172
15_26-10-10	METHANE	6	NICOTINIC ACID	30	500	60	6	484	131
9_26-10-10	METHANE	6	NICOTINIC ACID	30	1000	60	6.2	631	171
10_26-10-10	METHANE	6	NICOTINIC ACID	30	1000	60	6.2	637	173
5_26-10-10	METHANE	6	NICOTINIC ACID	30	10000	60	6.8	841	228
6_26-10-10	METHANE	6	NICOTINIC ACID	30	10000	60	6.6	847	230
8_3-11-10	METHANE	6	NICOTINIC ACID	30	500	90	5.9	381	103
9_3-11-10	METHANE	6	NICOTINIC ACID	30	500	90	6.3	537	146
6_3-11-10	METHANE	6	NICOTINIC ACID	30	1000	90	6.1	440	119
7_3-11-10	METHANE	6	NICOTINIC ACID	30	1000	90	6	460	125

4_3-11-10	METHANE	6	NICOTINIC ACID	30	10000	90	6.3	618	168
5_3-11-10	METHANE	6	NICOTINIC ACID	30	10000	90	6.2	483	131
16_26-10-10	METHANE	6	NICOTINIC ACID	30	500	120	6.1	406	110
17_26-10-10	METHANE	6	NICOTINIC ACID	30	500	120	6	367	100
11_26-10-10	METHANE	6	NICOTINIC ACID	30	1000	120	5.9	315	86
12_26-10-10	METHANE	6	NICOTINIC ACID	30	1000	120	5.9	352	96
7_26-10-10	METHANE	6	NICOTINIC ACID	30	10000	120	6.4	526	143
8_26-10-10	METHANE	6	NICOTINIC ACID	30	10000	120	6.2	328	89
13-26-10-10	METHANE	6	NICOTINIC ACID	30	10000	120	6.3	454	123

B.2 FLAME PROPAGATION TESTS

Table B. 10 – Results of flame propagation experiments for hybrid mixtures of methane – nicotinic acid.

ID	GAS SAMPLE	C (% v/v)	DUST SAMPLE	m (g/m^3)	v_f (m/s)
II_16-06-10	METHANE	-	NICOTINIC ACID	60	0
I_20-07-10	METHANE	-	NICOTINIC ACID	125	13.21
III_02-06-10	METHANE	-	NICOTINIC ACID	190	11.16
V_16-06-10	METHANE	-	NICOTINIC ACID	190	10.17
I_19-07-10	METHANE	4	NICOTINIC ACID	-	5.76
II_19-07-10	METHANE	4	NICOTINIC ACID	-	5.74
V-25-05-10	METHANE	5	NICOTINIC ACID	-	6.22
I_25-05-10	METHANE	6	NICOTINIC ACID	-	12.82
II_25-05-10	METHANE	6	NICOTINIC ACID	-	13.47
III_25-05-10	METHANE	6	NICOTINIC ACID	-	13.34
IV_25-05-10	METHANE	6	NICOTINIC ACID	-	9.41
IV_22-04-10	METHANE	7.3	NICOTINIC ACID	-	10.07
III_22-04-10	METHANE	7.3	NICOTINIC ACID	-	7.82
V_22-04-10	METHANE	7.3	NICOTINIC ACID	-	11.43
IX_07-06-10	METHANE	0.5	NICOTINIC ACID	60	11.47
I_16-06-10	METHANE	0.5	NICOTINIC ACID	60	9.21
III_07-06-10	METHANE	1	NICOTINIC ACID	60	13.90
VI_14-06-10	METHANE	1	NICOTINIC ACID	60	11.32
I_23-06-10	METHANE	1	NICOTINIC ACID	60	16.52
VIII_07-06-10	METHANE	2	NICOTINIC ACID	60	18.01
V_14-06-10	METHANE	2	NICOTINIC ACID	60	18.33
I_25-06-10	METHANE	2	NICOTINIC ACID	60	22.23
II_07-06-10	METHANE	3	NICOTINIC ACID	60	18.24
IV_14-06-10	METHANE	3	NICOTINIC ACID	60	17.91
VI_07-06-10	METHANE	4	NICOTINIC ACID	60	21.35
III_14-06-10	METHANE	4	NICOTINIC ACID	60	22.95
II_23-06-10	METHANE	4	NICOTINIC ACID	60	17.12
I_07-06-10	METHANE	5	NICOTINIC ACID	60	19.91
II_14-06-10	METHANE	5	NICOTINIC ACID	60	17.48
III_23-06-10	METHANE	5	NICOTINIC ACID	60	16.87
VII_07-06-10	METHANE	6	NICOTINIC ACID	60	23.32
I_14-06-10	METHANE	6	NICOTINIC ACID	60	24.57
III_16-06-10	METHANE	6	NICOTINIC ACID	60	25.53
I_04-06-10	METHANE	6	NICOTINIC ACID	60	23.63
II_04-06-10	METHANE	6	NICOTINIC ACID	60	20.66
IV_04-06-10	METHANE	6	NICOTINIC ACID	60	19.72
IV_20-07-10	METHANE	2	NICOTINIC ACID	125	12.26
IV_21-07-10	METHANE	2	NICOTINIC ACID	125	14.18
VII_20-07-10	METHANE	4	NICOTINIC ACID	125	18.06
V_21-07-10	METHANE	4	NICOTINIC ACID	125	13.86
V_20-07-10	METHANE	5	NICOTINIC ACID	125	12.17
VI_20-07-10	METHANE	6	NICOTINIC ACID	125	9.08
VI_21-07-10	METHANE	6	NICOTINIC ACID	125	8.06
IV_26-05-10	METHANE	0.5	NICOTINIC ACID	190	6.31
VI_16-06-10	METHANE	0.5	NICOTINIC ACID	190	15.36

III_26-05-10	METHANE	1	NICOTINIC ACID	190	13.76
VI_17-06-10	METHANE	1	NICOTINIC ACID	190	15.80
II_02-06-10	METHANE	1	NICOTINIC ACID	190	12.83
VI_26-05-10	METHANE	2	NICOTINIC ACID	190	10.52
V_17-06-10	METHANE	2	NICOTINIC ACID	190	15.14
II_26-05-10	METHANE	3	NICOTINIC ACID	190	10.75
IV_17-06-10	METHANE	3	NICOTINIC ACID	190	10.99
III_12-07-10	METHANE	3	NICOTINIC ACID	190	14.30
I_02-06-10	METHANE	3	NICOTINIC ACID	190	15.90
V_26-05-10	METHANE	4	NICOTINIC ACID	190	14.46
III_17-06-10	METHANE	4	NICOTINIC ACID	190	13.70
I_20-07-10	METHANE	4	NICOTINIC ACID	190	12.02
II_21-07-10	METHANE	4	NICOTINIC ACID	190	14.20
I_26-05-10	METHANE	5	NICOTINIC ACID	190	6.62
II_17-06-10	METHANE	5	NICOTINIC ACID	190	5.73
II_12-07-10	METHANE	5	NICOTINIC ACID	190	9.46
VII_26-05-10	METHANE	6	NICOTINIC ACID	190	6.34
VI_25-05-10	METHANE	6	NICOTINIC ACID	190	6.62
I_17-06-10	METHANE	6	NICOTINIC ACID	190	7.67
I_03-06-10	METHANE	6	NICOTINIC ACID	190	8.66
V_04-06-10	METHANE	6	NICOTINIC ACID	190	6.40

References

[1] NFPA 654: Standard for the Prevention of Fire and Dust Explosions from the Manufacturing, Processing, and Handling of Combustible Particulate Solids, 2000.

[2] Guy Colonna, NFPA Combustible Dust Hazard Codes and Standards, Symposium on Dust Explosion Hazard Recognition and Control: New Strategies, May 13-14, 2009, Baltimore, Maryland.

[3] ITT for Development of DUST-EXPERT, ITT reference: version 5, issued 13-Feb-95, HSE.

[4] ICHemE (2002). Accident Database. Rugby, UK: Institute of Chemical Engineers (IChemE).

[5] http://www.aria.developpement-durable.gouv.fr/

[6] http://www.umweltbundesamt.de/technik-verfahren-sicherheit-e/zema/index.html

[7] http://www.factsonline.nl/

[8] CSB. (2006). Investigation Report. Combustible Dust Hazard Study.

[9] Zalosh R., Grossel S., Kahn R., and Sliva D., 2005. "Dust Explosion Scenarios and Case Histories in the CCPS Guidelines for Safe Handling of Powders and Bulk Solids," 39th AIChE. Loss Prevention Symposium Session on Dust Explosions, Atlanta, April 2005.

[10] Bartknecht, W., Explosions, Springer-Verlag, Berlin Heidelberg New York, 1981.

[11] EPA & OSHA. 1999. EPA/OSHA Joint Chemical Accident Investigation Report, BPS, Inc., West Helena, Arkansas. EPA 550-R-99-003. www.epa.gov/OEM/docs/chem/bpsrpt.pdf

[12] Chatrathi & Going, (1998) Explosion Protection in Pharmaceutical Processing, Fike Corporation Safety Technology News, vol.10 Issue 1, Spring 1998.

[13] Chilworth, W. (2003), When dust clouds and solvent vapours mix and explode, Process Safety News(3), 2 (Chilworth Technology)

[14] Amyotte P. R., Pegg M. J., Khan F. I., Nifuku M., Yingxin T., Moderation of dust explosions, Journal of Loss Prevention in the Process Industries 20 (2007) 675–687

[15] Bisignano U., Esposito C., Marena G., Mazzei A., Mazzei N., Mazzoli G., Valutazione Del Rischio Infortunistico Derivante Da Esplosioni Di Sostanze In Polvere Durante La Manipolazione E Lo Stoccaggio, In: Atti del 3° Seminario di Aggiornamento dei Professionisti CONTARP - La Prevenzione che cambia, i ruoli, le strategie e le sinergie degli "attori" coinvolti, Napoli 24-26 marzo, 2004. INAIL CONTARP Centrale. p. 61-68.

[16] NFPA 68: Standard on Explosion Protection by Deflagration Venting, 1994.

[17] ASTM E 1226, Standard Test Method for Pressure and Rate of Pressure Rise for Combustible Dusts, 2005

[18] Eckhoff R. (2003) Dust Explosions in the Process Industries, 3rd Ed. Gulf Professional Publishing.

[19] Engler, C., Beitrage zur Kenntniss der Staubexplosionen, Chemische Industrie, (1885) 171-173.

[20] Pilão R., Ramalho E., Pinho C., Explosibility of cork dust in methane/air mixtures, Journal of Loss Prevention in the Process Industries 19 (2006) 17–23

[21] Denkevits A., Explosibility of hydrogen–graphite dust hybrid mixtures, Journal of Loss Prevention in the Process Industries 20 (2007) 698–707

[22] Amyotte, P.R., Mintz, K. J., Pegg, M. J., Sun, Y. H., The ignitability of coal dust-air and methane-coal dust-air mixture, Fuel vol.72 n°5 (1993) 671 – 679

[23] Pellmont G., Explosions und Zündverhalten von hybriden Gemischen aus brennbaren Stäuben und Brenngasen, PhD Thesis, Zürich: Swiss Federal Institute of Technology (EHT), (1979).

[24] Pellmont G., Minimum Ignition Energy of Combustible Dusts and Explosion Behaviour of Hybrid Mixtures. In 3rd International Symposium on Loss Prevention and Safety Promotion in the Process Industries, 3, (1980) 851 – 862, Basel, Switzerland.

[25] Amyotte P.R.,, Mintz K.J., Pegg M.J., Sun Y.H., Wilkie K.I., Effects of methane admixture, particle size and volatile content on the dolomite inerting requirements of coal dust, J Hazard Mat, 27/2 (1991) 187-203.

[26] Cashdollar K.L., Sapko MJ, Weiss ES, Hertzberg M, Laboratory and mine dust explosion research at the Bureau of Mines. In: Industrial dust explosions. ASTM Special Technical Publication (STP) 958. West Conshohocken, PA: American Society for Testing and Materials, (1987) 107–123.

[27] Cashdollar K. L., Coal dust explosibility. J Loss Prevent Proc, 9 (1996) 65–76.

[28] Chatrathi K., Dust and hybrid explosibility in a 1 m^3 spherical chamber, Process Saf Prog, 13/4) (1994) 183 – 189

[29] Foniok R., Hybrid Dispersive Mixtures and Inertized Mixtures of Coal Dust. Explosiveness and Ignitability, Staub Reinhalt. Luft,. 45 (1985) 151-154.

[30] Glassman I., Combustion, 3rd ed., San Diego, USA: Academic Press, 1996

[31] Bartknecht, W. (1989). Explosions: Course, prevention, protection. Berlin: Springer

[32] Bartknecht, W., Explosions: Course, prevention, protection. Springer-Verlag – New York (1981)

[33] Hertzberg M., Cashdollar K. L., Introduction to dust explosions. In M. Cashdollar, & K. L. Hertzberg, Symposium on Industrial Dust Explosions. ASTM STP 958, 5 (1987).

[34] Abbasi T., Abbasi S.A., Review Dust explosions–Cases, causes, consequences, and control, Journal of Hazardous Materials 140 (2007) 7–44

[35] Pilão R., Ramalho E., Pinho C., Overall characterization of cork dust explosion, Journal of Hazardous Materials B133 (2006) 183–195

[36] Dufaud O., Perrin L. and Traoré M., Dusts / vapours explosions: Hybrid behaviours?, J Loss Prevent Proc, 21/4 (2008) 481-484.

[37] Dufaud O., Perrin L., Traore M., Chazelet S., Thomas D., Explosions of vapour/dust hybrid mixtures: A particular class. Powder Technology, 190/1-2 (2009) 269-273.

[38] Dufaud O., Perrin L., Traore´ M., Chazelet S. and Thomas D., HYBRID MIXTURES EXPLOSIONS: WHEN VAPOURS MET DUSTS, In 12th International Symposium on Loss Prevention and Safety Promotion in the Process Industries, Edinburgh, UK, 2007

[39] Dufaud O., Perrin L., Traore M., Chazelet S., Thomas D., Explosions of vapour/dust hybrid mixtures: A particular class. Powder Technology, 190/1-2 (2009) 269-273.

[40] Landman G.V.R. (1995). Ignition behaviour of hybrid mixtures of coal dust, methane, and air. The Journal of the South African Institute of Mining and Metallurgy, January/February, 45–50.

[41] Denkevits A., Dust Explosion Experiments – Measurement of Explosion Indices of Graphite Dusts in Hydrogen- Containing Atmospheres, Report on EFDA, May 2005.

[42] Denkevits A., Hydrogen/dust explosion hazard in ITER: Effect of nitrogen dilution on explosion behaviour of hydrogen/tungsten dust/air mixtures, Fusion Engineering and Design, In Press, Corrected Proof, Available online 5 February 2010

[43] Mallard, E. e Le Chatelier, H. L., 1883, "Combustion des mélanges gazeux explosifs", Ann. Mines., 4, 274.

[44] Semenov, N. N., NACA Tech. Memo. No. 1282 (1951).

[45] Liberman M.A. Introduction to physics and chemistry of combustion: explosion, flame, detonation, Springer Verlag 2008

[46] Proust C., Experimental determination of the maximum flame temperatures and the laminar burning velocities for some combustible dust–air, Archivum Combustionis 13 (3-4) (1993), pp. 175–188.

[47] Andrews G.E., Bradley D., Determination of burning velocities: A critical review, Combustion and Flame, Volume 18, Issue 1, February 1972, Pages 133-153

[48] Proust C., Veyssiere B., Fundamental Properties of Flames Propagating in starch Dust-Air Mixtures, Combustion Science and Technology 62 (1988), pp. 149–172.

[49] Dobashi R., Flame Propagation During Dust Explosions, Proceedings of the 5th International Seminar on Fire and Explosion Hazards, Edinburgh, UK, 23-27 April 2007

[50] Cassel, H. M. (1964) "Some Fundamental Aspects of Dust Flames." Report Inv. 6551. Washington, DC: U.S. Bureau of Mines.

[51] Cashdollar K.L., Hertzberg M., Zlochower I.A., Effect of Volatility on Dust Flammability Limits for Coals, Giolsonite, and Polyethylene, 22nd Symp. (Int.) on Combustion, The Combustion Institute, 1757 (1988).

[52] Cashdollar K. L., Overview of dust explosibility characteristics, Journal of Loss Prevention in the Process Industries 13 (2000) 183–199

[53] Krause U., Kasch T., The influence of flow and turbulence on flame propagation through dust-air mixtures, Journal of Loss Prevention in the Process Industries 13 (2000) 291–298

[54] Wang S.F., Jia F., Pu Y.K., Gutkowski A., Effect of turbulence on flame propagation in cornstarch dust-air mixtures, Journal of Thermal Science, 2006, 15(2): 186.

[55] Schneider H., Proust Ch., Determination of turbulent burning velocities of dust air mixtures with the open tube method, Journal of Loss Prevention in the Process Industries, Volume 20, Issues 4-6, July-November 2007, Pages 470-476. Chatrathi K., Dust and hybrid explosibility in a 1 m^3 spherical chamber, Process Safety Progress, 13 (4), 1994, 183-189

[56] Proust C., Flame propagation and combustion in some dust-air mixtures, Journal of Loss Prevention in the Process Industries, Volume 19, Issue 1, January 2006, Pages 89-100.

[57] Proust Ch., A few fundamental aspects about ignition and flame propagation in dust clouds, Journal of Loss Prevention in the Process Industries 19 (2006) 104–120

[58] Van Wingerden, K. and Stavseng, L., Measurements of the laminar burning velocities in dust-air mixtures, VDI-Berichte 1272, pp. 553-564 (1996)

[59] Mazurkiewicz J., Jarosinski J., Wolanski P., Investigations of burning properties of cornstarch dust–air flame, Archivum Combustionis 13 (3–4) (1993), pp. 189–201.

[60] Chen, J. L., Dobashi, R., & Hirano, T. (1996). Mechanisms of flame propagation through combustible particle clouds. Journal of Loss Prevention in the Process Industries, 9(3), 225–229.

[61] Ju, W. J., Dobashi, R., & Hirano, T. (1998). Reaction zone structures and propagation mechanisms of flames in stearic acid particle clouds. Journal of Loss Prevention in the Process Industries, 11(6), 423–430.

[62] Han Ou-Sup, Yashima Masaaki, Matsuda Toei, Matsui Hidenori, Miyake Atsumi, Ogawa Terushige, Behaviour of flames propagating through lycopodium dust clouds in a vertical duct, Journal of Loss Prevention in the Process Industries 13 (2000) 449–457

[63] Han Ou-Sup, Yashima Masaaki, Matsuda Toei, Matsui Hidenori , Miyake Atsumi, Ogawa Terushige, A study of flame propagation mechanisms in lycopodium dust clouds based on dust particles' behaviour, Journal of Loss Prevention in the Process Industries 14 (2001) 153–160

[64] Bradley D., Dixon-Lewis G., El-Din Habik S., Lean flammability limits and laminar burning velocities of CH4-air-graphite mixtures and fine coal dusts, Combustion and Flame, Volume 77, Issue 1, July 1989, Pages 41-50

[65] Liu Y., Sun J., Chen D., Flame propagation in hybrid mixture of coal dust and methane, Journal of Loss Prevention in the Process Industries 20 (2007) 691–697

[66] Chen D. L., Sun J. H., Wang Q. S., Liu Y., Combustion Behaviours and Flame Structure of Methane/Coal Dust Hybrid in a Vertical Rectangle Chamber, Combustion Science and Technology, Vol. 180 (8) August 2008 , pages 1518 - 1528

[67] Taniguchi M., Kobayashi H., Kiyama K., Shimogori Y., Comparison of flame propagation properties of petroleum coke and coals of different rank, Fuel, 88(8), 2009, 1478-1484.

[68] Siwek R., Development of a 20 l Laboratory Apparatus and its Applications for the Investigation of Combustible Dust, Ciba Geigy AG, Basel, 1985.

[69] VDI 3673, Pressure Release of Explosions. Verein Deutscher Ingenieure, 1994

[70] International Organisation of Standardisation (ISO) (1985) Explosion Protection Systems. Part 1: Determination of Explosion Indices of Combustible Dusts, ISO-6184/1

[71] Cesana, C., Siwek, R. (2009). Operating instructions 20-l-apparatus 7.0. Adolf Kühner AG. Switzerland: CH-4127 Birsfelden.

[72] ASTM (1995) E 789-95 Standard Test Method for Dust Explosions in a 1.2-Litre Closed Cylindrical Vessel, Annual Book of ASTM Standards 2004. USA: ASTM International.

[73] ASTM (2002) E 2019-99 Standard Test Method for minimum ignition energy of a dust cloud in air, Annual Book of ASTM Standards 2002 (pp. 769–776). USA: ASTM International.

[74] Janes A., Chaineaux J., Carson D., Le Lore P.A., MIKE 3 versus HARTMANN apparatus: Comparison of measured minimum ignition energy (MIE), Journal of Hazardous Materials, Volume 152, Issue 1, 21 March 2008, Pages 32-39.

[75] Lee, J.H.S., Pu, Y.K., Knystautas, R., "Influence of turbulence on closed-volume explosion of dust-air mixtures", Archivum Combustionis 7: 279-297 (1987).

[76] Tamanini, F., "Turbulence effects on dust explosion venting", Plant/Operations Progress 9: 52-60 (1990).

[77] Eckhoff, R.K., "Influence of initial and explosion-induced turbulence on dust explosions in closed and vented vessels", Powder Technology 71: 181-187 (1992).

[78] Pu, Y.K., Jarosinski, J., Johnson, V.G., Kauffman, C.W., "Turbulence effect on dust explosions in the 20-liter spherical vessel", Proc 23rd Symposium Int Combustion, 1990, p.843/849.

[79] Van der Wel, P.G.J., Van Veen, J.P.W., Lemkowitz, S.M., Scarlett, B. and Van Wingerden, C.J.M., "An interpretation of dust explosion phenomena on the basis of time scales", Powder Technology, 71: 207-15 (1992).

[80] http://www.dguv.de/bgia/en/gestis/expl/index.jsp

[81] Di Benedetto A., Russo P., Amyotte P., Marchand N., Modelling the effect of particle size on dust explosions, Chemical Engineering Science, Volume 65, Issue 2, 16 January 2010, Pages 772-779

[82] Menon D., Dollimore D., Alexander K. S., A TG–DTA study of the sublimation of nicotinic acid, Thermochimica Acta, Volumes 392-393, 15 September 2002, Pages 237-241

[83] Dahoe, A.E., Cant, R.S., and Scarlett, B., "On the Decay of Turbulence in the 20-LiterExplosion Sphere", Flow Turbulence Combustion 67: 159–184 (2001).

[84] Dahoe, A. E., Zevenbergen, J. F., Lemkowitz, S. M., Scarlett, B., "Dust explosions in spherical vessels: the role of flame thickness in the validity of the 'cube-root law'," Journal of Loss Prevention in the Process Industries 9: 33–44 (1996).

[85] Lewis, B., and von Elbe, G., "Determination of the speed of flames and the temperature distribution in a spherical bomb from time-pressure explosion records", Journal of Chemical Physics, 2: 283–290 (1934).

[86] Tufano, V., Crescitelli, S., Russo, G., "Overall kinetic parameters and laminar burning velocity from pressure measurements in closed vessels", Combust. Sci. Technol. 31: 119-130 (1983).

[87] Pocheau, A., "Scale invariance in turbulent front propagation", Phys. Rev. E 49 : 1109-1122 (1994).

[88] Phylaktou, H., Andrews, G.E., Mounter, N. and Khamis, K. M., "An investigation into "rate of rise" detection systems for dust explosion suppression", IChE Symposium Series 130, 1992, p.525.

[89] Clavin, P. and Williams, F. A., J. Fluid Mech. 90: 589 (1979).

[90] Gieras, M., W. Glinka, R. Klemens P. Wolanski, "Investigation of flame structure during laminar and turbulent burning in dust–air mixtures" Conf. Dust Expl. Prot. People Equip. Env., 168, 1995.

[91] Tezok, F.I., Kauffman, C.W., Sichel, M. and Nichols, J.A., "Turbulent burning velocity measurements for dust air mixtures in a constant volume spherical bomb", Progress in Astronautics and Aeronautics 105: 184–195 (1986).

[92] Zhen, G. and W. Leukel, "Determination of Dust Dispersion Induced Turbulence and its Influence on Dust Explosions," Combust. Sci. Tech. 113-114: 629 (1996).

[93] van Wingerden, K., Arntzen, B.J., and Kosinski, P, "Modelling of dust explosions", VDI-Berichte 1601: 411 (2001).

[94] Gordon S., McBride B.J., Computer Program for Calculation of Complex Chemical Equilibrium Compositions and Applications. NASA RP 1311 (1994).

[95] Dahoe A.E., de Goey L.P.H., On the determination of the laminar burning velocity from closed vessel gas explosions, J Loss Prevent Proc, 16/6 (2003) 457-478.

[96] Cashdollar K.L., Zlochower I.A., Green G.M., Thomas R.A., Hertzberg M., Flammability of methane, propane, and hydrogen gases, J Loss Prevent Proc, 13/3-5 (2000) 327-340.

[97] Mashuga C.V., Crowl D.A., Application of the flammability diagram for evaluation of fire and explosion hazards of flammable vapours, Process Saf Prog, 17/3 (1998) 177 – 183.

[98] Senecal J., Beaulieu P., K_G: New data and analysis, Process Saf Prog. 17 (1998) 9-15.

[99] Bartknecht W., Explosionsschutz, Berlin: Springer-Verlag. Beck, H., Glienke, N., & Möhlmann, C, 1993.

[100] Cesana C., Final Report, Calibration-Round-Robin CaRo 07, B052 221, Adolf Kühner AG, Birsfelden, Switzerland, 2007.

[101] Cesana C., Final Report, Calibration-Round-Robin CaRo 03, B052 185, Adolf Kühner AG, Birsfelden, Switzerland, 2003.

[102] Cesana C., Final Report, Calibration-Round-Robin CaRo 98, B052 146,Adolf Kühner AG, Birsfelden, Switzerland, 1998.

[103] Di Benedetto A. and P. Russo, Thermo-kinetic modelling of dust explosions, Journal of Loss Prevention in the Process Industries 20, 303–309, 2007.

[104] Hertzberg M., Cashdollar K. L., Zlochower I. A., Flammability limit measurements for dusts and gases: Ignition energy requirements and pressure dependences, Symposium (International) on Combustion, Volume 21, Issue 1, 1988, Pages 303-313.

[105] Zhen G., Leuckel W., Effects of ignitors and turbulence on dust explosions, Journal of Loss Prevention in the Process Industries, Vol. 10, Issues 5-6, September-November 1997, Pages 317-324.

[106] Wang S.F., Zhang H., Jarosinski J., Gorczakowski A., Podfilipski J., Laminar burning velocities and Markstein lengths of premixed methane/air flames near the lean flammability limit in microgravity, Combustion and Flame, Vol. 157, Issue 4, 2010, Pages 667-675

[107] Gu X. J., Haq M. Z., Lawes M., Woolley R., Laminar burning velocity and Markstein lengths of methane–air mixtures, Combustion and Flame, Volume 121, Issues 1-2, April 2000, Pages 41-58

[108] Andrews G.E., Bradley D., The burning velocity of methane-air mixtures, Combustion and Flame, Volume 19, Issue 2, October 1972, Pages 275-288

[109] 94/9/EC Directive – ATEX 95 (100a) dated 23rd March 1994 - Equipment and protective systems intended for use in potentially explosive atmospheres

[110] 99/92/EC Directive – ATEX 137 dated 16 December 1999 - Minimum requirements for improving the safety and health protection of workers potentially at risk from explosive atmospheres

[111] Eckhoff R., Design of electrical equipment for areas containing combustible dust Why dust standards cannot be extensively harmonised with gas standards, Journal of Loss Prevention in the Process Industries 13 (2000) 201–208.

[112] Eckhoff R., Differences and similarities of gas and dust explosions: A critical evaluation of the European 'ATEX' directives in relation to dusts, Journal of Loss Prevention in the Process Industries 19 (2006) 553–560

[113] http://www.csb.gov/about/mission.aspx

[114] OSHA (2008), "Combustible Dust National Emphasis Program" (NEP); document CPL 03-00-006 Available at: www.osha.gov/OshDoc/Directive_pdf/CPL_03-00-008.pdf

[115] Blair, A.S., Dust explosion incidents and regulations in the United States, Journal of Loss Prevention in the Process Industries, 20 (4-6), (2007), 523-529